Spring 7-3-2012

Multiscale Investigation of Acid Mine Drainage: the Effect of Organic Carbon Cycling on Microbial Activity and Pyrite Oxidation

Tesfayohanes W. Yacob
University of Colorado at Boulder, embushu@gmail.com

Multiscale investigation of acid mine drainage: the effect of organic carbon cycling on microbial activity and pyrite oxidation

by

TESFAYOHANES WELDEGHEBRIEL YACOB

B. Sc. Chemical Engineering, Addis Ababa University, 2005

A thesis submitted to the

Faculty of the Graduate School of the

University of Colorado in partial fulfillment

of the requirement for the degree of

Doctor of Philosophy

Department of Civil, Environmental and Architectural Engineering

2012

This thesis entitled:

Multiscale investigation of acid mine drainage: the effect of organic carbon cycling on microbial activity and pyrite oxidation

Written by Tesfayohanes Weldeghebriel Yacob
has been approved for the Department of Civil, Environmental and Architectural Engineering

JoAnn Silverstein

Harihar Rajaram

Mark Hernandez

Diane McKnight

Richard Smith

Date 04/06/2012

The final copy of this thesis has been examined by the signatories, and we
Find that both the content and the form meet acceptable presentation standards
Of scholarly work in the above mentioned discipline.

Yacob, Tesfayohanes Weldeghebriel (Ph.D., Civil Engineering)

Multiscale investigation of acid mine drainage: the effect of organic carbon cycling on microbial activity and pyrite oxidation

Thesis directed by Professor JoAnn Silverstein

Acid mine drainage (AMD) generation from abandoned waste rock piles is a serious environmental problem. One proposed solution is the use of organic carbon to bring about biogeochemical changes that can slow down AMD. The growth of mine waste rock enrichments on a glucose substrate was studied in batch cultures and a monod kinetic model was developed. Various concentrations of soluble microbial products (SMPs) of these enrichments were studied for their interaction with ferric iron and the resulting effect on pyrite oxidation. Four Waste rock packed columns were run in series and the chemical and biological indicators of interest measured for the rock pore liquid and column bulk liquid effluent. The growth experiment results gave a maximum specific growth rate of 0.13 ± 0.01 (1/hr). The enrichments were able to grow from pH 1.6 to 6.0 and had a pH optimum between 2.5 and 3.0. A dissolved oxygen half saturation constant of 0.11 ± 0.05 mg/l was obtained indicating the high sensitivity of the organisms to oxygen. SMPs were able to reduce the pyrite oxidation rate by up to 90% with lysis derived SMPs having a much higher impact than growth derived SMPs for an equivalent SMP-DOC (dissolved organic carbon). A mathematical relationship was developed to predict the rate of pyrite oxidation given an SMP-DOC concentration. The column experiments showed that rock pores contain up to 16 times higher iron and sulfate concentrations compared to column bulk liquid effluents. These and other microbial evidence suggest high pyrite oxidation rate is maintained at rock pores and that bulk liquid effluent concentrations are

controlled by diffusional exchange with rock pores as indicated by a tracer test. Results of the growth and SMP-ferric iron interaction study can be incorporated to AMD models and used to predict remediation effects of carbon addition. Waste rock AMD generation results can be used as preliminary guides to design efficient carbon delivery schemes to reactive sites of waste rock piles.

ACKNOWLEDGEMENTS

I would like to thank:

The National Science Foundation, for providing financial support in the form of a grant (NSF # CBET 0854510).

My advisor JoAnn Silverstein, for being an encouraging and patient mentor throughout the years.

Harihar Rajaram, for providing a continuous advice and feedback on research questions.

Kristina Minchow , Logan Calihan , Travis Tasker, Sachin Pandey, and Jelena Basta for a great help in the lab and for useful research discussions.

Joy Jenkins, for teaching me many laboratory techniques as well as introducing me to acid mine drainage remediation research.

Benjamin Andre, for his help in learning matlab and the many useful research discussions.

Sanjay Mohanty, Aditya kausik, Timothy Dittrich, and Krishna Madhavan for providing encouragement and accountability in the form of a Ph.D. support group.

Graduate school colleagues from Civil Engineering, for many years of friendship.

My uncle and his family: Abraham, Mebrat, Sabra, and Omega: for lovingly hosting me for 5+ years. I specially thank my uncle for his relentless encouragement throughout graduate school.

My brothers and sisters, for being supportive and loving. I specially thank my brother Mussie for his financial support.

My Parents, for their loving and continuous care they provided throughout the years. I thank my Dad for his continuous mentoring during my time in grade school and his continuous encouragement thereafter.

God, for all the wonderful things he has done in my life.

CONTENTS

Chapter Pages

CHAPTER 1. INTRODUCTION 1
1.1 Problem definition 1
1.2 Environmental impact 3
1.3 Generation mechanism and factors 5
1.3.1 Chemistry 5
1.3.2 Biology 6
1.3.3 Physical space for reaction 7
1.3.4 Hydrology and transport 8
1.3.5 Putting it together 11
1.4 Current AMD prevention and remediation techniques 12
1.5 Organic carbon in mine waste rock piles 14
1.6 Organic carbon based prevention of AMD 17
1.7 Research questions 21
1.8 Research focus 23
1.9 References 25

CHAPTER 2. THE GROWTH KINETICS OF HETEROTROPHIC MINE WASTE ROCK ENRICHMENTS ON GLUCOSE: THE EFFECT OF PH AND DISSOLVED OXYGEN 31
2.1 Introduction 32
2.2 Materials and Methods 35
2.2.1 Enrichment of cultures 35
2.2.2 Limited glucose growth 35
2.2.3 pH effect on growth 36
2.2.4 Limited DO growth 37
2.2.5 Analytical methods 37
2.2.6 Monod modeling 37
2.3 Results and Discussion 40
2.3.1 Limited glucose growth 40
2.3.2 Limited DO growth 43
2.3.3 pH effect on growth 45
2.3.4 Phospholipid fatty acid analysis (PLFA) 49
2.4 Conclusion 51
2.5 References 52

CHAPTER 3. INTERACTION OF FERRIC IRON WITH SOLUBLE MICROBIAL PRODUCTS DECREASES PYRITE OXIDATION 55

3.1 Introduction 56
3.2 Materials and Methods 60
3.2.1 Enrichment of cultures 60
3.2.2 Obtaining SMPs (growth and lysis products) 60
3.2.3 Pyrite oxidation experiments 60
3.2.4 SMP apparent molecular weight fractionation and pyrite oxidation experiments 61
3.2.5 Biodegradation of lysis derived SMPs 62
3.2.6 Deferoxamine mesylate complexation experiments 62
3.2.7 SMP characterization 63
3.2.8 Analytical methods 64
3.3 Results and Discussion 65
3.3.1 Enrichment of cultures 65
3.3.2 SMP and pyrite oxidation activity 65
3.3.3 Deferoxamine mesylate experiment results 75
3.3.4 Modeling effects of Fe-SMP and Fe-DFAM complexes 76
3.3.5 Implications 86
3.4 Conclusions 88
3.5 References 89

CHAPTER 4. THE ROLE OF PORE REACTIONS ON ACID MINE DRAINAGE GENERATION IN WASTE ROCK 93
4.1 Introduction 94
4.1.1 AMD introduction 94
4.1.2 Waste rock piles 94
4.2 Materials and Methods 97
4.2.1 Research set up 97
4.2.2 Flow experiments 97
4.2.3 Porosity and saturation measurement 99
4.2.4 Rock pore liquid measurement 99
4.2.5 Enumeration of microorganisms 100
4.2.6 Tracer test 101
4.2.7 Analytical methods 101
4.3 Results and Discussion 103
4.3.1 Column effluent results 103
4.3.2 Microorganism enumeration (MPN) results 109
4.3.3 Saturation and porosity measurement results 111
4.3.4 Pore liquid chemistry measurement results 113
4.3.5 Tracer test results 115
4.3.6 Geochemical modeling 117

4.3.7 Implications 119
4.4 Conclusions 121
4.5 References 122

CHAPTER 5. SUMMARY AND CONCLUSIONS 125
5.1 Summary of research 125
5.1.1 Chapter 2 – Growth kinetics 126
5.1.2 Chapter 3-SMP ferric iron interaction 127
5.1.3 Chapter 4-Waste rock AMD generation 127
5.2 Conclusions 128
5.2.1 Chapter 2 128
5.2.2 Chapter 3 128
5.2.3 Chapter 4 129
5.3 Recommendations for future research endeavors 131

BIBILIOGRAPHY 132

LIST OF TABLES

Table Pages

Table 2-1. Slopes of a best line fit to a plot of the natural logarithm of biomass density vs. time. Relative activity was calculated by dividing the slopes by the largest slope value. 46

Table 3-1. SEC-DOC based amw distribution for the growth and lysis derived SMPs. The percentages were calculated by using the areas obtained from the integration of the DOC response curve in Figure 3-8. 72

Table 3-2. Fluorescence model (PARAFAC) results for growth and lysis derived SMPs. The model output predictions for the 13 components were grouped into four categories and summed up to generate percentage values. 75

Table 4-1. Selected PHREEQC speciation results for the average pore liquid chemistry results of C5. The input for the speciation contained mg/l of, Fe^{3+} – 15,100, Fe^{2+}-100, SO_4^{2-}78,700, Al-31, Cu-2.2, Zn-74, Mn-8.4, Mg-10, Cd-0.5, Pb-177, K-12,643, Na-0 and Ca-9,887. The pH was 1.6 and the pE was set at 12. 119

LIST OF FIGURES

Figure Page

Figure 1-1. Hydrograph for Leadville, CO. Graph was developed from 32 year of average monthly snow fall, rain precipitation, and daily snow depth data. 10

Figure 1-2. DOC interactions in a waste rock pile: The growth of heterotrophic organisms off carbon substrate leads to the formation of EPS and SMPs and can lead to oxygen and nutrient competition and iron and sulfate reduction. Formation of heterotrophic EPS can lead to reactive sulfide site blockage, reduce oxygen diffusion into rock pores and can sorb metals including iron oxides. SMPs can complex ferrous and ferric iron and also serve as a substrate for heterotrophic microorganisms. Some of the organic carbon substrate and produced SMPs can sorb into ferric iron oxide precipitates found on the surface of the waste rocks and in the AMD liquid. 20

Figure 2-1. Mineral media containing 1.7 g/l glucose and 0.2 g/l yeast extract at a pH of 3.0 was inoculated with an exponential phase culture obtained from mine waste rock enrichments. Substrate depletion was tracked by measuring the glucose concentration and the biomass growth monitored by reading the optical density at 510 nm in a direct reading spectrophotometer. Error bars indicate the difference of the measurements for duplicate experiments from the average measurements (n=2). 41

Figure 2-2. A calibration curve for converting optical density to dry cell mass density was obtained from selected samples within the growth phase of an experiment. Culture liquid samples were filtered through pre dried 0.22 um syringe nylon filters followed by drying and weighing to determine the cell mass density. Optical density was measured at 510 nm using a direct reading spectrophotometer. Horizontal and vertical error bars indicate the respective difference of the measurements for the duplicate experiments from the average measurements (n=2). 42

Figure 2-3. Glucose depletion and biomass dry weight increase data from limited glucose growth experiments were fitted to a Monod kinetics model. The modeled parameters were maximum specific growth rate, cellular yield and half saturation constant for glucose. A MATLAB nonlinear least square optimization routine was used to minimize the residuals and obtain the best fit parameters. 43

Figure 2-4. A plot of dissolved oxygen consumption experimental data and model fit. Glucose, yeast extract and mineral containing media in a BOD bottle was inoculated with exponential phase culture. A YSI 5905 DO probe was fitted to the BOD bottle and the dissolved oxygen data recorded about every second using a mini com terminal connected with a YSI DO meter. 45

Figure 2-5. Biomass plots for variable pH growth experiments. Glucose, yeast extract and mineral media solutions were acidified to different initial pHs using 3N HCl. The adjusted media were inoculated with filtered and re suspended exponential phase cultures. The measured optical density results were converted to dry cell density using a calibration curve and plotted. 47

Figure 2-6. A plot of the best fit pH relative activity continuous function and experimentally determined activities. Dots represent experimentally determined relative activity, while the line is for the best fit continuous function. 48

Figure 3-1. $Fe(H_2DFA)^{2+}$, a bishydroxamate configuration of the DFA siderophore complexed with ferric iron at pH < 4, after Kalinowski et al., 2000. 63

Figure 3-2. Substrate depletion curve for a second transfer culture with an initial glucose concentration of 20 g/l. 65

Figure 3-3. Ferrous iron produced during growth derived SMP solution pyrite oxidation experiments. Experiments were done in flasks containing 2.0 g of pyrite in 200 ml of pH 1.8 solutions and about 90 mg/l of initial ferric iron. Two solutions containing 28 and 53 mg/l growth derived SMP-DOC were used. Error bars indicate difference of the plotted average values from the duplicate flask measurements for each SMP-DOC concentration used. 66

Figure 3-4. Ferrous iron produced during lysis derived SMP solution pyrite oxidation experiments. Experiments were done in flasks containing 2.0 g of pyrite in 200 ml of pH 1.8 solutions and about 90 mg/l of initial ferric iron. Three solutions containing 27, 78, and 236 mg/l lysis derived SMP-DOC were used. Error bars indicate difference of the plotted average values from the duplicate flask measurements for each SMP-DOC concentration used. 68

Figure 3-5. Ferrous iron production during ultra-filtered lysis derived SMP solution pyrite oxidation experiments containing 1.0 g of pyrite in 100 ml of pH 1.8 solutions and about 80 mg/l of initial ferric iron. Three solutions

containing 164, 167, and 267 mg/l SMP-DOC were used corresponding to the <1 KDa , <10 KDa, and unfiltered bulk solutions. Error bars indicate difference of the plotted average values from the duplicate flask measurements for each SMP-DOC concentration used. 69

Figure 3-6. DOC measurements of the biodegradation experiment carried out with an initial lysis derived SMP-DOC of 500 mg/l, inoculated with an active acidophilic heterotrophic culture. One treatment contained an initial ferric iron concentration of 90 mg/l whereas the second did not contain any ferric iron. The control was not inoculated with an active culture and did not contain ferric iron. 70

Figure 3-7. A plot of ferrous iron production during pyrite oxidation experiments with filtered biodegraded SMPs containing 1.25 g pyrite in pH 1.8, 125 ml solutions. The SMP with (Fe3) and without (Fe3) refer to the original biodegradation experiment. Both biodegraded solutions were filtered and adjusted to about 90 mg/l ferric iron and had 91 and 95 mg/l SMP-DOC. The control from the biodegradation experiment was also filtered and adjusted to about 93 mg/l ferric iron and had 476 mg/l SMP-DOC. The pyrite oxidation control did not contain any SMPs. The error bars indicate difference of the plotted average values from the duplicate flask measurements for each tested case. 71

Figure 3-8. Size exclusion chromatograph of growth and lysis derived SMPs. The DOC response in mV was monitored online. The response time was converted to molecular weight using a calibration curve prepared by injecting known weight dextran standards. 73

Figure 3-9. Lysis products fluorescence characterization results (clock wise from top right : the actual EEM, the modeled EEM, the residuals, and the residuals on a percent basis). 74

Figure 3-10. Growth products fluorescence characterization results (clock wise from top right : the actual EEM, the modeled EEM, the residuals, and the residuals on a percent basis). 74

Figure 3-11. Fitted data of the pyrite oxidation experiments with lysis derived SMPs. Symbols represent experimental data and the lines are obtained using equations of the first-order rate models obtained from the nonlinear regressions. 77

Figure 3-12. Fitted data of the pyrite oxidation experiments with growth derived SMPs. Symbols represent experimental data and the lines are obtained using equations of the first-order rate model obtained from the nonlinear regressions. 78

Figure 3-13. Ferrous iron production during pyrite oxidation experiments containing deferoxamine mesylate. Experiments were done in 200 ml, pH 1.8 solutions and contained 2.0 g of pyrite and initial ferric iron concentration of about 85 mg/l ferric iron. Symbols represent experimental data and the lines are obtained using equations of first-order rate models obtained by nonlinear regression. 82

Figure 3-14. First order pyrite oxidation rate constants as a function of SMP-DOC concentrations. Data from UF experiments are for apparent molecular weight fractions <1 KDa, and <10 KDa. The biodegradation experiments data are from the two biodegraded filtrates with the one containing ferric iron prior to biodegradation. The unfiltered bulk UF treatment and the sterile biodegradation treatment are added to the three lysis experiments and make up the above 5 lysis derived SMP data points. The DFAM treatments contained 129, 257, and 386 mg/l DFAM-DOC. Error bars represent 95% confidence intervals for the rate constants. 83

Figure 3-15. SMP pyrite oxidation Inhibition model run results for all the SMP treatments. The best fit line represents the inhibition model predicted rate constants at the best fit inhibition constant, $ksmp$ of 21.7 mg/l SMP-DOC. The 95% confidence levels on $ksmp$ were used to generate a lower and upper bound predictions for K. The inhibition model was run for all SMP treatments (n=12). 85

Figure 3-16. SMP pyrite oxidation Inhibition model run results for lysis derived SMP treatments. The best fit line represents the inhibition model predicted rate constants at the best fit inhibition constant, $ksmp$ of 7.5 mg/l SMP-DOC. The 95% confidence levels on $ksmp$ were used to generate a lower and upper bound predictions for K. The inhibition model was run for all lysis derived SMP treatments including the ultra-filtered and biodegraded SMP (n=10). 86

Figure 4-1. Schematics of the column experiment set up. The end of the cylindrical part of the columns had a perforated plate allowing the free drainage of liquid to the conical part. Column 1 has a recirculating reservoir which was daily wasted and fed with water to maintain a 5 day residence time. Liquid from the reservoir was applied at 11 ml/min to column 2 and in series to all the other columns. 98

Figure 4-2. Ferric iron concentration for effluents of columns 1-5. The ferrous iron concentrations for all columns were mostly less than 20 mg/l. The

ferric iron was calculated as a difference of the total soluble iron and soluble ferrous iron measurements. 105
Figure 4-3. Measured pH for effluents of columns 1-5. pH measurements were done on 0.22 µm filtered samples and were undertaken within an hour of sample collection. 106
Figure 4-4. Sulfate and ferric iron concentrations for selected samples of column 5 effluent. Please note the separate y axes. 106
Figure 4-5. Humidity measurement results at a depth of 30.5 cm for columns 2-5 along with ambient humidity measurements. 107
Figure 4-6. Metal analysis of selected elements for column 5 effluent on days 21, 92 and 191. A separate right axis has been made for zinc concentrations for a better display of the data. 107
Figure 4-7. Metal analysis results of selected elements for effluent of columns 1-5 on day 191. A separate right axis has been made for zinc concentrations for a better display of the data. 108
Figure 4-8.The ferric iron production is the net moles of ferric iron released from each of columns 2-5 per kg of waste rock per second. 109
Figure 4-9. MPNs of iron oxidizing organisms for column effluent and pore liquid samples of columns 2-5. Error bars represent the standard errors predicted for each test. 110
Figure 4-10. MPNs of acidophilic heterotrophs done for column effluent and pore liquid of columns 2-5. Error bars represent the standard errors predicted for each test. 110
Figure 4-11. Average rock porosity for samples of columns 2-5 (n=30). Error bars represent standard deviation for the results. 112
Figure 4-12. Average water saturation for samples of columns 2-5 (n=30). Error bars represent standard deviation for the results. 112
Figure 4-13. A plot of the average water saturation of rock samples in all columns at each of the 5 depths. Error bars represent standard deviation for the results. 113
Figure 4-14. Pore liquid and column effluent total soluble iron concentrations for columns 2-5. Error bars represent standard deviation of results (n=3). 115
Figure 4-15. Bromide molar concentration for C5 effluent. The peak bromide concentration was 0.0189 M and appeared 2.6 hours after the tracer injection. A day into the tracer injection 58% of the tracer mass was recovered. 117

CHAPTER 1. INTRODUCTION

1.1 Problem definition

Acid mine drainage, AMD, is produced by the oxidation of sulfide minerals, primarily pyrite, by ferric iron and oxygen and is characterized by low pH, high metals and sulfate content. The process of mining disturbs the existing land vegetation and topography of the mined area. It typically increases the exposed surface area of rocks exposed to water and air. Construction of pits, adits, shafts, tunnels and other structures increase the flow of air and water to sulfide minerals. As part of an effort to access the commercial grade ore, waste rocks are removed and usually deposited at a nearby site.

Waste rock containing commercial grade ores are typically crushed, ground, and milled to fine sizes of less than a millimeter, in order to ready them for different separation and extraction techniques. Following the needed extraction of resources, this fine sized and usually wet material makes what is called a tailings waste. As metal and other precious resources are typically found in low concentrations, it is common to generate 95 times more waste rock and tailings waste as compared to the final product volume. At the end of the mining operation, if the mine is not closed properly, continuing oxidation of sulfide in pits for surface mining and in adits and shafts for underground mining produces AMD.

Depending on the topography and hydrology of the area, the AMD produced may contaminate ground water aquifers and surface water bodies. The other major sources of concern for AMD generation are the tailing and waste rock piles. Lottermoser (2003) estimates that more than 15,000 Mt/year of waste rock and soil covering a surface area of approximately

100 million hectares is disturbed during mining for metals and coal. Modern mining rules require mining companies to prepare a plan on closing down a mine including the sealing of adits and shafts, fencing open pits, proper storing and monitoring of tailings and waste rock, landscaping and re-vegetation works (Lottermoser 2003). However, a significant number of abandoned mines are found all over the world from mining that occurred through mid-way of the 20th century. A 1993 report titled “The Burden of Gilt “by an environmental organization estimated that there were more than 550,000 abandoned mines in the United States (Lyon *et al.*, 1993). The United States Bureau of Land Management has an inventory of 31,000 abandoned mine lands of which 75% are still waiting investigation to determine a remediation course of action (BLM, 2011). The focus of this research is on abandoned waste dumps and specifically on waste rock piles.

1.2 Environmental impact

The drainage from tailings and waste rock piles as well as from open mine adits and shafts can form a pool of highly contaminated water. Pools of liquid having pH <2 with orders of magnitude higher metal concentrations above drinking water limits are commonly found around mine wastes, while in rare cases negative pHs are also observed (Nordstrom and Alpers, 1999). These waters, if not isolated by a fence, can pose direct health dangers to children and adventurers as well as grazing animals such as deer. The pool of liquid and the drainage can also join streams, rivers and other surface water bodies.

A study of the impact of AMD on 64,300 stream reaches in the Mid-Atlantic and Southeastern United States showed that about 2% were acidic and another 2% were heavily affected by it although not acidic (Herlihy *et al.*, 1990). Depending on the nature of the geologic formation underneath the mine waste, some of the drainage can contaminate ground water aquifers. The contaminated ground water may discharge to surface water bodies at a different location. On mixing with surface water bodies, the AMD is diluted and in most cases the ferric iron in the drainage is precipitated as ferric hydroxide. Typically, AMD impacted stream beds are covered with orange iron hydroxide precipitates. There is a dynamic interaction of the soluble metals with the stream bed in the form of sorption, de-sorption, complexation and colloid facilitated transport. Thus the solubility of the metals in the AMD affected surface waters is controlled by a number of water chemistry factors prevailing in the liquid and stream beds.

Plants and animals living in AMD impacted surface waters can be affected by chemical and biological changes induced by specific metals and/or acidic conditions (Pond *et al.*, 2008). It has been documented that some AMD impacted streams and rivers contain none or much fewer fish compared to their neutral counterparts (Warner 1971; Gray, 1998). Ferric iron precipitates have been documented to affect fish gill and thus their respiratory functions (Jansen and Groman, 1993 **;** Dalzell and Macfarlane, 1999).

Sorption of heavy metals onto sediments exposed to AMD is also a serious concern and can inhibit plant growth on the sediments. AMD contaminated industrial water sources, depending on the pH and concentration of metals and sulfate, can cause corrosion to steel and concrete containing process equipment and lines. Water treatment plants whose sources are affected by AMD are forced to spend extra resources to clean it up with techniques such as reverse osmosis, nanofiltration, and ion exchange.

1.3 Generation mechanism and factors

1.3.1 Chemistry

The acidity that releases metals from the waste rock mainly results from the oxidation of sulfide. At low pH, ferric iron is the dominant oxidant yielding ferrous iron, oxidized sulfur species, and acidity (equation 1-1). Oxygen can also directly oxidize pyrite (equation 1-2). This is particularly considered important during the initial formation of AMD in a fresh mine waste. Ferric iron, depending on the pH may be present in various forms and this affects sulfide oxidation and thus AMD generation. The formation of soluble and solid ferric-hydroxide species, as well as other secondary minerals of iron is thus an important control on ferric iron concentration (equation 1-3).

Above pH of 3, at which ferric iron precipitates out, organic ligands can complex ferric iron and maintain the solubility leading to continued pyrite oxidation (Brothers *et al.*, 1996). This however, is generally not significant because of the scarcity of organic ligands in mine waste rock environments. The conversion of the sulfide oxidation product ferrous iron back to ferric iron (equation 1-4) can happen with or without microorganisms and is an important step because it keeps the AMD generation cycle going. Below pH 4, the rate of conversion by iron oxidizing microorganisms is many orders of magnitude higher than by just oxygen (Singer and Stumm, 1970). This cyclic nature of the regeneration of the oxidant leads to accumulation of metals, sulfate and increasing acidity.

$$FeS_2 + 14Fe^{3+} + 8H_2O \rightarrow 15Fe^{2+} + 2SO_4^{2-} + 16H^+ \qquad (1\text{-}1)$$

$$FeS_2 + 3.5O_2 + H_2O \rightarrow Fe^{2+} + 2SO_4^{2-} + 2H^+ \qquad (1\text{-}2)$$

$$Fe^{3+} + 3H_2O \leftrightarrow Fe(OH)_3 + 3H^+ \quad (1\text{-}3)$$

$$4Fe^{2+} + O_2 + 4H^+ \rightarrow 4Fe^{3+} + 2H_2O \quad (1\text{-}4)$$

The above sulfide representation is for the dominant form, pyrite. Other sulfide minerals such as arsenopyrite, marcasite, and pyrrhotite also undergo similar types of reactions. The dissolution of minerals such as calcite, and dolomite can affect AMD by consuming acidity and precipitating the oxidant ferric iron as shown in equation 1-5 (Stromberg and Banwart, 1999; Dopson *et al.*, 2009). Aluminum and ferric hydroxide species can also provide pH buffering. This is important as the pH affects the activity of ferric iron and that of the acidophilic iron oxidizers.

$$CaCO_3 + 2H^+ \leftrightarrow Ca^{2+} + CO_2 + H_2O \quad (1\text{-}5)$$

The interaction of sulfide mineral dissolution products with metals released from sulfide oxidation can result in secondary minerals such as jarosite and gypsum.

1.3.2 Biology

Microorganisms are very important in the cyclic nature of AMD formation. Their importance is mainly below pH 4. At this low pH, the bulk of the oxidation of ferrous iron and sulfate species take place by acidophilic autotrophic microorganisms. Autotrophic iron oxidizing organisms use the ferrous iron as an electron donor while using oxygen as the terminal electron acceptor. *A.ferrooxidans*, *L.ferrooxidans and A.thioxidans* are the most abundant iron oxidizers isolated from waste rock piles. Studies have shown *L.ferrooxidans* to have a lower pH optimum at pH (1.5-2.0), while *A.ferrooxidans* has an optimum of pH 2.5-3.0 (Coram and Rawlings, 2002; Meruane and Vargas, 2003). Some strains close to *L.ferrooxidans* have been shown to fix

nitrogen (Tyson *et al.*, 2005). Studies have shown the attachment of iron oxidizing bacteria to sulfide surfaces using biofilm (Gehrke *et al.*, 1998). These bacteria have been shown to excrete molecules that concentrate ferric iron within the biofilm. The microenvironments are thought to increase the rate of sulfide oxidation significantly, thus increasing the release of ferrous iron.

Heterotrophic organisms are also present in AMD environments. Research has indicated that these organisms mainly thrive from the microbial products excreted by the autotrophic iron and sulfur oxidizing organisms (Johnson and Hallberg, 2003). This can be considered a mutualistic relationship as some of these products have been shown to inhibit the growth of iron oxidizing organisms (Johnson and Hallberg, 2003). Acidophilic heterotrophs such as *Acidiphilium cryptum , Acidiphilium* SJH, and *Acidiphilium acidophilum* have all been shown to reduce soluble and precipitated ferric iron forms under different conditions of pH, and oxygen (Bridge and Johnson, 2000; Johnson and Bridge, 2002; Kusel *et al.*, 2002). Bilgin et al. (2005) has shown that the initial pH influences the microbial reduction of the ferric-hydroxide species present and the pH increase resulting from the reduction. Microbial iron reduction has thus important implications on the rate of sulfide oxidation. Few reports of low pH microbial sulfate reduction exist in the literature. Although not studied widely, acidophilic eukaryotes have been identified in mining waste (Gross and Robbins, 2000; Baker *et al.*, 2009; Das *et al.*, 2009) and may be more important than previously thought.

1.3.3 Physical space for reaction

Iron and sulfur oxidizers in a waste rock pile can either grow inside the pores of rocks, or in the bulk liquid. Waste rock piles that contain fine tailings size material have more porous

zones allowing bulk liquid to better saturate this fine material. In waste rock piles with little or no fines, bulk liquid flow can be dominated by film flow over waste rock surfaces. The dependence of Iron and sulfur oxidizers on the sulfide oxidation product, ferrous iron, creates an advantage for the microorganisms to attach themselves to sulfide surfaces. This is in addition to other advantages common to all attached growing microorganisms.

As aerobic organisms, the ability to obtain dissolved oxygen will dictate how deep iron and sulfur oxidizers can grow inside a rock pore. In large rock piles, other than the convection of oxygen gas, an inflow of freshly oxygenated water will influence where the microorganisms are most abundantly present within a pile. This is particularly important as the unsaturated flow in a pile will have preferential flow with uneven distribution throughout the pile. In some cases a limitation of a CO_2 source may impact the distribution of the autotrophic organisms. Rocks with more carbonate minerals can provide dissolved inorganic carbon species and thus may be more colonized.

The residence time of rock pore and bulk liquid can correspond to an accumulation of more ferric iron as a result of reactant and product build up. This increased concentration is also associated with higher sulfide oxidation rate, which in turn produces more ferrous iron and sulfate species for iron and sulfur oxidizers. Thus the cyclic nature of AMD is affected by the residence time of the liquid present in contact with the sulfide mineral.

1.3.4 Hydrology and transport

It is important to understand the transport of liquid through a waste rock pile to understand the generation of AMD as well as the transport of the drainage to the environment.

The far from uniform flow of liquid through an unsaturated waste rock pile affects the critical residence time of the liquid at the sulfide interface as well as the availability of oxygen to iron and sulfur oxidizers. It also affects the exchange of the sulfide reaction products among rock pore liquid, bulk film liquid, and matrix liquid through diffusion and advection within a pile.

The level of water saturation of waste rocks in a pile depends on factors such as the amount and duration of liquid precipitation (rain), the snow melt duration and amount, the physical make-up of the pile and evaporation. Evaporation in turn depends on the humidity level in a pile, solar insolation, and the ambient temperature of the location where the pile is in (Carey *et al.*, 2005). A three year study of a mine waste rock pile 5 km south east of Leadville, Colorado and the dead zone surrounding it reported that only during snow melt, typically occurring for about two weeks, did actual drainage out of the pile occur with low pH. For the rest of the year there was no significant drainage leaving the pile because the precipitation the pile received was being absorbed into the soil and rock pores (Vaughn *et al.*, 1999).

NOAA data from a Leadville CO weather station was used to make a hydrograph by calculating a 32 year (1977 to 2008) average monthly snow fall and rain precipitation (Figure 1-1). Based on a daily snow depth data, the snow accumulation from October through May was assumed to melt in April and May. The hydrograph shows that for a significant portion of a year, liquid input to a pile is about an eighth of the peak liquid input occurring during snow melt. The hydrograph is shown as a general trend for waste piles found in mountainous temperate climates. Depending on where a waste rock pile is located, the hydrograph will greatly depend on the local climate.

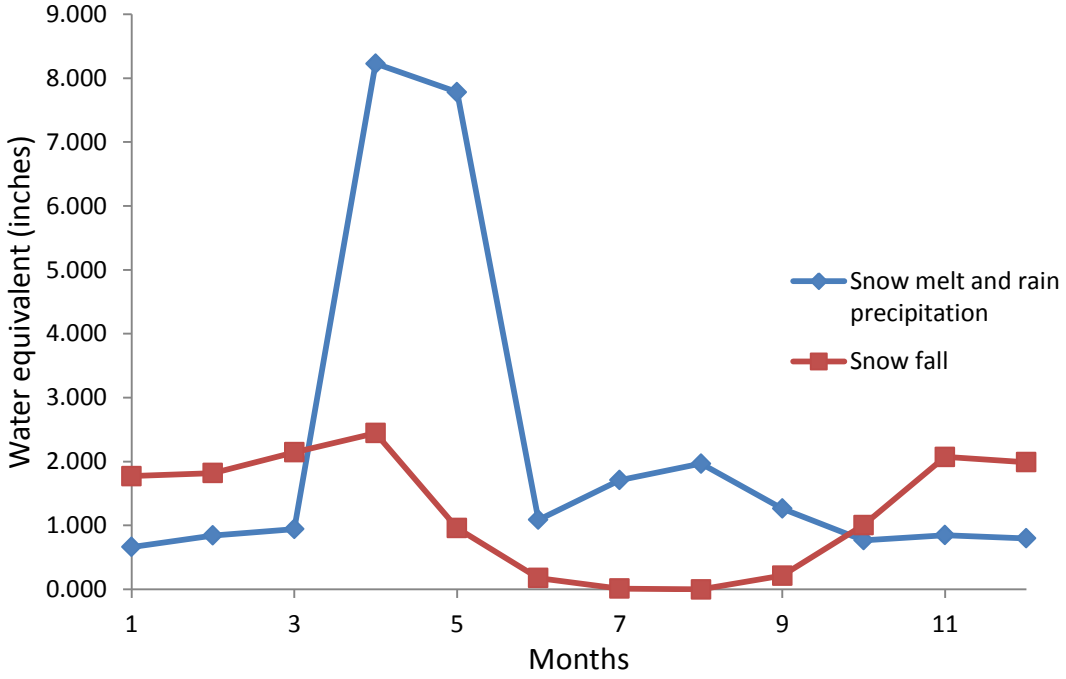

Figure 1-1. Hydrograph for Leadville, CO. Graph was developed from 32 year of average monthly snow fall, rain precipitation, and daily snow depth data.

Nichol et al. (2005) showed that during the wet times of a waste rock pile, the initial drainage from the pile appeared 2 to 12 hours following a large rainfall event. On the other hand, it took days to weeks for the initial spring snow melt drainage to appear following dry season of a pile. This indicates that the snow melt may have first filled some of the pore spaces in the individual rocks before starting to flow out of the pile. Liquid transport inside an unsaturated pile follows preferential flow paths which change over time and whose flow rates vary up to an order of magnitude (Nichol *et al.*, 2005; Tokunaga *et al.*, 2005; Stockwell *et al.*, 2006). The average residence time of the preferential flow streams in the pile will be higher during dry times of the pile than the wet times as the flow rates of these preferential paths decrease during dry times (Nichol *et al.*, 2005).

1.3.5 Putting it together

The formation of AMD from a waste rock pile thus depends on a lot of factors. The main steps of AMD generation are the sulfide oxidation and the ferrous to ferric iron oxidation. In rate comparisons of laboratory experiments it has been shown that the oxidation of sulfide is usually the rate limiting step (Blowes *et al.*, 2003). In field conditions the rate of AMD formation is much less predictable. The sulfide content of rocks, the sizes of rocks, and the porosity of rocks control the available reactive sulfide surface area. The local pH is affected by microbial activity, mineralogy, and hydrology. Ferric iron oxidant concentration is influenced by factors such as microbial activity, local pH, saturation and dissolution of ferric iron minerals, and liquid residence time. The microbial activity is dependent upon local pH, ferrous iron availability, and dissolved oxygen. The transport of oxygen happens through advection and diffusion from a liquid and gas phase to the bulk, film, and rock pore liquid. This transport is in turn influenced by hydrology, individual rock sizes, porosities, water saturation, mineralogy, and physical arrangement. Indeed, it is a very complex system.

Apart from the effect of local liquid residence times on ferric iron concentration and sulfide oxidation, a buildup of reaction products can occur as the bulk liquid progresses along a flow path. Local evaporation within a waste rock pile can lead to evaporation and solidification of metal and iron sulfate minerals. These solid phases can then be dissolved and possibly transported out of the pile during a wet season (Gilchrist *et al.*, 2009).

1.4 Current AMD prevention and remediation techniques

Most commonly used AMD prevention techniques focus on preventing oxygen and/or water from reaching the reactive areas of the mine waste. These include flooding or sealing of underground mines, storage in sealed waste heaps, capping the base of waste rock piles and placing a cover over waste rock piles (Yanful and Orlandea, 2000; Kyhn and Elberling, 2001; Johnson and Hallberg, 2005; Huang *et al.*, 2008). The success of the above mentioned techniques depends on a number of factors such as physical properties of the pile, the sulfide content and the mineralogy of the waste. Other prevention methods being researched include: coating of the sulfide surface with phosphate and hydrogen peroxide (Huang and Evangelou, 1994), addition of anionic surfactants and organic acids to inhibit iron oxidizing organisms and mixing of mine waste with alkaline materials.

AMD preventative practices above work better for newly designed waste rock piles as they require disturbance of the pile such as placing the rocks under water, removing and replacing parts of the pile, and forming structures that can minimize oxygen and water from entering the interior of the pile. For the numerous abandoned waste rock piles implementation of the above preventative methods will involve expensive moving and construction techniques and thus may not be a realistic solution.

AMD remediation techniques treat AMD once it has formed and mainly work with neutralization of the waste and formation of precipitates; sulfate and iron reduction reactions consume protons and form hydrogen sulfide which precipitates heavy metals (Lindsay *et al.*, 2008). Chemicals such as calcium oxide, calcium carbonate, sodium carbonate and sodium

hydroxide have been used for the purpose of neutralization of the waste while chemical oxidants such as hydrogen peroxide are added to oxidize ferrous iron (Johnson and Hallberg, 2005). Neutralization of the waste and oxidation of the ferrous iron is followed up by ferric oxide based precipitate formation which contains the metals in the AMD.

The other method designed to treat AMD with relatively neutral pH (5 and above) that uses the precipitation of hydroxide and other mineral precipitates with metals is done by using aerobic wetlands. Aerobic wetlands are usually constructed to have shallow depth to allow enough oxygenation of the liquid to promote oxidation of ferrous iron. Anaerobic wetlands use sulfate reducing bacteria (SRBs) and iron reducing bacteria (IRBs) to generate alkalinity and sulfide. Locally found organic substrates are usually used as a substrate for the organisms. Permeable reactive barriers are used to treat AMD contaminated groundwater and work by utilization of SRBs and IRBs in the presence of an organic carbon source and an alkalinity source such as limestone designed in a way to have enough permeability to allow flow through the barrier (Waybrant *et al.*, 2002; Amos *et al.*, 2004).

Remediation techniques involve collecting and treating the AMD on a continuous basis. They require expenses for construction of the collection system and pumping of the drainage to the treatment site. There is a continuous need for the neutralization chemicals used and has significant sludge disposal costs.

1.5 Organic carbon in mine waste rock piles

Acid mine drainage systems are generally deficient in organic matter content. Rain brings about 1 to 2.5 mg/L of dissolved organic carbon (DOC) content (Thurman, 1985). Snow, the principal form of precipitation in mountain mined sites, can have a DOC content ranging from 0.5 to 5 mg/L (Thurman, 1985). The other source of organic carbon is believed to be the iron and sulfur oxidizing autotrophic community which fix carbon dioxide to produce organic carbon (Schaeffer and Umbreit, 1963; Bond *et al.*, 2000; Tyson *et al.*, 2004; Banfield *et al.*, 2005). Cell lyses is another source.

Iron and sulfur oxidizing organisms have also been shown to excrete organic molecules and acids such as pyruvic acid which have been shown to be poisonous above certain concentrations (Schaeffer and Umbreit, 1963; Borichewski, 1967; Bhatnagar and Singh, 1991). AMD generation experiments done in a waste rock containing tank run in unsaturated conditions by Jenkins (2006) had 25-40 mg/L DOC of which 83% was shown to be degraded by a BDOC test done with *Acidiphilium cryptum*. In comparison a tank run under saturated conditions and which was producing much lower AMD had only 3-5 mg/L DOC. This is an indication that the activity and the amount of iron oxidizing bacteria influence the production of organic carbon.

Autotrophic acidophilic iron oxidizing organisms which are primarily responsible for generating AMD have been shown to have a symbiotic relation with heterotrophic organisms that help them keep the concentration of organic molecules and acids that may potentially be poisonous to them (Borichewski, 1967; Fortin *et al.*, 1996; Marchand and Silverstein, 2003).

Mixed cultures of iron oxidizing and acidophilic heterotrophic organisms grown with and without glucose in a saturated oxygen condition were shown to have higher soluble iron oxidation rate than the pure iron oxidizing organism's culture (Marchand, 2000; Marchand and Silverstein, 2003).

Organic carbon is used as a substrate by heterotrophic organisms which can use oxygen, ferric iron and sulfate as their electron acceptors depending on species, pH and oxygen level in the system. The purpose of soluble microbial products (EPS) produced by IOB is not clear. It is generally known that bacteria are able to control SMP production and gear it to their advantage. Patidar and Tare (2008) showed that SMPs formed by sulfate and manganese reducing bacteria complex Fe, Ni, Zn, and Co in anaerobic degradation of sulfide laden organics. SMP production increased with increasing sulfide content resulting in higher trace metal availability to the microorganisms in the system. Iron reducing bacteria are also known to produce cytochromes to help them exchange electrons with precipitated ferric iron oxides. *Shewanella oneidensis* produces an outer-membrane cytochrome called OmcA which binds to -Fe_2O_3 and exchanges electrons (Eggleston *et al.*, 2008). Some bacteria are also known to produce siderophores which chelate ferric ions and increase their solubility in solution (Hayen and Volmer, 2006).

Iron oxidizing bacteria produce extra polymeric substances (EPS) which they use for a variety of purposes including forming a reaction zone close to a sulfide surface in which very high concentrations of ferric iron are complexed (Gehrke *et al.*, 1998; Gehrke *et al.*, 2001). The high concentration of the sulfide oxidant near the reaction surface increases the rate of sulfide oxidation as this rate positively depends on ferric iron concentration (McKibben and Barnes,

1986; Williamson and Rimstidt, 1994). The attachment of the Iron oxidizing microorganisms in the EPS to the negatively charged sulfide surface is facilitated by the positive charges of the ferric iron in the EPS. EPS of *A.ferrooxidans* grown on iron were shown to be mostly composed of simple sugars (rhamnose, fucose, xylose, mannose, glucose, glucuronic acid) and fatty acids with glucuronic acid shown to complex ferric iron (Gehrke *et al.*, 1998; Gehrke *et al.*, 2001).

1.6 Organic carbon based prevention of AMD

AMD environments are usually characterized by low pH, low organic carbon content and scarce nutrients and thus favor acidophilic chemo lithotrophic organisms such as iron and sulfur oxidizing bacteria to heterotrophic ones. Organic carbon additions to AMD generating systems have been shown to lead to higher pH and reduced soluble metals and sulfate in drainages (Marchand, 2000; Bilgin, 2004; Sturman, 2004; Jenkins, 2006). It has also been shown that iron oxidizing bacteria decrease and heterotrophic organisms capable of reducing iron and sulfur increase during carbon addition and in some of the studies for a limited time afterwards (Sturman, 2004; Jenkins, 2006). The studies have shown that carbon addition has the potential to inhibit AMD months after addition of carbon to the system is stopped (Sturman, 2004; Jenkins, 2006). Carbon addition can potentially be cheaper than the other preventative and remediation methods for waste rock piles if the frequency of carbon addition can be decreased to an economical time frame depending on the particular waste rock pile considered. Possible permanent remediation effects in the form of physical and biogeochemical changes resulting from the carbon addition can decrease the frequency of carbon addition.

Limited research has been done to assess the mechanisms that bring AMD inhibition during carbon addition. Some of the hypotheses for the possible mechanisms are competition for oxygen between iron oxidizing and heterotrophic organisms, complexation of ferric iron with heterotrophic SMPs resulting in reduced ferric iron availability for reaction with sulfide, and coverage of waste rock surface with heterotrophic biofilm thereby decreasing contact

between iron oxidizing bacteria and the reactive surface area of the rock (Johnson, 1995; Marchand and Silverstein, 2002).

The rate of consumption of dissolved oxygen (DO) by heterotrophic organisms depends on their growth kinetics, which will depend on the affinity to and availability of substrate, nutrients, growth factors, and DO. The pH optimum of the microorganisms is also an important factor. Marchand (2000) reported an average DOC consumption rate of 27.9 mg C /L-day in limited oxygen fill and draw pyrite oxidation experiments with *A. acidophilum* and *A. ferrooxidans*. During the experiment higher DOC consumption rates were followed by a significant decrease of DO from the system. In a waste rock pile, DO depletion and resulting competition between iron oxidizing and heterotrophic organisms as a result of carbon addition may be much more significant in the pore space reaction sites that have more diffusion limitations compared to outer surface reactive sites of waste rocks.

Jenkins (2006) reported significant biofilm formation following the addition of organic carbon to waste rock containing tanks. Heterotrophic biofilm can block iron oxidizing microorganism's access to rock surface and pore reaction sites. The biofilm cover can provide additional diffusion resistance to the rock surface and pores potentially affecting transport of oxygen, iron, and sulfur species. Biofilms have also been shown to sorb metals (Ferris *et al.*, 1989).

Marchand (2000) showed decreased pyrite oxidation when doing abiotic experiments with cell free solutions of iron oxidizing and AMD heterotrophic microorganisms. He postulated that this may be because of a possible complexation of ferric iron by SMPs causing it to be less active. He also reported that size exclusion experiments showed that the elution time of up to

62% of the total organic carbon (TOC) detected overlapped with the elution time of ferric iron in the cell free solutions. This is an indication of possible complexation. Depending on the concentration of the SMPs, direct inhibition of the iron oxidizing organisms is possible as some organic acids can potentially disrupt cell membrane functions leading to imbalance of intracellular H^+ (Borichewski, 1967; Bhatnagar and Singh, 1991). The concentration of SMPs is most likely proportional to the amount of utilized organic carbon substrate. Huang *et al.* (2008) showed that the effluent of SMPs in sequencing batch reactors for a biological waste water treatment system was directly proportional to the influent organic carbon. A schematic of the various DOC interactions in a mine waste environment is shown in Figure 1-2.

Iron reduction can contribute to AMD inhibition in a limited oxygen environment by increasing the pH of the system and removing the primary pyrite oxidant (ferric iron). Iron reduction has been shown to occur in the presence organic carbon substrates at pH greater than 3.5 resulting in an increase of pH to about 6 (Bilgin *et al.*, 2004; Bilgin *et al.*, 2005). Sulfate reduction mostly happens at a near neutral pH (Rampinelli *et al.*, 2008) under limited oxygen conditions and results in precipitation of metals and can also contribute to remediation once the system pH increases. Some studies have shown the presence of acid tolerant sulfate reducers active at a pH of 3 (Johnson and Bridge, 2002; Kusel *et al.*, 2002).

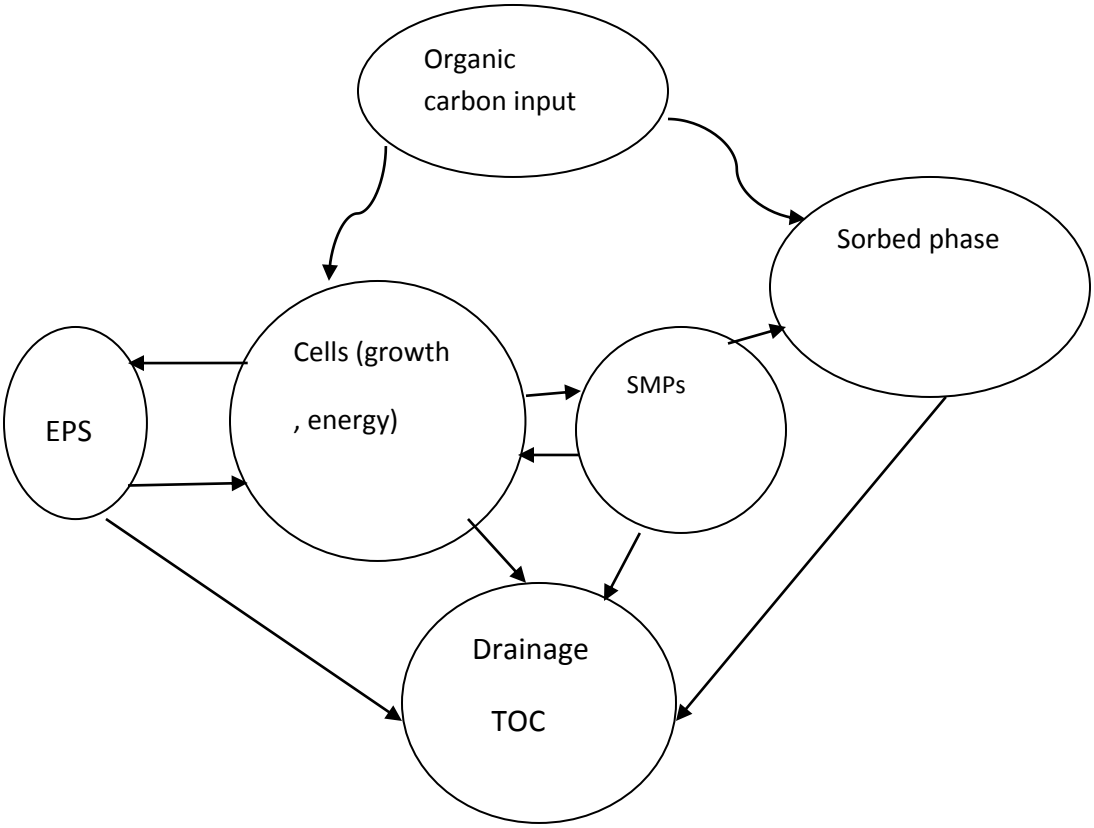

Figure 1-2. DOC interactions in a waste rock pile: The growth of heterotrophic organisms off carbon substrate leads to the formation of EPS and SMPs and can lead to oxygen and nutrient competition and iron and sulfate reduction. Formation of heterotrophic EPS can lead to reactive sulfide site blockage, reduce oxygen diffusion into rock pores and can sorb metals including iron oxides. SMPs can complex ferrous and ferric iron and also serve as a substrate for heterotrophic microorganisms. Some of the organic carbon substrate and produced SMPs can sorb into ferric iron oxide precipitates found on the surface of the waste rocks and in the AMD liquid.

1.7 Research questions

The knowledge about the mechanisms of AMD generation in waste rock piles can provide a basis for designing and evaluating an organic carbon based prevention of AMD. The delivery of an organic carbon source to active reaction sites within a waste rock pile may result in greater preventative effect. The understanding of this requires the knowledge of how pile scale parameters such as unsaturated water flow affect microbial and chemical reactions at the various sulfide liquid interfaces. Many investigations have been done to characterize and investigate big waste rock piles looking at the effect of geochemical and flow characteristics (Stromberg and Banwart, 1994; Tran *et al.*, 2003; Sracek *et al.*, 2004; Stockwell *et al.*, 2006; Azam *et al.*, 2007). However, well designed and controlled laboratory waste rock column experiments to elucidate the effect of rock pore water residence time, liquid flow rate variations, and liquid distribution on the biogeochemical reactions of AMD have not been done.

The understanding of the transformation of an added organic carbon source is needed to quantify and evaluate the preventative effect carbon addition will have on AMD generation. There is only limited information available on the growth of acidophilic heterotrophs in waste rock piles. Few studies have looked at laboratory experiments of pure acidophilic isolates (Bridge and Johnson, 2000; Kusel *et al.*, 2002; Marchand and Silverstein, 2002). Thus there is a need to study the various factors affecting the growth of acidophilic heterotrophs in waste rock environments. The investigation of the utilization of ferric iron and sulfate as terminal electron acceptors by acidophilic heterotrophs during the oxidation of carbon is needed. In waste rock

piles, mineral formations with these ions may complicate these investigations and thus need to be addressed.

Work on soluble microbial products of acidophilic heterotrophs and their interaction with ferric iron is also very limited (Marchand, 2000). The SMPs must be characterized and the conditions of their formation need to be investigated. The various factors that affect organics-ferric interaction have to be studied and resulting pyrite oxidation inhibition has to be quantified. The competition for oxygen expected between acidophilic autotrophs and heterotrophs at the sulfide mineral interface has to also be studied in laboratory and field scale tests.

Another relevant study need is on the various forms of organic carbon sources and their rate of utilization when added to a waste rock pile. Sulfide oxidation in most waste rock piles is considered to be a long term problem on the order of tens of years, if not much more. The duration of an AMD preventative effect with a given dosage of an organic carbon substrate will partly depend on the continued presence of the substrate through a slow release and/or reuse of soluble microbial products. Thus, understanding the transport and storage of soluble microbial products in the bulk and rock pore liquids is important. Another important aspect of the long term prevention effect is the production of heterotrophic biofilms and the coverage of rock surfaces and pores with it. This can result in the decrease of the available reactive sulfide area and cause transport limitations for oxygen and other reaction products. Thus, the various aspects of the production and stability of heterotrophic biofilms have to be studied.

1.8 Research focus

There were three main objectives for this dissertation.

1. The first objective of the dissertation was the growth study of acidophilic waste rock enrichments. The focus was on acidophilic heterotrophs which form the backbone of the proposed strategy of organic carbon induced competitive microbial prevention of AMD. The study was done by quantifying the growth kinetics using a glucose substrate and looking at effects of dissolved oxygen, and pH. Limited domain level population characterization was done.
2. The enhanced growth of acidophilic heterotrophs in mine waste rock environments during the addition of an organic carbon substrate can lead to increased microbial products of both growth and decay origin. The second objective of this dissertation was the investigation of the effect of microbial products of acidophilic heterotrophs on pyrite oxidation by ferric iron. The effect of the growth and lysis derived SMPs on pyrite oxidation was quantified by doing experiments with various concentrations of the organics. A related strategy was the characterization of these microbial products. The focus for the characterization was based on their molecular size and optical (fluorescence) properties. The role of the molecular size of the SMPs on their inhibition of pyrite oxidation was also investigated. The potential for biodegradation of these microbial products and the resulting effect this will have on their interaction with ferric iron was also investigated.

3. The third objective was the investigation of generation of AMD from waste rock packed columns. This investigation was focused on identifying the roles of rock pore liquid chemistry and biology on AMD generation in waste rock piles. The first strategy for this was the measurement of iron, other metals, sulfate and microorganisms in a bulk liquid and rock pore liquid samples obtained from waste rock packed column experiments. The second was quantifying selected rock samples' porosity and water saturation under a given liquid flow rate through waste rock packed columns. The third strategy was the use of a conservative tracer to understand and quantify the transport controls of the bulk and rock pore liquids and the diffusive exchange between them in the columns.

1.9 References

Amos, R. T., Mayer, K. U., Blowes, D. W. and Ptacek, C. J. (2004). Reactive transport modeling of column experiments for the remediation of acid mine drainage. *Environmental Science & Technology* **38**(11): 3131-3138.

Azam, S., Wilson, G. W., Herasymuik, G., Nichol, C. and Barbour, L. S. (2007). Hydrogeological behaviour of an unsaturated waste rock pile: a case study at the Golden Sunlight Mine, Montana, USA. *Bulletin of Engineering Geology and the Environment* **66**(3): 259-268.

Baker, B. J., Tyson, G. W., Goosherst, L. and Banfield, J. F. (2009). Insights into the Diversity of Eukaryotes in Acid Mine Drainage Biofilm Communities. *Applied and Environmental Microbiology* **75**(7): 2192-2199.

Banfield, J. F., Verberkmoes, N. C., Hettich, R. L. and Thelen, M. P. (2005). Proteogenomic approaches for the molecular characterization of natural microbial communities. *Omics-a Journal of Integrative Biology* **9**(4): 301-333.

Bhatnagar, M. and Singh, G. (1991). Growth-inhibition and leakage of cellular material from thiobacillus-ferrooxidans by organic-compounds. *Journal of Environmental Biology* **12**(4): 385-399.

Bilgin, A. A. (2004). Enhancement of bacterial iron respiration as a means to inhibit acid mine drainage. Ph.D. thesis. *University of Colorado.*

Bilgin, A. A., Silverstein, J. and Hernandez, M. (2005). Effects of soluble ferri - Hydroxide complexes on microbial neutralization of acid mine drainage. *Environmental Science & Technology* **39**(20): 7826-7832.

Bilgin, A. A., Silverstein, J. and Jenkins, J. D. (2004). Iron respiration by Acidiphilium cryptum at pH 5. *Fems Microbiology Ecology* **49**(1): 137-143.

BLM. (2011). "http://www.blm.gov/wo/st/en/prog/more/Abandoned_Mine_Lands/abandoned_mine_site.html" Feb 2011. Retrieved 2/12, 2012. Bureau of Land Management.

Blowes , D. W., Ptacek , C. J., Jambor , J. L. and Weisener , C. G. (2003). The geochemistry of acid mine drainage. *Treatise on geochemistry*. B. S. Lollar. Toronto, Canada., *Elsevier*. **9:** 149-204.

Bond, P. L., Smriga, S. P. and Banfield, J. F. (2000). Phylogeny of microorganisms populating a thick, subaerial, predominantly lithotrophic biofilm at an extreme acid mine drainage site. *Applied and Environmental Microbiology* **66**(9): 3842-3849.

Borichewski, R.M. (1967). Keto acids as growth-limiting factors in autotrophic growth of thiobacillus thiooxidans. *Journal of Bacteriology* **93**(2): 597-&.

Bridge, T. A. M. and Johnson, D. B. (2000). Reductive dissolution of ferric iron minerals by Acidiphilium SJH. *Geomicrobiology Journal* **17**(3): 193-206.

Brothers, L. A., Engel, M. H. and Elmore, R. D. (1996). The late diagenetic conversion of pyrite to magnetite by organically complexed ferric iron. *Chemical Geology* **130**(1-2): 1-14.

Carey, S. K., Barbour, S. L. and Hendry, M. M. (2005). Evaporation from a waste-rock surface, Key Lake, Saskatchewan. *Canadian Geotechnical Journal* **42**(4): 1189-1199.

Coram, N. J. and Rawlings, D. E. (2002). Molecular relationship between two groups of the genus Leptospirillum and the finding that Leptosphillum ferriphilum sp nov dominates South African commercial biooxidation tanks that operate at 40 degrees C. *Applied and Environmental Microbiology* **68**(2): 838-845.

Dalzell, D. J. B. and Macfarlane, N. A. A. (1999). The toxicity of iron to brown trout and effects on the gills: a comparison of two grades of iron sulphate. *Journal of Fish Biology* **55**(2): 301-315.

Das, B. K., Roy, A., Koschorreck, M., Mandal, S. M., Wendt-Potthoff, K. and Bhattacharya, J. (2009). Occurrence and role of algae and fungi in acid mine drainage environment with special reference to metals and sulfate immobilization. *Water Research* **43**(4): 883-894.

Dopson, M., Lovgren, L. and Bostrom, D. (2009). Silicate mineral dissolution in the presence of acidophilic microorganisms: Implications for heap bioleaching. *Hydrometallurgy* **96**(4): 288-293.

Eggleston, C. M., Voros, J., Shi, L., Lower, B. H., Droubay, T. C. and Colberg, P. J. S. (2008). Binding and direct electrochemistry of OmcA, an outer-membrane cytochrome from an iron reducing bacterium, with oxide electrodes: A candidate biofuel cell system. *Inorganica Chimica Acta* **361**(3): 769-777.

Ferris, F. G., Schultze, S., Witten, T. C., Fyfe, W. S. and Beveridge, T. J. (1989). Metal interactions with microbial biofilms in acidic and neutral ph environments. *Applied and Environmental Microbiology* **55**(5): 1249-1257.

Fortin, D., Davis, B. and Beveridge, T. J. (1996). Role of Thiobacillus and sulfate-reducing bacteria in iron biocycling in oxic and acidic mine tailings. *Fems Microbiology Ecology* **21**(1): 11-24.

Gehrke, T., Hallmann, R., Kinzler, K. and Sand, W. (2001). The EPS of Acidithiobacillus ferrooxidans - a model for structure-function relationships of attached bacteria and their physiology. *Water Sci Technol* **43**(6): 159-67.

Gehrke, T., Telegdi, J., Thierry, D. and Sand, W. (1998). Importance of extracellular polymeric substances from Thiobacillus ferrooxidans for bioleaching. *Applied and Environmental Microbiology* **64**(7): 2743-2747.

Gilchrist, S., Gates, A., Szabo, Z. and Lamothe, P. J. (2009). Impact of AMD on water quality in critical watershed in the Hudson River drainage basin: Phillips Mine, Hudson Highlands, New York. *Environmental Geology* **57**(2): 397-409.

Gray, N. F. (1998). Acid mine drainage composition and the implications for its impact on lotic systems. *Water Research* **32**(7): 2122-2134.

Gross, S. and Robbins, E. I. (2000). Acidophilic and acid-tolerant fungi and yeasts. *Hydrobiologia* **433**(1-3): 91-109.

Hayen, H. and Volmer, D. A. (2006). Different iron-chelating properties of pyochelin diastereoisomers revealed by LC/MS. *Analytical and Bioanalytical Chemistry* **385**(3): 606-611.

Herlihy, A. T., Kaufmann, P. R., Mitch, M. E. and Brown, D. D. (1990). Regional estimates of acid-mine drainage impact on streams in the mid-atlantic and southeastern united-states. *Water Air and Soil Pollution* **50**(1-2): 91-107.

Huang, G. T., Jin, G., Wu, J. H. and Liu, Y. D. (2008). Effects of glucose and phenol on soluble microbial products (SMP) in sequencing batch reactor systems. *International Biodeterioration & Biodegradation* **62**(2): 104-108.

Huang, X. and Evangelou, V. P. (1994). Suppression of pyrite oxidation rate by phosphate addition. *Environmental Geochemistry of Sulfide Oxidation* **550**: 562-573.

Jansen, M. and Groman, D. (1993). The Effect of High Concentrations of Iron on Impounded American Lobsters: A Case Study. *Journal of Aquatic Animal Health* **5**(2).

Jenkins, J. D. (2006). Role of flow and organic carbon on acid mine drainage remediation in waste rock. Ph.D. thesis. *University of Colorado***.**

Johnson, D. B. (1995). Acidophilic microbial communities - candidates for bioremediation of acidic mine effluents. *International Biodeterioration & Biodegradation* **35**: 41-58.

Johnson, D. B. and Bridge, T. A. M. (2002). Reduction of ferric iron by acidophilic heterotrophic bacteria: evidence for constitutive and inducible enzyme systems in Acidiphilium spp. *Journal of Applied Microbiology* **92**(2): 315-321.

Johnson, D. B. and Hallberg, K. B. (2003). The microbiology of acidic mine waters. *Research in Microbiology* **154**(7): 466-473.

Johnson, D. B. and Hallberg, K. B. (2005). Acid mine drainage remediation options: a review. *Science of the Total Environment* **338**(1-2): 3-14.

Kusel, K., Roth, U. and Drake, H. L. (2002). Microbial reduction of Fe(III) in the presence of oxygen under low pH conditions. *Environmental Microbiology* **4**(7): 414-421.

Kyhn, C. and Elberling, B. (2001). Frozen cover actions limiting AMD from mine waste deposited on land in Arctic Canada. *Cold Regions Science and Technology* **32**(2-3): 133-142.

Lindsay, M. B. J., Ptacek, C. J., Blowes, D. W. and Gould, W. D. (2008). Zero-valent iron and organic carbon mixtures for remediation of acid mine drainage: Batch experiments. *Applied Geochemistry* **23**(8): 2214-2225.

Lottermoser , B. (2003). Mine wastes: characterization, treatment and environmental impacts. Berlin, Heidelberg, and New York. *Springer*.

Lyon, J. S., Hilliard, T. J. and Bethell, T. N. (1993). Burden of gilt Washington, DC, *Mineral Policy Center*.

Marchand, E. A. (2000). The role of induced heterotrophic microbial growth in mitigating the effects of acid mine drainage. Ph.D. thesis. *University of Colorado.*

Marchand, E. A. and Silverstein, J. (2002). Influence of heterotrophic microbial growth on biological oxidation of pyrite. *Environmental Science & Technology* **36**(24): 5483-5490.

Marchand, E. A. and Silverstein, J. (2003). The role of enhanced heterotrophic bacterial growth on iron oxidation by Acidithiobacillus ferrooxidans. *Geomicrobiology Journal* **20**(3): 231-244.

McKibben, M. A. and Barnes, H. L. (1986). Oxidation of pyrite in low-temperature acidic solutions - rate laws and surface textures. *Geochimica Et Cosmochimica Acta* **50**(7): 1509-1520.

Meruane, G. and Vargas, T. (2003). Bacterial oxidation of ferrous iron by Acidithiobacillus ferrooxidans in the pH range 2.5-7.0. *Hydrometallurgy* **71**(1-2): 149-158.

Nichol, C., Smith, L. and Beckie, R. (2005). Field-scale experiments of unsaturated flow and solute transport in a heterogeneous porous medium. *Water Resources Research* **41**(5).

Nordstrom, D. K. and Alpers, C. N. (1999). Negative pH, efflorescent mineralogy, and consequences for environmental restoration at the Iron Mountain Superfund site, California. *Proceedings of the National Academy of Sciences of the United States of America* **96**(7): 3455-3462.

Patidar, S. K. and Tare, V. (2008). Soluble microbial products formation and their effect on trace metal availability during anaerobic degradation of sulfate laden organics. *Water Science and Technology* **58**(4): 749-755.

Pond, G. J., Passmore, M. E., Borsuk, F. A., Reynolds, L. and Rose, C. J. (2008). Downstream effects of mountaintop coal mining: comparing biological conditions using family- and genus-level macroinvertebrate bioassessment tools. *Journal of the North American Benthological Society* **27**(3): 717-737.

Rampinelli, L. R., Azevedo, R. D., Teixeira, M. C., Guerra-Sa, R. and Leao, V. A. (2008). A sulfate-reducing bacterium with unusual growing capacity in moderately acidic conditions. *Biodegradation* **19**(5): 613-619.

Schaeffer, W. I. and Umbreit, W. W. (1963). Phosphotidylinositol as a wetting agent in sulfur oxidation by thiobacillus thiooxidans. *Journal of Bacteriology* **85**(2): 492-&.

Singer, P. C. and Stumm, W. (1970). Acidic mine drainage . Rate-determining step. *Science* **167**(3921): 1121-&.

Sracek, O., Choquette, M., Gelinas, P., Lefebvre, R. and Nicholson, R. V. (2004). Geochemical characterization of acid mine drainage from a waste rock pile, Mine Doyon, Quebec, Canada. *Journal of Contaminant Hydrology* **69**(1-2): 45-71.

Stockwell, J., Smith, L., Jambor, J. L. and Beckie, R. (2006). The relationship between fluid flow and mineral weathering in heterogeneous unsaturated porous media: A physical and geochemical characterization of a waste-rock pile. *Applied Geochemistry* **21**(8): 1347-1361.

Stromberg, B. and Banwart, S. (1994). Kinetic modeling of geochemical processes at the aitik mining waste rock site in northern sweden. *Applied Geochemistry* **9**(5): 583-595.

Stromberg, B. and Banwart, S. A. (1999). Experimental study of acidity-consuming processes in mining waste rock: some influences of mineralogy and particle size. *Applied Geochemistry* **14**(1): 1-16.

Sturman, P. J. (2004). Control of acid rock drainage from mine tailings through the addition of dissolved organic carbon. Ph.D. thesis. Montana State University.

Thurman, E. M. (1985). Organic geochemistry of natural waters. Dordrecht; Hingham; Boston, MA, USA, *Kluwer Academic*.

Tokunaga, T. K., Olson, K. R. and Wan, J. M. (2005). Infiltration flux distributions in unsaturated rock deposits and their potential implications for fractured rock formations. *Geophysical Research Letters* **32**(5).

Tran, A. B., Miller, S., Williams, D. J., Fines, P. and Wilson, G. W. (2003). Geochemical and mineralogical characterisation of twocontrasting waste rock dumps – the INAP waste rock dumpcharacterization project. 6th International Conference onAcid Rock Drainage, *Austral. Inst. Mining Metall. Publ. Ser***:** 939–948.

Tyson, G. W., Chapman, J., Hugenholtz, P., Allen, E. E., Ram, R. J., Richardson, P. M., Solovyev, V. V., Rubin, E. M., Rokhsar, D. S. and Banfield, J. F. (2004). Community structure and metabolism through reconstruction of microbial genomes from the environment. *Nature* **428**(6978): 37-43.

Tyson, G. W., Lo, I., Baker, B. J., Allen, E. E., Hugenholtz, P. and Banfield, J. F. (2005). Genome-directed isolation of the key nitrogen fixer Leptospirillum ferrodiazotrophum sp nov from an acidophilic microbial community. *Applied and Environmental Microbiology* **71**(10): 6319-6324.

Vaughn, R. B., Stanton, M. R. and Horton, R. J. (1999). A year in the life of a mine dump: A diachronic case study. *Tailings and Mine Waste'99*, Balkema.

Warner , R. (1971). Distribution of Biota in a Stream Polluted by Acid Mine-Drainage *ohio journal of science* **71**: 202-215.

Waybrant, K. R., Ptacek, C. J. and Blowes, D. W. (2002). Treatment of mine drainage using permeable reactive barriers: Column experiments. *Environmental Science & Technology* **36**(6): 1349-1356.

Williamson, M. A. and Rimstidt, J. D. (1994). The kinetics and electrochemical rate-determining step of aqueous pyrite oxidation. *Geochimica Et Cosmochimica Acta* **58**(24): 5443-5454.

Yanful, E. K. and Orlandea, M. P. (2000). Controlling acid drainage in a pyritic mine waste rock. Part II: Geochemistry of drainage. *Water Air and Soil Pollution* **124**(3-4): 259-284.

CHAPTER 2. THE GROWTH KINETICS OF HETEROTROPHIC MINE WASTE ROCK ENRICHMENTS ON GLUCOSE: THE EFFECT OF PH AND DISSOLVED OXYGEN

Abstract

The addition of an organic carbon source to mine waste can stimulate native heterotrophic organisms and create a competition with iron oxidizing organisms for oxygen and attachment sites resulting in passivation of acid mine drainage. There is a need to study the growth of native acidophilic heterotrophic organisms on organic carbon substrates and quantify the effect of environmental factors such as pH and dissolved oxygen (DO) on the growth. Mine waste rock enrichments were grown in batch flasks containing glucose as substrate, supplemental yeast extract and mineral media. The effect of DO and pH on the growth was studied. Phospholipid fatty acid analysis was done on the enrichments to get domain level compositional information. The enrichments consumed glucose at a specific growth rate of 0.13 hr^{-1} and had a yield of 0.51 g dry cells/ g glucose. The half saturation constant for oxygen was found to be 0.11 mg/l. They were able to grow from pH 1.5 to 6.0. Nearly half of the active enrichments were shown to be of eukaryotic origin. The study shows the presence of AMD organisms capable of metabolizing simple sugars under low pH conditions and points to the need for studying the metabolism of various locally found organic carbon substrates by acidophilic heterotrophic enrichments.

2.1 Introduction

Acidophilic heterotrophic organisms have been detected since the early 1980's in mine and mine waste samples (Harrison, 1981; Berthelot *et al.*, 1993). The major source of organic carbon in mining waste environments is the CO_2 fixation by iron and sulfur oxidizing organisms (Baker and Banfield, 2003; Johnson and Hallberg, 2009). Heterotrophic organisms in acidic waters are believed to play a pivotal role in acid mine drainage (AMD) generation by consuming low molecular weight aliphatic and carboxylic acid compounds that could otherwise be toxic to the autotrophic consortia (Bhatnagar and Singh, 1991; Johnson, 1995; Baker and Banfield, 2003). The low pH, heavy metal loading and low energy sources have limited AMD microorganisms to a handful of species (Baker and Banfield, 2003).

Nearly all heterotrophic organisms detected in AMD environments are able to utilize oxygen as an electron acceptor (Baker and Banfield, 2003). However, due to the abundance of ferric iron at a pH below 3.0, ferric iron reduction is also an important process (Marchand and Silverstein, 2003; Bilgin *et al.*, 2005). The redox potential of ferric/ferrous iron couple is very close to the oxygen/water couple below pH 2 (Bridge and Johnson, 2000; Johnson and Bridge, 2002). Johnson and McGinness (1991) showed that about 20 of 50 aerobic acidophilic heterotrophic strains tested were able to reduce ferric iron. The ability to reduce ferric iron has been seen to be unaffected by the level of dissolved oxygen (DO) in *Acidiphilium SJH*, while it was very important in the case of *A. acidophilum* (Johnson and Bridge, 2002) . *Acidiphilium cryptum* JF-5 was shown to reduce ferric iron at pH 3 from both soluble and precipitated forms with the reduction dependent on the level of oxygen (Kusel *et al.*, 2002).

At circum-neutral and higher pHs more sulfate reducers are present (Bilgin *et al.*, 2007; Johnson and Hallberg, 2009). AMD environments contain high concentrations of sulfate and at higher pHs, precipitation of ferric iron may reduce the concentration enough to allow sulfate to be the preferred electron acceptor. Lu *et al.* (2011) have shown however the presence of low pH acidophilic organisms coupling organic carbon oxidation with sulfate reduction. They showed that significant reduction of sulfate occurred at pH 2. Sulfate reducers have also been cultured from tailing pore liquid samples of pH 3-4 (Fortin *et al.*, 1996). They however were not able to grow them at low pH in laboratory and hypothesized that they may be thriving in reduced and more neutral pH microenvironments.

Prevention of AMD generation through the addition of organic carbon sources to mine waste has been proposed to result in biogeochemical changes such as the competition for dissolved oxygen and attachment sites between iron oxidizing organisms and acidophilic heterotrophs (Marchand and Silverstein, 2002; Marchand and Silverstein, 2003; Jenkins, 2006; Johnson *et al.*, 2008). It has also been shown that carbon addition could result in sulfate and ferric iron reduction resulting in pH increase and minimization of the sulfide oxidant, ferric iron (Bilgin *et al.*, 2005; Bilgin *et al.*, 2007). Since the acidophilic heterotrophic consortia in a mine waste are carbon limited, the addition of an external carbon source will initiate metabolization.

Depending on the levels of pH and DO in mine waste microenvironments, the electron acceptors may be oxygen, ferric iron or sulfate. In terms of preventing AMD, the consumption of oxygen by acidophilic heterotrophs is an important consideration as most iron oxidizers are strictly aerobic. In addition, the reduction of ferric iron can benefit remediation by removing the dominant low pH sulfide oxidant. The production of soluble microbial products (SMPs) and

extra polymeric substances (EPS) can result in reduction of the activity of ferric iron and the covering of reactive sulfide surfaces respectively (Marchand and Silverstein, 2002). Understanding the kinetics of organic carbon substrate utilization and the associated effect of pH and DO on growth is important to quantify the remediation effect of a carbon substrate in a mine waste. It is also important to investigate the occurrence and kinetics of ferric and sulfate reduction and the geochemical conditions that influence it. Coupled with other studies, the growth kinetics can help quantify the consumption of DO and the production SMPs and EPS.

Model AMD organism/organisms can be used to study the microbial utilization of an organic carbon substrate. However, identifying the right model organism is a challenge. It has been previously shown that pure strains like *A. ferrooxidans* and *Acidiphilium cryptum* commonly believed to be prevalent and studied in detail were not an important constituent of some AMD environmental enrichments (Edwards *et al.*, 1999; Jenkins, 2006). An alternative approach is to use environmental enrichments to study the kinetics of growth and substrate metabolization and the various factors affecting it. This also provides an advantage of being more relevant to the specific mine waste of remediation interest. This study used environmental enrichments from a mine waste rock pile near Leadville, Colorado to quantify the growth kinetics using glucose as substrate. The effect of pH and DO on growth was also investigated. Phospholipid fatty acid analysis was performed to get insights into the domain level composition of the consortium.

2.2 Materials and Methods

2.2.1 Enrichment of cultures

Mine waste rocks from an abandoned pile near Leadville, CO were immersed in water and aerated to establish an active culture. Part of this solution was then added into a pH 3.0 solution composed of 1 g/l glucose, 0.10 g/l yeast extract and mineral media comprising of 2.0 g/l $(NH_4)_2SO_4$, 0.1 g/l KCl, 0.5 g/l K_2HPO_4, and 0.5 g/l $MgSO_4.7H_2O$. pH adjustments were made using 3N trace metal grade HCl. Enrichments were undertaken in 250 ml Erlenmeyer flasks covered with cheese cloth and put on an orbital shaker set at 125 rpm. Sterile techniques were followed throughout the experiment. These enrichments were used as inoculant for subsequent experiments. An assay of phospholipid fatty acid analysis (Microbial Insights Inc., Knoxville, TN) was done on one batch of the enrichment for an active biomass count and domain level characterization.

2.2.2 Limited glucose growth

Glucose limited experiments were done using 1.7 g/l glucose and 0.2 g/l yeast extract added to the mineral solution described above at pH 3.0. Cultures were twice transferred in to the media to keep them at exponential phase. The third time transfer was used for the actual experiment. Experiments were done in duplicate 250 ml flasks covered with cheese cloth and put on an orbital shaker set at 125 rpm. Samples were analyzed for glucose concentration, initial and final pH, optical density and dry cell weight content. Initial and final samples were also used to do microbial enumeration using the most probable number assay (MPN). The

media described above with 50 g/l resazurin was incubated in serial dilutions in an 8 by 12 well micro plate. The change of resazurin from a pink color to colorless was used to identify growth wells and the MPN was estimated using a statistical table (Rowe *et al.*, 1977).

A separate of line of cultures were grown on glucose and mineral solution without yeast extract. This was done to assess the ability of the enrichments to grow without a supplemental complex media.

2.2.3 pH effect on growth

5 g/l glucose and 0.5 g/l yeast extract were added to the mineral solution described above at pH 3.0. Cultures were twice transferred in to the media to keep them at exponential phase. Mineral media solution at various pHs was prepared (1.0), (1.5), (2.0), (2.5), and (3.0) by using 1N HCl. Thereafter, the exponential phase inoculant was filtered, rinsed and suspended in each of the different pH mineral media solutions described above and used as an inoculant. A 10% by volume inoculant was used. Flasks containing the experimental solution were covered with cheese cloth and put on an orbital shaker set at 125 rpm. Samples were taken to measure pH, glucose concentration, and optical density.

The effect of higher pH on the growth of the consortium was checked by growing a buffered pH 6 culture along with a control at pH 3. The same exponential phase culture used for the pH 1.0-3.0 experiments was used. The media used was 1 g/l glucose and 0.1 g/l yeast extract and the same mineral media used throughout the study with the exception of an increased KH_2PO_4 concentration, 12.2 g/l, adjusted to pH 3 and 6. The inoculant was rinsed and suspended in the respective media.

2.2.4 Limited DO growth

A biological oxygen demand test (BOD) bottle was filled with 1.0 g/l glucose, 0.1 g/l yeast extract substrate and previously described mineral media solution at pH 3.0. A 10% by volume exponential phase inoculum was used. A YSI DO probe was fitted to the BOD bottle and the consumption of the DO was recorded while the BOD bottle contents were continuously mixed using a magnetic stirrer.

2.2.5 Analytical methods

Glucose was measured using a YSI 2700 select membrane biochemistry analyzer. pH was measured using an Accumet combination electrode and meter. DO was measured using a YSI 5905 bod probe and meter. The dissolved oxygen data was exported to a computer every second using minicom terminal software through a data cable connected with the YSI DO meter. Optical density measurements were done at 540 nm using a Hach DR2000 direct reading spectrometer. Nylon filters used for cell mass density measurements were of size 0.22 µm and were rinsed, oven dried (105 degree C) for 24 hours and kept at a room temperature in a desiccator prior to use. Following filtration of a known amount of culture liquid, filters were again dried in 105 degree c for 24 hours and allowed to cool in a desiccator and weighed.

2.2.6 Monod modeling

The acidophilic heterotrophic growth was quantified by assuming growth limitations to result from glucose substrate, dissolved oxygen, and pH. The reduction of the maximum specific growth rate, μ_m (1/hr) can be modeled as being affected by the lowest limitation factor

(glucose, dissolved oxygen or pH) or an interaction of these three limiting factors (equation 2-1).

The glucose concentration and cell mass density data from the limited glucose growth experiments was used to model the growth parameters using the equations 2-1 and 2-3.

$$\frac{dS}{dt} = \mu_m \frac{X}{Y} * \min or\ product\ of\ (\frac{S}{Ks+S}, \frac{DO}{K_{DO}+DO}, f(pH)) \quad \text{.....(2-1)}$$

$$\frac{dX}{dt} = \mu_m X \frac{S}{Ks+S} \qquad \text{(2-2)}$$

$$\frac{dS}{dt} = \mu_m \frac{X}{Y} \frac{S}{Ks+S} \qquad \text{(2-3)}$$

Where S is glucose concentration (g/l), X is concentration of dry cells in g/l, μ_m is maximum specific growth rate (1/hr), Y is cellular yield per unit mass of substrate (g dry cells/ g glucose), Ks is half saturation constant of glucose (g/l), DO is dissolved oxygen concentration (mg/l), K_{DO} is oxygen half saturation constant (mg/l), and $f(pH)$ is the relative activity at a given pH.

Equation 2-2 and 2-3 were coupled and solved by numerically integrating them in Matlab. A Matlab nonlinear least squares regression function was used to find the parameters μ_m, Y and Ks (Andre *et al.*, 2009).

The analysis of the oxygen depletion data was undertaken by assuming a no growth Monod model as shown in equation (2-4). The term Q= $\frac{\mu_m Xo}{Y_o}$, is the specific oxygen uptake rate in mg/l-hr DO and was solved for along with K_{DO}.

$$\frac{dDO}{dt} = \frac{\mu_m Xo}{Y_O} \frac{DO}{K_{DO} + DO} \qquad \text{(2-4)}$$

DO is the dissolved oxygen concentration in mg/l, and K_{DO} is the half saturation constant of oxygen in mg/l. Xo is the initial biomass in dry cells (mg/l) and Yo is the dry cellular yield for dissolved oxygen in mg dry cell /mg dissolved oxygen.

2.3 Results and Discussion

2.3.1 Limited glucose growth

The consortium degraded the 1.7 g/l glucose in just over 24 hours (Figure 2-1). The optical density increased from 0.1 to about 0.9. From the cell weight data, a yield of 0.51 g dry cell mass/g glucose was calculated. The linear relationship established between the dry cell weight concentration and the optical density (Figure 2-2) was used to generate dry cell mass densities to be used as a modeling data for all optical density readings. A pH drop from an initial value of 3.2 to 2.54 occurred over the span of the glucose consumption. The steepness of the pH drop was directly proportional to the rate of consumption of glucose. This suggests that it could be because of the dissolution of acidic metabolization end products such as carbon dioxide or the consumption of ammonia from the salt media during growth (Gemmell and Knowles, 2000). The average initial and final MPNs obtained were $2.62*10^6 \pm 1.10*10^6$ and $2.98*10^7 \pm 1.65*10^7$ respectively. Monod kinetic model best fit for the glucose limited growth data gave a μ_m of 0.13 ± 0.01 (1/hr), K_s of 0.22 ± 0.12 g/l glucose, and a yield Y of 0.52 ± 0.02 g dry cells/ g glucose (Figure 2-3). The margins of error represent the 95% confidence interval around the parameters. The obtained μ_m of 0.13 (1/hr) was much higher than a previous study done on the glucose consumption of *Acidiphilum cryptum*. Andre and Stroncek (2008) performed glucose growth experiments using *Acidiphilum cryptum* at 35^oC and they calculated a μ_m of 0.05 (1/hr). This is in fact further evidence that *Acidiphilum cryptum* is not a good AMD model heterotrophic organism. Another study of the glucose kinetics by the facultative autotroph *Thiobacilus acidophilus* revealed a μ_m of 0.084 (1/hr) (Pronk *et al.*, 1990).

The culture lines grown without yeast extract were also able to grow without any issues for multiple transfers. The time frame it took for an exponential phase culture to consume a given glucose concentration media without yeast extract was similar to the media containing yeast extract, with the difference being less than 2 hours out of a generally 24 hour growth period. This suggests supplemental complex media is not necessarily required to support the growth of these enrichments.

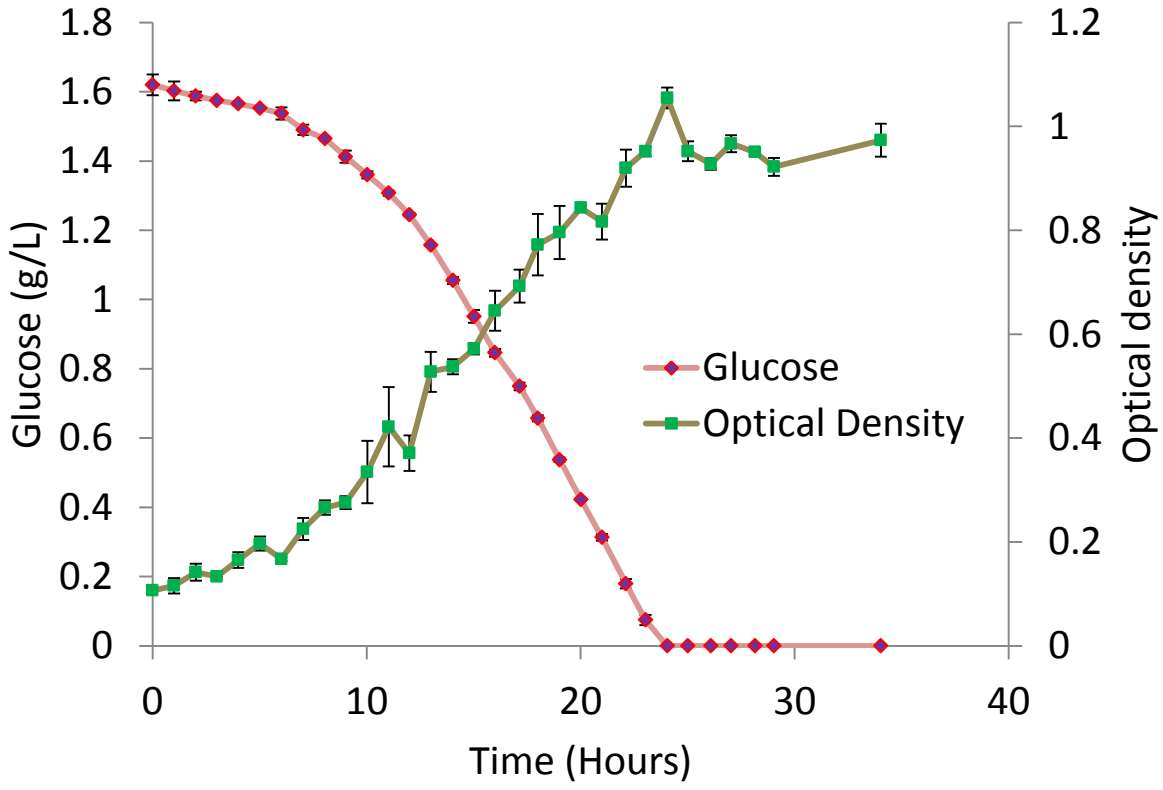

Figure 2-1. Mineral media containing 1.7 g/l glucose and 0.2 g/l yeast extract at a pH of 3.0 was inoculated with an exponential phase culture obtained from mine waste rock enrichments. Substrate depletion was tracked by measuring the glucose concentration and the biomass growth monitored by reading the optical density at 510 nm in a direct reading spectrophotometer. Error bars indicate the difference of the measurements for duplicate experiments from the average measurements (n=2).

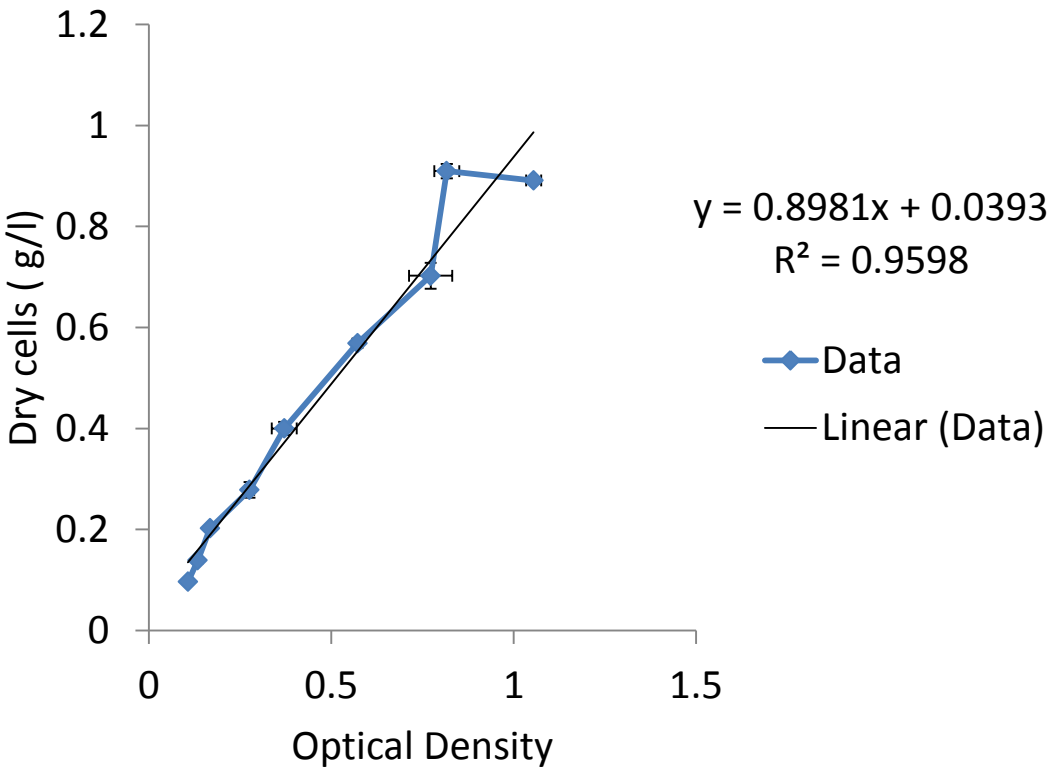

Figure 2-2. A calibration curve for converting optical density to dry cell mass density was obtained from selected samples within the growth phase of an experiment. Culture liquid samples were filtered through pre dried 0.22 um syringe nylon filters followed by drying and weighing to determine the cell mass density. Optical density was measured at 510 nm using a direct reading spectrophotometer. Horizontal and vertical error bars indicate the respective difference of the measurements for the duplicate experiments from the average measurements (n=2).

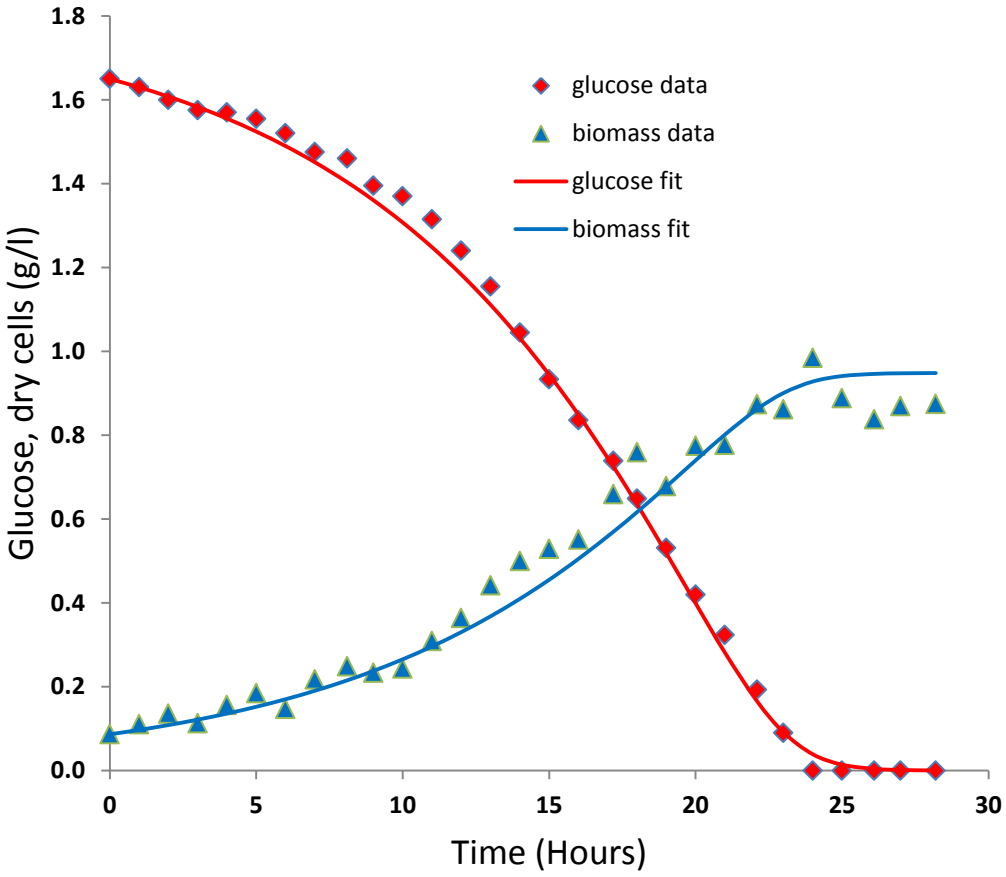

Figure 2-3. Glucose depletion and biomass dry weight increase data from limited glucose growth experiments were fitted to a Monod kinetics model. The modeled parameters were maximum specific growth rate, cellular yield and half saturation constant for glucose. A MATLAB nonlinear least square optimization routine was used to minimize the residuals and obtain the best fit parameters.

2.3.2 Limited DO growth

The initial DO concentration measured following the equilibration of the DO probe was 4.8 mg/l. The oxygen consumption rate initially increased up to a DO concentration of about 3.5 mg/l. After this concentration, the DO consumption appeared to proceed at a constant rate until about 0.33 to 0.37 mg/l DO. Somewhere in between 0.33 and 0.37 mg/l DO, a sharp drop of the oxygen consumption rate occurred. A no growth Monod kinetic model was used to

model the portion of the data with the apparent constant oxygen consumption rate, i.e. below 3.5 mg/l DO. To improve the asymptotic behavior of the chosen model, a factor of 0.2 mg/l DO was added to result of the numerical integration step for $\frac{dDO}{dt}$; this was done before calculation of the residual for the optimization step. The model run gave a half saturation constant, Ko_2 of 0.11 ± 0.05 mg/l DO. The specific oxygen uptake rate, Q was 0.084 ± 0.002 mg/l-hr DO (figure 2-4). Liu *et al.* (1988) has shown that the activity of the iron oxidizer *A. ferrooxidans* gets limited in the range of 0.29-0.7 mg/l DO with growth ceasing at 0.2 mg/l DO. Thus the tested AMD enrichments can limit the activity of certain iron oxidizing organisms as they actually have a comparable or higher dissolved oxygen sensitivity.

Kusel *et al.* (2002) has demonstrated the reduction of ferric iron at 4% oxygen in the gas phase by *Acidiphilum cryptum*. It is thus possible that the environmental consortium can undergo ferric iron reduction along with oxygen respiration as the dissolved oxygen concentration decreases. In waste rock pile applications, this is in fact an advantage as it can allow both the competition for oxygen with iron oxidizing microorganisms as well as limiting the availability of ferric iron as an oxidant of sulfidic minerals.

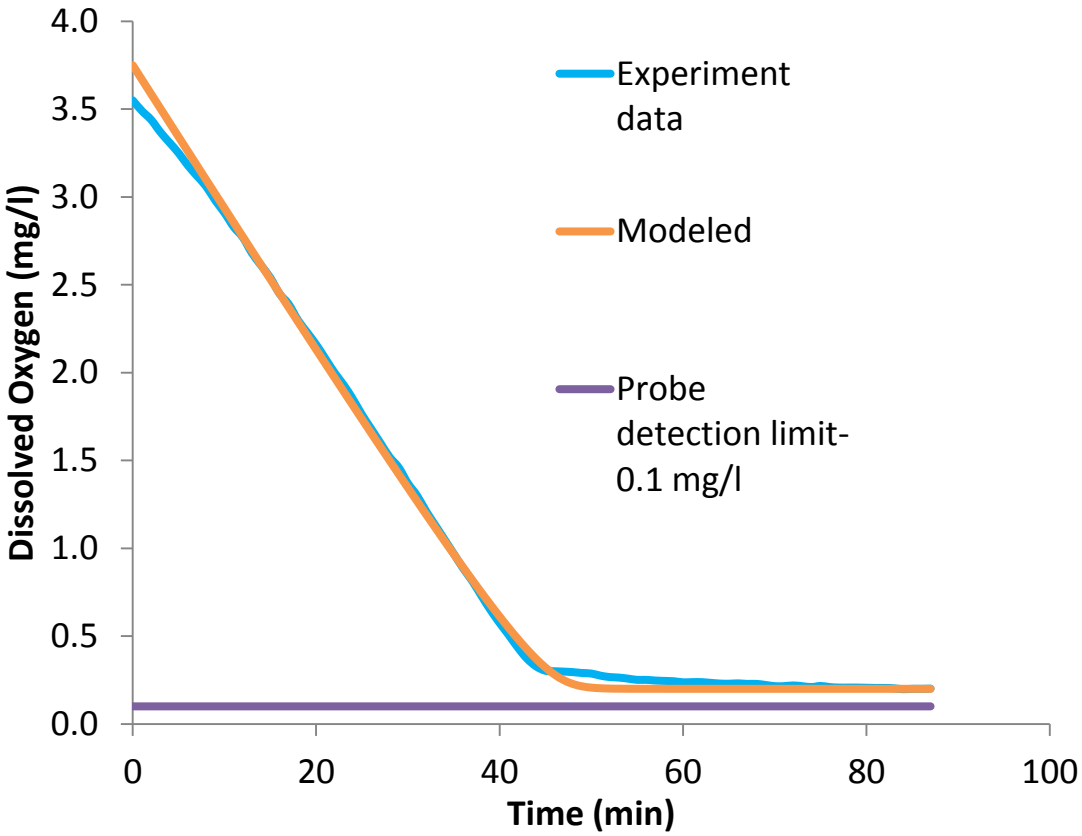

Figure 2-4. A plot of dissolved oxygen consumption experimental data and model fit. Glucose, yeast extract and mineral containing media in a BOD bottle was inoculated with exponential phase culture. A YSI 5905 DO probe was fitted to the BOD bottle and the dissolved oxygen data recorded about every second using a mini com terminal connected with a YSI DO meter.

2.3.3 pH effect on growth

The optical density measurements were converted to dry cell mass density using the calibration curve depicted in Figure 2-2. The dry cell mass density results showed that the highest rate of growth was at pH 3 (Figure 2-5). Growth decreased with decreasing pH values, with almost no growth at pH 1.0. All the starting pH values decreased with the consumption of the glucose. The measured initial and final pH pairs for the experiments were (3.01, 2.25), (2.53, 2.13), (2.05, 1.91), (1.59, 1.51), and (1.11, 1.07). Slope of the best fit line to a plot of ln X vs. t

was calculated and compared for the different pH growth results. X is the biomass growth in dry cell mass density and t is the time elapsed since start of the growth. The results are summarized in table 2-1. The buffered pH 6.0 and pH 3.0 control experiments showed that at pH 6.0 growth was slower than pH 3.0 by only about 20% as measured by the biomass slope method described above. The buffering for the pH 6.0 experiment was effective; the system only exhibited a pH change from 5.96 to 5.88.

Table 2-1. Slopes of a best line fit to a plot of the natural logarithm of biomass density vs. time. Relative activity was calculated by dividing the slopes by the largest slope value.

Initial pH	slope (1/hr)	Relative activity
1.11	0.005	0.09
1.59	0.025	0.45
2.05	0.027	0.47
2.53	0.054	0.96
3.01	0.056	1.00
5.98	--	0.80

The pH relative activities were converted to a continuous function by using the equation

$$f(pH) = \frac{1+2(10^{\frac{L-H}{2}})}{1+10^{(pH-H)}+10^{(L-pH)}} \quad \text{(2-5)}$$

Where $f(pH)$ is the relative activity for a culture at a given initial pH; L and H are the parameters used for adjusting the curve to the lower and higher end of the pH data respectively. The best fit parameters for the pH experiment data were 1.79 for L and 9.0 for H. Figure 2-6 shows the best fit curve.

The pH experiment results suggest that the environmental enrichments tested have a pH optimum around pH (2.5-3.0). The consortium was more sensitive to lower pHs than the tested higher pH of 6.0. Unlike *A. cryptum,* which is incapable of growth below pH 1.9 (Harrison,

1981), results from this experiment show the environmental consortium capable of growth at pH 1.5, albeit at a lower rate than the optimal pH range.

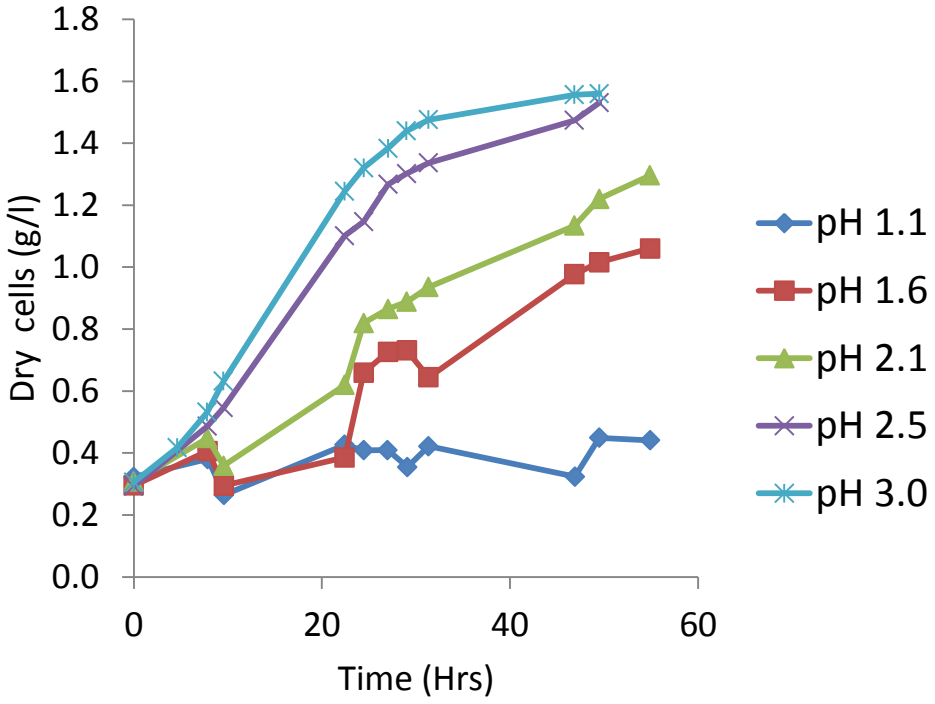

Figure 2-5. Biomass plots for variable pH growth experiments. Glucose, yeast extract and mineral media solutions were acidified to different initial pHs using 3N HCl. The adjusted media were inoculated with filtered and re suspended exponential phase cultures. The measured optical density results were converted to dry cell density using a calibration curve and plotted.

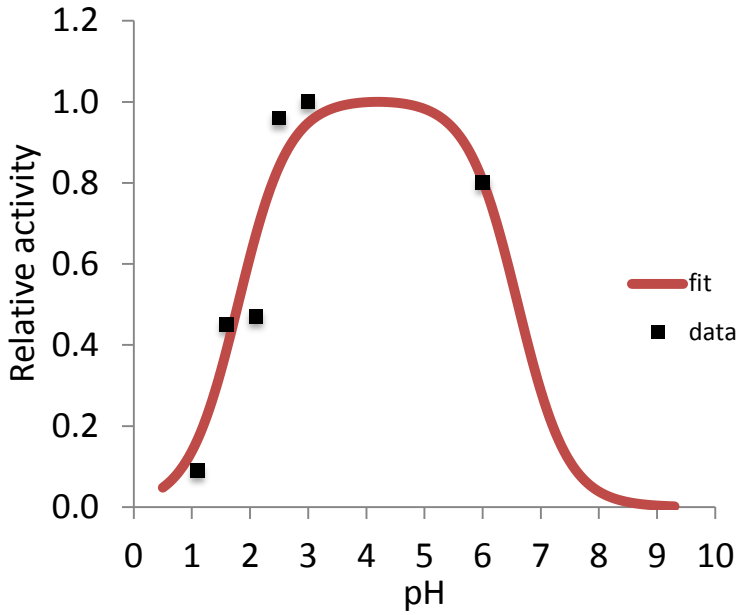

Figure 2-6. A plot of the best fit pH relative activity continuous function and experimentally determined activities. Dots represent experimentally determined relative activity, while the line is for the best fit continuous function.

The overall glucose consumption rate for the acidophilic heterotrophs can then be expressed as:

$$\frac{dS}{dt} = 0.13\frac{X}{0.52} * \min of\left(\frac{S}{0.2+S}, \frac{DO}{0.01+DO}, f(pH)\right) \text{.....(2-6)}$$

$$\frac{dS}{dt} = 0.13\frac{X}{0.52} * \frac{S}{0.2+S} * \frac{DO}{0.01+DO} * f(pH) \text{.....(2-7)}$$

, $f(pH)$ is the pH relative activity function developed above , X is dry cells in g/l, S is glucose concentration in g/l and DO is dissolved oxygen concentration in mg/l.

Equation 2-6 and 2-7 above represent the pure non interactive and multiplicative interactive methods respectively for reducing the maximum substrate utilization rate given multiple limitation factors.

2.3.4 Phospholipid fatty acid analysis (PLFA)

PLFA analysis was done for the acidophilic heterotroph enrichment for a domain level characterization (Microbial Insights Inc., Knoxville, Tn). The particular tested culture was grown to exponential phase on 1g/l glucose and 0.1 g/l yeast extract in the same salt media previously described at pH 3.0 using the original waste rock extract as inoculum. The enrichment did not show any sign of algae growth. The PLFA analysis indicated the presence of prokaryotic and eukaryotic organisms in about 1:1 ratio. The total PLFA/ml detected was 154,245 pico moles. An active microbial number of $3.08*10^9$ /ml was also obtained from the PLFA. The results of the PLFA suggest eukaryotes are present and active and account for about 50% of the consortium. This is an important finding and points to the need for characterizing and studying the metabolic activities of eukaryotic members of environmental AMD enrichments. Eukaryotes have recently been shown to be abundantly present at below pH 1.0 mine waste waters (Baker *et al.*, 2009). There is an increasing interest to know more about the role of these domain in mine waste generation as well as remediation (Das *et al.*, 2009).

All mechanisms of remediation of mine waste by organic carbon depend on the growth of acidophilic heterotrophs. The results of this study can be used to make quantitative predictions about the growth of heterotrophic organisms in mine waste sites. If coupled with a growth model for iron oxidizing organisms, the ensuing competition for oxygen can be modeled. The growth model can also be used to predict the production of soluble microbial products and extracellular polymeric substances given equilibrium production data of the same. As organic carbon remediation of mine waste sites progress, increase of pH is expected at microenvironments where sulfide oxidation takes place. As demonstrated in this study,

acidophilic heterotrophs are capable of growth at higher pH of up to 6.0 and can help maintain the remediation effect for a longer time.

2.4 Conclusion

It has been shown that environmental enrichments from AMD waste rock piles degrade glucose over a wide range of pH values. These organisms were able to efficiently utilize glucose down to very low levels of DO. The use of environmental enrichments to study metabolic responses to remediation actions can yield more relevant results as compared to using pure model strains. About half of the active AMD enrichments were eukaryotes suggesting the importance of this consortium.

2.5 References

Andre, B. and Stroncek, J. (2008). Kinetics study of Acidiphilium Cryptum in glucose media. University of Colorado. Personal communication.

Andre, B. J., Rajaram, H. and Silverstein, J. (2009). Generation of acid mine drainage: Reactive transport models incorporating geochemical and microbial kinetics. Ph.D. thesis. University of Colorado.

Baker, B. J. and Banfield, J. F. (2003). Microbial communities in acid mine drainage. *Fems Microbiology Ecology* **44**(2): 139-152.

Baker, B. J., Tyson, G. W., Goosherst, L. and Banfield, J. F. (2009). Insights into the Diversity of Eukaryotes in Acid Mine Drainage Biofilm Communities. *Applied and Environmental Microbiology* **75**(7): 2192-2199.

Berthelot, D., Leduc, L. G. and Ferroni, G. D. (1993). Temperature studies of iron-oxidizing autotrophs and acidophilic heterotrophs isolated from uranium mines. *Canadian Journal of Microbiology* **39**(4): 384-388.

Bhatnagar, M. and Singh, G. (1991). Growth-inhibition and leakage of cellular material from thiobacillus-ferrooxidans by organic-compounds. *Journal of Environmental Biology* **12**(4): 385-399.

Bilgin, A. A., Harrington, J. M. and Silverstein, J. (2007). Enhancement of bacterial iron and sulfate respiration for in situ bioremediation of acid mine drainage sites: a case study. *Minerals & Metallurgical Processing* **24**(3): 139-144.

Bilgin, A. A., Silverstein, J. and Hernandez, M. (2005). Effects of soluble ferri - Hydroxide complexes on microbial neutralization of acid mine drainage. *Environmental Science & Technology* **39**(20): 7826-7832.

Bridge, T. A. M. and Johnson, D. B. (2000). Reductive dissolution of ferric iron minerals by Acidiphilium SJH. *Geomicrobiology Journal* **17**(3): 193-206.

Das, B. K., Roy, A., Koschorreck, M., Mandal, S. M., Wendt-Potthoff, K. and Bhattacharya, J. (2009). Occurrence and role of algae and fungi in acid mine drainage environment with special reference to metals and sulfate immobilization. *Water Research* **43**(4): 883-894.

Edwards, K. J., Gihring, T. M. and Banfield, J. F. (1999). Seasonal variations in microbial populations and environmental conditions in an extreme acid mine drainage environment. *Applied and Environmental Microbiology* **65**(8): 3627-3632.

Fortin, D., Davis, B. and Beveridge, T. J. (1996). Role of Thiobacillus and sulfate-reducing bacteria in iron biocycling in oxic and acidic mine tailings. *Fems Microbiology Ecology* **21**(1): 11-24.

Gemmell, R. T. and Knowles, C. J. (2000). Utilisation of aliphatic compounds by acidophilic heterotrophic bacteria. The potential for bioremediation of acidic wastewaters contaminated with toxic organic compounds and heavy metals. *Fems Microbiology Letters* **192**(2): 185-190.

Harrison, A. P. (1981). Acidiphilium-cryptum gen-nov, sp-nov, heterotrophic bacterium from acidic mineral environments. *International Journal of Systematic Bacteriology* **31**(3): 327-332.

Jenkins, J. D. (2006). Role of flow and organic carbon on acid mine drainage remediation in waste rock. Ph.D. thesis. *University of Colorado***.**

Johnson, D. B. (1995). Acidophilic microbial communities - candidates for bioremediation of acidic mine effluents. *International Biodeterioration & Biodegradation* **35**: 41-58.

Johnson, D. B. and Bridge, T. A. M. (2002). Reduction of ferric iron by acidophilic heterotrophic bacteria: evidence for constitutive and inducible enzyme systems in Acidiphilium spp. *Journal of Applied Microbiology* **92**(2): 315-321.

Johnson, D. B. and Hallberg, K. B. (2009). Carbon, Iron and Sulfur Metabolism in Acidophilic Micro-Organisms. *Advances in Microbial Physiology, Vol 54*. R. K. Poole. 54: 201-255.

Johnson, D. B. and McGinness, S. (1991). Ferric iron reduction by acidophilic heterotrophic bacteria. *Applied and Environmental Microbiology* **57**(1): 207-211.

Johnson, D. B., Yajie, L. and Okibe, N. (2008). "Bioshrouding" - a novel approach for securing reactive mineral tailings. *Biotechnology Letters* **30**(3): 445-449.

Kusel, K., Roth, U. and Drake, H. L. (2002). Microbial reduction of Fe(III) in the presence of oxygen under low pH conditions. *Environmental Microbiology* **4**(7): 414-421.

Liu, M. S., Branion, R. M. R. and Duncan, D. W. (1988). The effects of ferrous iron, dissolved-oxygen, and inert solids concentrations on the growth of thiobacillus-ferrooxidans. *Canadian Journal of Chemical Engineering* **66**(3): 445-451.

Lu, J., Chen, T. H., Wu, J., Wilson, P. C., Hao, X. Y. and Qian, J. H. (2011). Acid tolerance of an acid mine drainage bioremediation system based on biological sulfate reduction. *Bioresource Technology* **102**(22): 10401-10406.

Marchand, E. A. and Silverstein, J. (2002). Influence of heterotrophic microbial growth on biological oxidation of pyrite. *Environmental Science & Technology* **36**(24): 5483-5490.

Marchand, E. A. and Silverstein, J. (2003). The role of enhanced heterotrophic bacterial growth on iron oxidation by Acidithiobacillus ferrooxidans. *Geomicrobiology Journal* **20**(3): 231-244.

Pronk, J. T., Meesters, P. J. W., Vandijken, J. P., Bos, P. and Kuenen, J. G. (1990). Heterotrophic growth of thiobacillus-acidophilus in batch and chemostat cultures. *Archives of Microbiology* **153**(4): 392-398.

Rowe, R., Todd, R. and Waide, J. (1977). Microtechnique for most-probable-number analysis. *Applied and environmental microbiology* **33**(3): 675-680.

CHAPTER 3. INTERACTION OF FERRIC IRON WITH SOLUBLE MICROBIAL PRODUCTS DECREASES PYRITE OXIDATION

Abstract

Microbial growth in mine waste produces soluble microbial products (SMP), both growth and lysis derived. Experiments were conducted to study the interaction of SMP with soluble ferric iron, particularly formation of complexes that reduce the effectiveness of (Fe3) as the primary oxidant of pyrite in acid mine drainage generation. The rate of pyrite oxidation at pH 1.8 by ferric iron in sterile suspensions decreased in the presence of all SMP. However, for equivalent dissolved organic carbon (DOC) concentrations, the rate of ferrous iron production was significantly lower with lysis derived SMPs, 0.0136 hr^{-1}, compared with growth products, 0.0756 hr^{-1}, and a control, 0.1075 hr^{-1}. Fractionation of the SMP by ultrafiltration indicated that lower molecular weight organic compounds (<1 KDa) dominated the lysis products. The inhibition effect of SMP was similar to, but weaker than that of a known organic complexing agent, DFAM. After biodegradation of soluble lysis products the remaining fraction of DOC still reduced oxidation rate by 82% compared with an organic-free medium.

3.1 Introduction

After initial weathering of mine waste rock and reduction of pore water pH below 4, acid mine drainage (AMD) is formed by chemical oxidation of pyrite by ferric iron, producing ferrous iron and sulfuric acid (3-1). Regeneration of ferric iron by iron oxidizing bacteria maintains the AMD cycle as long as pyritic minerals, oxygen and water are present (3-2).

$FeS_2 + 14Fe^{3+} + 8H_2O \rightarrow 15Fe^{2+} + 2SO_4^{2-} + 16H^+$ ……(3-1)

$4Fe^{2+} + O_2 + 4H^+ \rightarrow 4Fe^{3+} + 2H_2O$..... (3-2)

In the abiotic reaction (3-1), the ratio of ferrous iron (Fe2) produced to ferric iron (Fe3) consumed is 1.07.

Mining for metals and coal produces disturbed waste rock and soil at an estimated rate of over 15,000 Mt/year, covering a surface area of approximately 100 million hectares – equivalent to or greater than all the solids displaced by natural processes such as landslides and earthquakes (Lottermoser 2003). Often this waste rock is deposited at mine sites above tree line and the microbial ecology of waste rock is dominated by chemolithotrophic bacteria, primarily iron and sulfur oxidizing organisms using electrons from iron sulfide minerals and fixing both CO_2 and N_2 (Tyson *et al.*, 2004; Tyson *et al.*, 2005). It has been reported that these primary producers sustain a complex population of heterotrophic organisms whose growth is probably limited by the internal cycling of organic carbon and nitrogen products of the chemolithotrophs (Bond *et al.*, 2000; Edwards *et al.*, 2000; Gross and Robbins, 2000).

Addition of an external source of organic carbon to mine waste has been shown to stimulate the growth of heterotrophic acidophiles, including iron and sulfate reducing bacteria when oxygen is depleted (Johnson, 1995; Marchand and Silverstein, 2002; Bilgin *et al.*, 2004).

This causes disruption to the autotrophic regeneration of ferric iron and raises the system pH. However, another effect of stimulating heterotrophic growth is increased production of soluble microbial products. A decrease in pyrite oxidation was observed when cell free extracts from *A. ferrooxidans and Acidiphilium acidophilum* cultures were added to a pyrite suspension. Marchand and Silverstein (2002) suggested that an interaction resembling complexation or chelation had occurred between ferric iron and soluble microbial products (SMP), and that the complexed iron was less reactive with pyrite.

Bacteria and fungi mediate the dissolution of iron and other metals by producing low molecular weight compounds like hydroxamate and catecholate siderophores (Kalinowski *et al.*, 2000). These compounds are often produced in iron-limited conditions to solubilize iron and facilitate transport into cells for metabolic activities (McKnight and Morel, 1980; Neilands, 1995; Hayen and Volmer, 2006). Most siderophores such as Pyochelin (Hayen and Volmer, 2006), ferrichrome and enterobactin (Neilands, 1995) are <1 KDa in molecular weight. They have a high complex formation constant of 10^{30} or greater when there are three bidentate ligands coordinating ferric iron (Neilands, 1995). C-type cytochromes have been shown to play an active role in ferric reductase complex enzyme activity in G. *sulfurreducens* during iron reduction (Magnuson *et al.*, 2000). Although most of the siderophore studies have been done for circumneutral and higher pH conditions, ferrous iron uptake regulation (fur) genes coding for iron transporters have been found in Acidithiobacili and Leptosprillium genera (Osorio *et al.*, 2008). Low molecular weight organic acids produced by Arthrobacter growing on hornblende promoted iron dissolution from the mineral surfaces, but the affinity of these compounds for ferric iron was lower than that of the siderophore desferrioxamine B (Kalinowski *et al.*, 2000).

Natural organic matter has also been shown to chelate and complex ferric iron and other metals (McKnight *et al.*, 1983; Luther *et al.*, 1992; McKnight *et al.*, 1992; Breault *et al.*, 1996; Luther *et al.*, 1996; Rose and Waite, 2003; Rose and Waite, 2005; Liu *et al.*, 2011). The reported association of ferric iron has mainly been with lower MW fractions (100-5000 Da) with preference to groups containing aromatic moieties, carboxylic acid groups and amino acid residues (McKnight *et al.*, 1992; Luther *et al.*, 1996). Brothers *et al.* (1996) demonstrated the effect of ferric iron chelation by salicylate, oxalate and acetylacentonate at pHs of around 7. They showed that pyrite oxidation was significantly enhanced due to the chelation effect of the above ligands. Other low molecular weight organic compounds (amu < 1 KDa) were found to complex ferric iron in sea water supplemented with $Fe(OH)_3$ at neutral pH (Chen *et al.*, 2004).

Soluble microbial products from waste water anaerobic digestion have been shown to complex copper and nickel ions with the 1-10 KDa molecular weight fractions having the highest capacity (Kuo and Parkin, 1996; Holakoo *et al.*, 2006). Studies have reported changes in the reactivity of ferric and ferrous iron complexed with organic ligands. Gao and Zepp (1998) reported that complexation of ferric iron by deferoxamine mesylate (DFAM), a commercial methane sulfonate form of the siderophore desferrioxamine B, inhibited iron photoreduction and reduced the rate of photooxidation of colored dissolved organic matter. Iron complexed by nitrilotriacetic acid (FeNTA) increased the rate of biodegradation of 2-aminobenzothiazole (ABT) by Rhodococcus rhodochrous (Bunescu *et al.*, 2008) and reductive degradation of RDX was enhanced when Fe(2) was complexed with catechol and thiol ligands, tiron and meso-2,3-dimercaptosuccinic acid (DMSA) (Kim and Strathmann, 2007).

The addition of organic carbon to drainage in mine waste rock has been proposed as a remediation strategy (Marchand and Silverstein, 2002; Marchand and Silverstein, 2003; Johnson *et al.*, 2008). The primary goal of this research was investigating the role of soluble microbial products produced by microbial populations growing in mine waste rock on the activity of ferric iron in pyrite oxidation. In addition, the stability of organo-iron complexes, characteristics of SMP reacting with ferric iron, and the effect of SMP-DOC molecular weight and concentration were investigated. Experiments using the complexing agent DFAM were carried out to compare the complexing activity of SMP to a strong organic chelating agent active at low pH conditions.

3.2 Materials and Methods

3.2.1 Enrichment of cultures

Experiments focused on SMP from heterotrophic organisms, assumed to proliferate after addition of organic matter to waste rock. Rocks from an abandoned mine near Leadville, CO were immersed in water and aerated to establish an active culture of suspended and attached microorganisms. Flasks containing glucose and mineral media comprised of 0.81 g/l NH_4Cl, 0.1 g/l KCl , 0.17 g/l K_2HPO_4 , 0.5 g/l $MgSO_4.7H_2O$, 0.19 g/l $CaCl_2.2H_2O$, and 0.02 g/l $FeSO_4.7H_2O$ were inoculated with the waste rock suspension. The first transfer culture was grown in 1 g/l glucose, while the second transfer received 20 g/l initial glucose and was used to obtain both growth and lysis SMP. Culture media were adjusted to pH 3 using 3N trace metal grade HCl (Fisher Scientific). The growth of the cultures was tracked by measuring glucose consumption.

3.2.2 Obtaining SMPs (growth and lysis products)

Growth products were obtained by filtering the second transfer culture within hours of complete glucose consumption. The lysis products were obtained by autoclaving a portion of the suspension followed by filtration. Both samples were filtered through pre-washed 0.22 µm cellulose acetate filters (GE Osmonics).

3.2.3 Pyrite oxidation experiments

Pyrite oxidation experiments were carried out by mixing 2.5 g of acid washed pyrite either with the growth or lysis products and ferric iron at a pH of 1.8. Pyrite was obtained from

Ward Scientific Company as cubes and was crushed and sieved to obtain a 75-90 µm size range. Pyrite granules were cleaned with 6N boiling HCl and rinsed with acetone to extract any precipitated or sorbed iron and organic matter (Moses *et al.*, 1987). ACS grade FeCl3.6H2O was used to prepare the stock ferric iron solution. All solutions were acidified to the desired pH using 3N HCl.

The lysis products were diluted to obtain 27, 78, and 236 mg/l SMP-DOC equivalent solutions. Solutions containing growth-derived SMP at 28 mg/l and 53 mg/l SMP-DOC equivalent solutions were used. Control flasks media had pyrite, ferric iron and acid with no growth or lysis products. The total solution volume was 200 ml with ferric iron concentration of 90 mg/l. Replicate flasks were used for all conditions. Flasks were incubated on a shake table at 125 rpm and sampled for pH, soluble ferrous and total iron, sulfate, and DOC.

3.2.4 SMP apparent molecular weight fractionation and pyrite oxidation experiments

The lysis derived SMP solution was filtered through 1 kDa and 10 kDa cutoff cellulose ultrafiltration membranes in a Millipore XFUF 07601 filtration cell pressurized to 75 psi with nitrogen gas. The membranes were pre-soaked in reagent grade water for 1 day to remove preservatives and easily leachable organics (Dong *et al.*, 2010). A 1:1 filtrate to retentate volume ratio was used to ensure proper filtration. The <1 kDa, <10 kDa filtered solutions, and the bulk unfiltered solution were used for pyrite oxidation experiments by adding pyrite and the needed stock (Fe3) in each solution to result in a 90 mg/l ferric iron concentration for a total volume of 100 ml.

3.2.5 Biodegradation of lysis derived SMPs

The biodegradability of the lysis SMP complexes was tested by adding the filtered lysis SMP solution to a media containing 90 mg/l ferric iron, an exponential phase culture of acidophilic heterotrophs, and minerals. A positive control contained lysis SMP, minerals and an exponential phase microorganism culture with no iron added, and a negative control had lysis SMP solution and minerals but no inoculum or iron. All flasks were incubated on a shake table set at 125 rpm. Samples were filtered through 0.22 µm nylon filters and analyzed for DOC. At the end of the biodegradation experiment, the solutions were filtered through 0.22 µm cellulose acetate filters to remove microorganisms. Appropriate amount of ferric iron stock was added to the media in the flasks that had no iron added initially to obtain a concentration of 90 mg/l. pH was adjusted to 1.8 using 3N HCl, and 1.25 g pyrite was added to all flasks. The flasks containing SMP, ferric iron, and pyrite suspensions were incubated on a shake table at 125 rpm and sampled for pH, ferrous and total soluble iron over the pyrite oxidation reaction period.

3.2.6 Deferoxamine mesylate complexation experiments

It was hypothesized that SMP molecules had a complexation type interaction with ferric iron. For comparison, a suspension of pyrite with ferric iron was incubated with a known hydroxamate complexing agent, deferoxamine mesylate (DFAM), which chelates (Fe3) but not (Fe2) (Kalinowski et al., 2000). DFAM is a commercial product similar in structure and activity to the bacterial siderophore desferrioxamine (DFA). At pH values below 4, ferric ion is chelated by DFA in the monohydroxamate and bishydroxamate configuration (Figure 3-1).

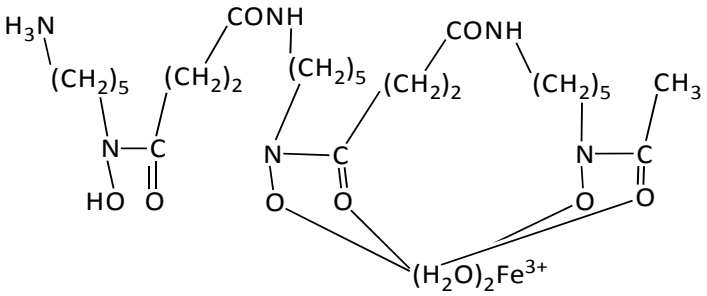

Figure 3-1. $Fe(H_2DFA)^{2+}$, a bishydroxamate configuration of the DFA siderophore complexed with ferric iron at pH < 4, after Kalinowski et al., 2000.

DFAM stock solution was diluted to a solution containing about 90 mg/l ferric iron and adjusted to pH 1.8 using HCl for a final deferoxamine mesylate concentration of 270, 540, and 812 mg/l corresponding to DOC concentrations of 129, 257, and 386 mg/l respectively. Pyrite oxidation experiments with DFAM were carried out by the method described above for SMP solutions. In addition, the analysis of samples for total iron was done using ICP-OES (LEGS Laboratory, Department of Geological Sciences, University of Colorado-Boulder).

3.2.7 SMP characterization

Molecular weight distribution of growth and lysis-derived SMP was done using size exclusion chromatography followed by TOC analysis (SEC-TOC) of eluted fractions. Two-ml samples were injected on to a Toyopearl HW-50 resin-packed column connected to an Agilent LC apparatus. An eluent composed of 2.4 mM NaH_2PO_4, 1.6 mM Na_2HPO_4 and 25 mM Na_2SO_4 at pH 6.8 was pumped at a rate of 1 ml/min at 34 bar. A TOC analyzer (GE Sievers Instruments)

was used for measuring the DOC content of the column outlet. A calibration curve was made by injecting dextran molecular weight standards.

Fluorescence excitation and emission (EEM) scans were done on samples of growth and lysis derived SMP using Fluoromax 4 fluorometer (Horiba Scientific). An excitation of 350 to 550 nm with a 10 nm increment was used and the resulting emission monitored on 240 to 450 nm at 2 nm steps. Samples with UV absorbance UVA254 of 0.2 or higher were diluted. The EEM scan results were corrected for lamp output, inner filter effects, and raman peaks. A 13-component PARAFAC DOM model (Cory and McKnight, 2005) was used to compare the fluorescence signatures to that of components previously identified in well characterized NOM samples.

3.2.8 Analytical methods

Glucose was measured using a YSI 2700 select membrane analyzer (YSI Yellow Springs, OH). Soluble ferrous and total iron concentrations were measured using the 1-10 phenanthroline method. Hydroxylamine HCl was used to reduce (Fe3) to (Fe2) followed by the color producing complexation reaction with 1-10 phenanthroline. (Fe3) was calculated as the difference of the (Fe tot) and (Fe2). Sulfate was measured on a Dionex ion chromatograph (DX-500) using an anion column (AS14) and a CD20 conductivity detector. An 8 mM Na_2CO_3 and a 1.0mM NaHCO3 eluent was used. DOC was measured using a Shimadzu DOC analyzer. pH was measured using an Accumet combination electrode and meter.

3.3 Results and Discussion

3.3.1 Enrichment of cultures

SMP was produced from the second of two transfers of cells extracted from mine waste rock and grown on glucose. The 20 g/l glucose substrate was typically depleted in 8-10 days (Figure 3-2).

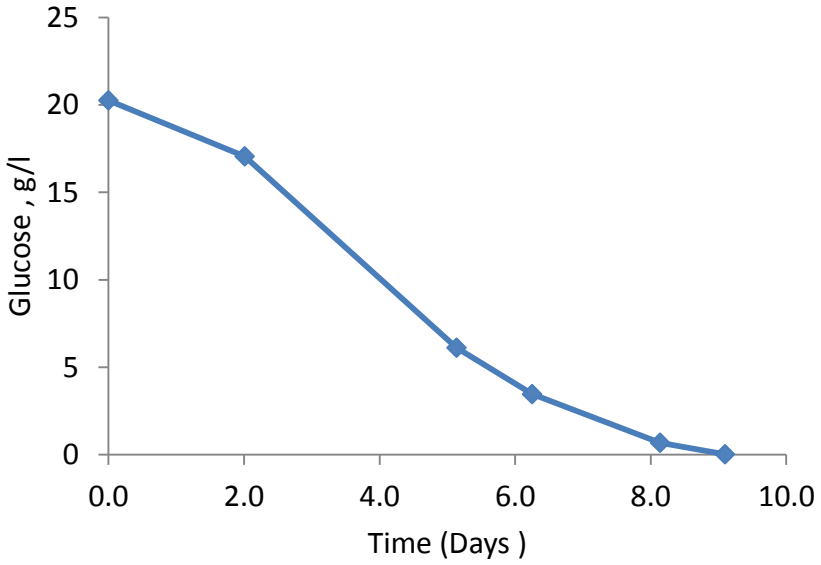

Figure 3-2. Substrate depletion curve for a second transfer culture with an initial glucose concentration of 20 g/l.

3.3.2 SMP and pyrite oxidation activity

The growth-derived SMP was obtained by filtering the culture liquid within hours of the consumption of glucose (Figure 3-2). The concentration of growth-derived SMP ranged from 57 to 77.9 with an average of 65.8 mg/l. Two dilutions of SMP-DOC were used for pyrite oxidation experiments, 28 and 53 mg/l DOC, along with an organic-free control. Initial ferric iron in the

flasks averaged 88.5±0.5 mg/l. The rate of pyrite oxidation, as measured by ferrous iron accumulation, was greatest in the organic-free control and decreased with increasing SMP-DOC concentration (Figure 3-3). Recovery of soluble ferrous iron after 27 hours was 97.3 percent of the stoichiometric amount (Equation 1) in the control flask; 87.1 percent in the flask containing 28 mg/l SMP-DOC; and 74.3 percent in the flask with 53 mg/l DOC.

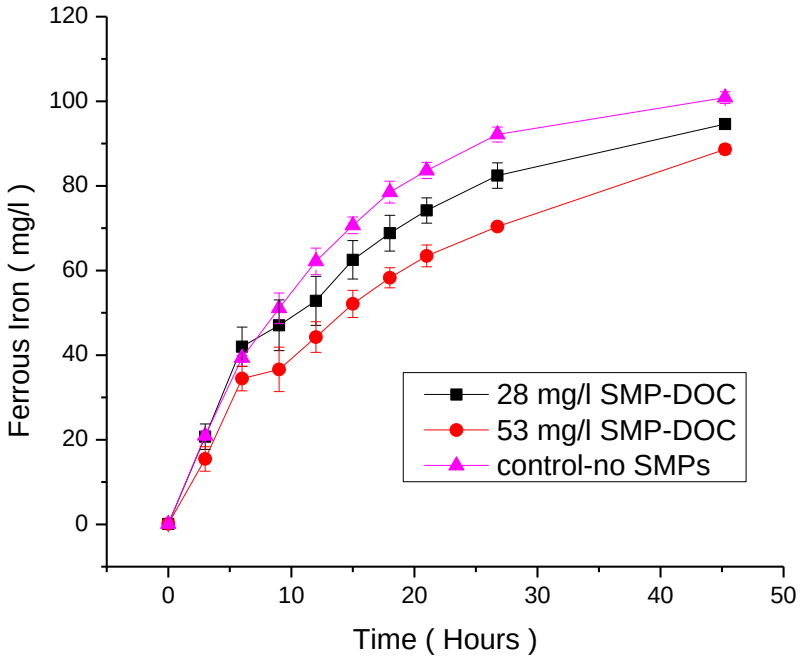

Figure 3-3. Ferrous iron produced during growth derived SMP solution pyrite oxidation experiments. Experiments were done in flasks containing 2.0 g of pyrite in 200 ml of pH 1.8 solutions and about 90 mg/l of initial ferric iron. Two solutions containing 28 and 53 mg/l growth derived SMP-DOC were used. Error bars indicate difference of the plotted average values from the duplicate flask measurements for each SMP-DOC concentration used.

Lysis-derived SMP was produced by autoclaving and filtering samples from the culture growth flasks within hours of the glucose consumption. The DOC concentration of the filtrate averaged 773 ± 55 mg/l. Because of the higher concentration of the autoclaved SMP solution, a

greater range of SMP concentration was tested for the effect on ferric iron oxidation activity: 27, 78, and 236 mg/l SMP-DOC, along with an organic-free control. The initial ferric iron concentration in the flasks averaged 88.1 ± 4.1 mg/l. As in the growth-derived SMP, ferrous iron accumulation was fastest in the control, with 92.7 % of expected production of soluble ferrous iron within 25 hours (Figure 3-4). Also, as with the growth-derived SMP, increasing concentration of lysis-derived SMP-DOC slowed the rate of pyrite oxidation and ferrous iron accumulation (Figure 3-4). Reduction of ferric iron oxidation activity was significantly greater in the presence of lysis-derived SMP compared with growth products. After 45 hours, only 43.9 percent of the expected concentration of dissolved ferrous iron had been produced in the flasks containing 27 mg/l lysis-derived SMP-DOC, compared with 99.6 percent in the same period in the flask with 28 mg/l growth-derived SMP-DOC.

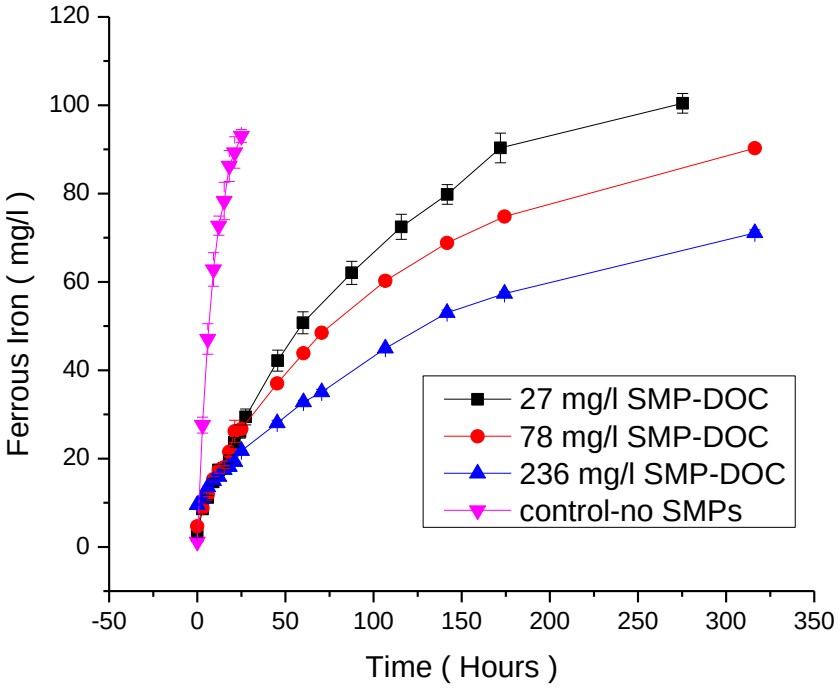

Figure 3-4. Ferrous iron produced during lysis derived SMP solution pyrite oxidation experiments. Experiments were done in flasks containing 2.0 g of pyrite in 200 ml of pH 1.8 solutions and about 90 mg/l of initial ferric iron. Three solutions containing 27, 78, and 236 mg/l lysis derived SMP-DOC were used. Error bars indicate difference of the plotted average values from the duplicate flask measurements for each SMP-DOC concentration used.

Experiments to investigate the apparent molecular weight (amw) fraction of SMP most effective in reducing ferric iron oxidation activity were carried out after ultrafiltration and collection of filtered lysis-derived SMP samples. The lysis SMP solution DOC before ultrafiltration was 325 mg/l. The fraction of SMP with amw <1 KDa contained 207 mg/l DOC and the fraction with amw <10 KDa had 223 mg/l DOC, indicating that low molecular weight organic compounds dominated the SMP, constituting 64% of the total DOC and 93% of the DOC < 10 KDa. This is consistent with a bimodal distribution of <1 KDa and >10 KDa fractions commonly

seen in effluents of biological processes such as wastewater bio reactors (Boero *et al.*, 1996; Huang *et al.*, 2008) .

For pyrite oxidation experiments, the initial adjusted ferric iron concentration for the unfiltered bulk solution, <1 KDa, <10 KDa, and no SMP control solution averaged 81.8 ± 1.9 mg/l. The SMP-DOC concentration for the unfiltered bulk solution, <1 KDa, and <10 KDa flasks were 267, 164, and 177 mg/l, respectively. As before, the pyrite oxidation (ferrous iron accumulation) rate appeared to decrease proportionally to the SMP-DOC concentration (Figure 3-5).

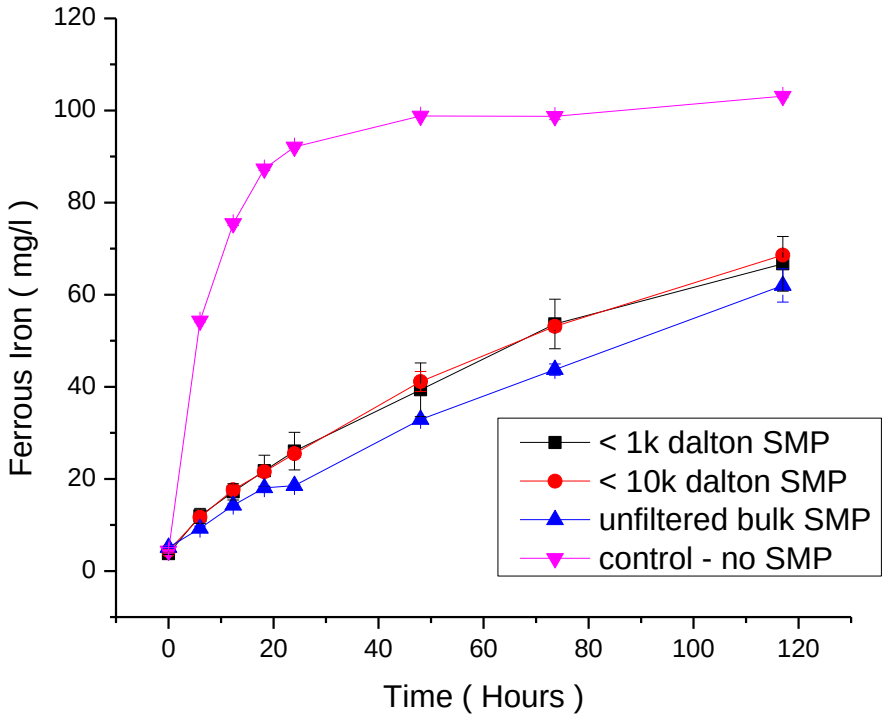

Figure 3-5. Ferrous iron production during ultra-filtered lysis derived SMP solution pyrite oxidation experiments containing 1.0 g of pyrite in 100 ml of pH 1.8 solutions and about 80 mg/l of initial ferric iron. Three solutions containing 164, 167, and 267 mg/l SMP-DOC were used corresponding to the <1 KDa , <10 KDa, and unfiltered bulk solutions. Error bars indicate difference of the plotted average values from the duplicate flask measurements for each SMP-DOC concentration used.

Variable effects of biodegradation on organo-metal complexes and metal availability have been reported ranging from little or none to significant increases in released metals, including iron and uranium, depending on the organic ligand composition, bacteria present and environmental conditions such as pH and redox potential (Francis and Dodge, 1993; Ganesh *et al.*, 1997; Dudal *et al.*, 2005). Approximately 80% of the 500 mg/l initial SMP-DOC was consumed in the inoculated flasks within 60 hours, with and without added ferric iron; whereas DOC was constant in the sterile control (Figure 3-6). The pyrite oxidation experiments with the filtered biodegradation experiment solutions showed that both biodegraded filtrates reduced pyrite oxidation as compared to the control with no SMP (Figure 3-7).

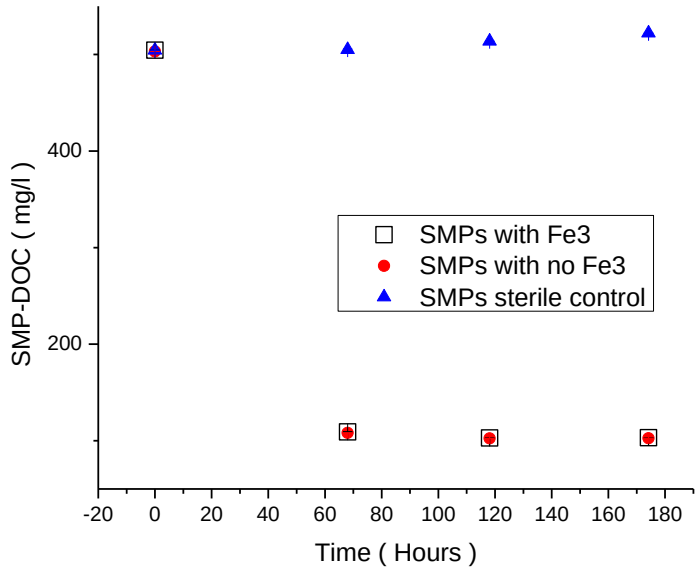

Figure 3-6. DOC measurements of the biodegradation experiment carried out with an initial lysis derived SMP-DOC of 500 mg/l, inoculated with an active acidophilic heterotrophic culture. One treatment contained an initial ferric iron concentration of 90 mg/l whereas the second did not contain any ferric iron. The control was not inoculated with an active culture and did not contain ferric iron.

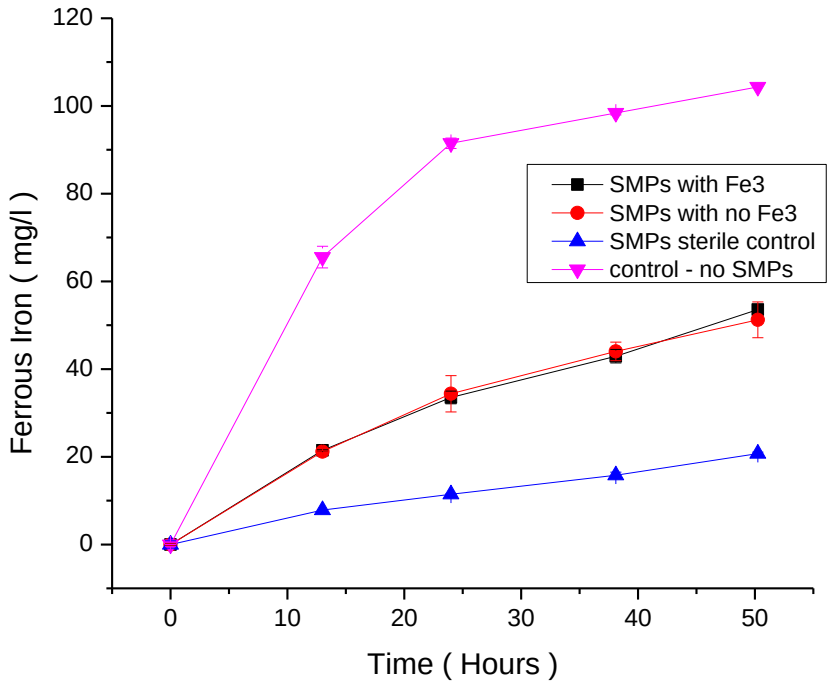

Figure 3-7. A plot of ferrous iron production during pyrite oxidation experiments with filtered biodegraded SMPs containing 1.25 g pyrite in pH 1.8, 125 ml solutions. The SMP with (Fe3) and without (Fe3) refer to the original biodegradation experiment. Both biodegraded solutions were filtered and adjusted to about 90 mg/l ferric iron and had 91 and 95 mg/l SMP-DOC. The control from the biodegradation experiment was also filtered and adjusted to about 93 mg/l ferric iron and had 476 mg/l SMP-DOC. The pyrite oxidation control did not contain any SMPs. The error bars indicate difference of the plotted average values from the duplicate flask measurements for each tested case.

The SEC results showed that almost the entire growth product DOC was less than 10 KDa, with the largest fraction between 1 KDa and 10 KDa. There was a greater distribution of apparent molecular weights in the autoclaved cell products (lysis SMP), with a significant fraction of less than 1 KDa (Figure 3-8). The grouped SEC-TOC amw fraction data for both the growth and lysis SMP after integration of peak areas are compared in Table 3-1.

Table 3-1. SEC-DOC based amw distribution for the growth and lysis derived SMPs. The percentages were calculated by using the areas obtained from the integration of the DOC response curve in Figure 3-8.

Apparent Molecular Weight (KDa)	Lysis products DOC (%)	Growth products DOC (%)
<1	52.8	25.5
1-10	22.5	72.8
>10	24.7	1.7

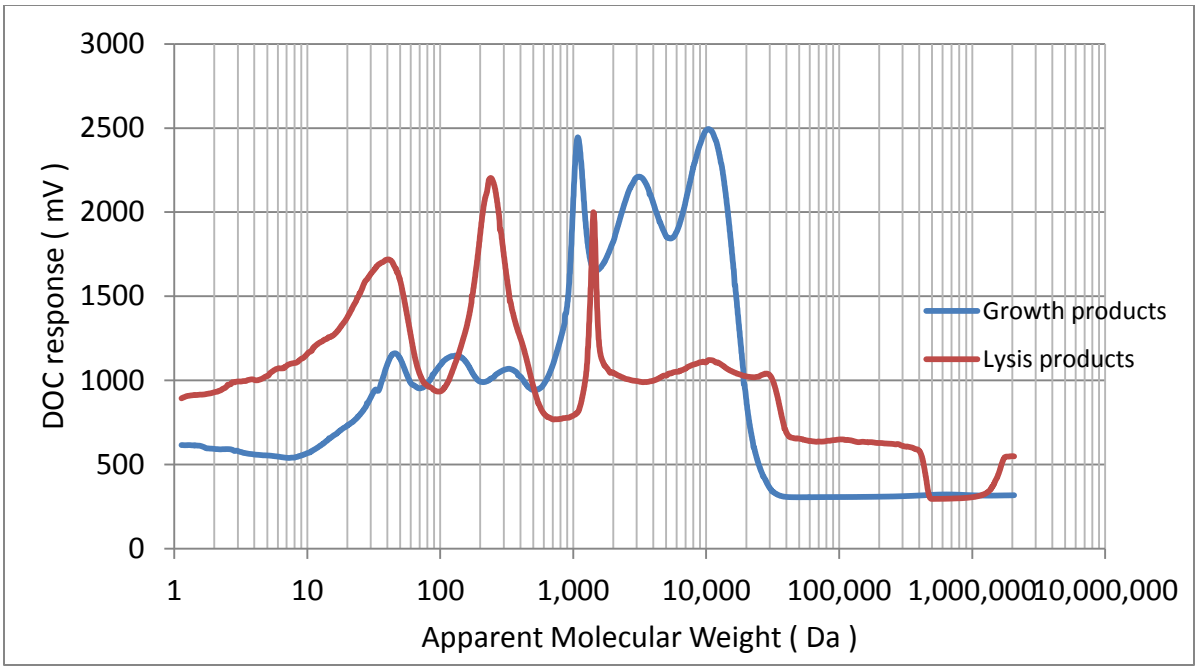

Figure 3-8. Size exclusion chromatograph of growth and lysis derived SMPs. The DOC response in mV was monitored online. The response time was converted to molecular weight using a calibration curve prepared by injecting known weight dextran standards.

The corrected fluorescence EEMs of growth and lysis SMP are consistent with spectra for organic matter of microbial origin (Figures 3-9 and 3-10). The output from a 13 component PARAFAC model showed the presence of protein like components accounting for 75 % of the fluorophores in the lysis products and 44 % for growth products (Table 3-2).

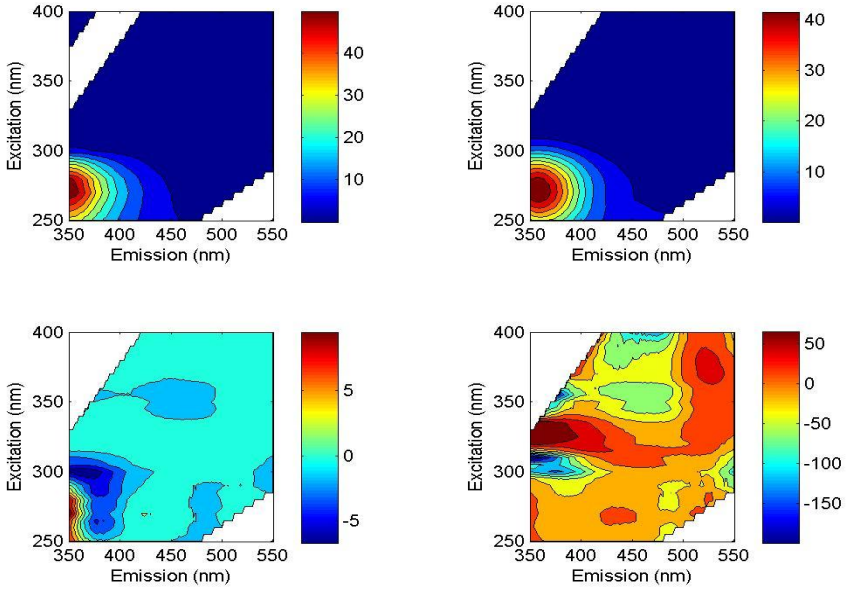

Figure 3-9. Lysis products fluorescence characterization results (clock wise from top right : the actual EEM, the modeled EEM, the residuals, and the residuals on a percent basis).

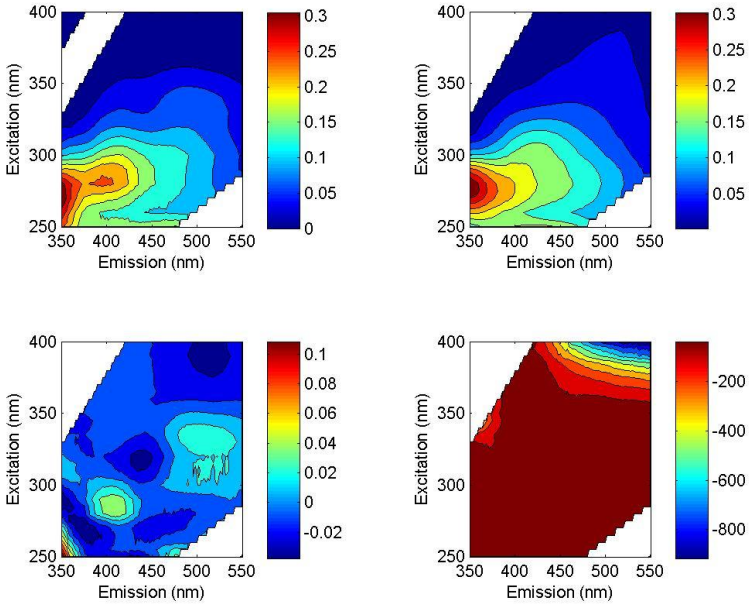

Figure 3-10. Growth products fluorescence characterization results (clock wise from top right : the actual EEM, the modeled EEM, the residuals, and the residuals on a percent basis).

Table 3-2. Fluorescence model (PARAFAC) results for growth and lysis derived SMPs. The model output predictions for the 13 components were grouped into four categories and summed up to generate percentage values.

PARAFAC Components	Growth derived SMPs (Percent abundance)	Lysis derived SMPs (Percent abundance)
Oxidized quinone-like (Q1, Q2, Q3)	16%	11%
Reduced quinone-like (SQ1, SQ2, HQ)	12%	11%
Protein-like (tryptophan and tyrosine)	44%	76%
Unknown (C1, C3, C6, C10)	27%	2%

3.3.3 Deferoxamine mesylate experiment results

The average total iron concentrations for the DFAM pyrite oxidation experiments were 89.8 ± 2.8 mg/l. The initial ICP-MS and 1-10 phenathroline total iron measurements showed a difference of 20.1, 45.3, and 65.6 mg/l iron for the 270, 540, and 812 mg/l DFAM concentration treatments respectively. The molar ratios of the iron differences to the DFAM concentrations (1.05 to 1.14) were very close to the theoretical DFAM:Fe complexation ratio of 1. The iron differences between the two measurement methods are likely the result of the complexation of ferric iron by DFAM inhibiting the hydroxylamine reduction of ferric iron step in the 1-10 phenathroline iron test method. The pyrite oxidation results also showed a plateau in the ferrous iron production at concentrations of about 76.8, 51.3, and 25.6 mg/l ferrous iron for the

270, 540, and 812 mg/l DFAM concentration treatments respectively. This is in comparison with the 106.2 mg/l ferrous iron plateau for the control. Calculation of the ferric iron reacted to give the above plateau ferrous iron concentrations showed that the initially DFAM complexed ferric iron may not have undergone any reaction with pyrite. Control flasks containing only DFAM and pyrite in pH 1.8 solutions, did not produce any measurable ferrous iron suggesting no direct leaching of pyrite by DFAM was happening.

3.3.4 Modeling effects of Fe-SMP and Fe-DFAM complexes

Assuming a 1st order Ferric iron consumption, pyrite not limiting, a first order rate constant was obtained for all the pyrite oxidation experiments.

$$\frac{d(Fe^{3+})}{dt} = -k * Fe^{3+}$$

$$Fe^{3+}(t) = (Fe^{3+})_o * \exp(-kt)$$

$$Fe^{2+}(t) = 1.07 * \left((Fe^{3+})_0 - Fe^{3+}(t)\right) = 1.07 * (Fe^{3+})_0 * (1 - \exp(-kt))$$

where $Fe^{2+}$and Fe^{3+} are total soluble ferrous and ferric iron concentrations in mg/l respectively and t is time in hours. $(Fe^{3+})_o$ denotes the initial total soluble ferric iron concentration in mg/l. The 1.07 factor accounts for the net ferrous iron production in the batch experiment, 15 g Fe^{2+} produced per 14 grams Fe^{3+} consumed in pyrite oxidation (reaction 1-1). A Matlab function for a nonlinear regression algorithm was used to estimate a value for k by minimizing the residual, R = $(Fe^{2+})(t)$ - $(1.07*(Fe^{3+})_0*(1-\exp(-kt)))$ for the ferrous iron profile data and initial ferric iron concentration, $(Fe^{3+})_0$. 95% confidence intervals for the parameters were obtained from a different Matlab function which uses the asymptotic standard error (ASE) method for nonlinear regression. Bootstrapping of residuals with replacement to the best fit

data was also used to generate 1000 new data sets and parameters (K) for each treated case and the 95% confidence intervals determined. Since the two confidence intervals were close to each other, the ASE method generated confidence intervals are reported here. The K's obtained for the growth and lysis SMP solutions were all significantly different from each other and from the controls with no SMPs. The fitted first order model lines and iron profile data for growth and lysate SMP are shown in Figures 3-11 and 3-12 respectively. Figure 3-14 shows the rate constants for all the pyrite oxidation experiments including the ultra-filtered, biodegraded, and DFAM solutions.

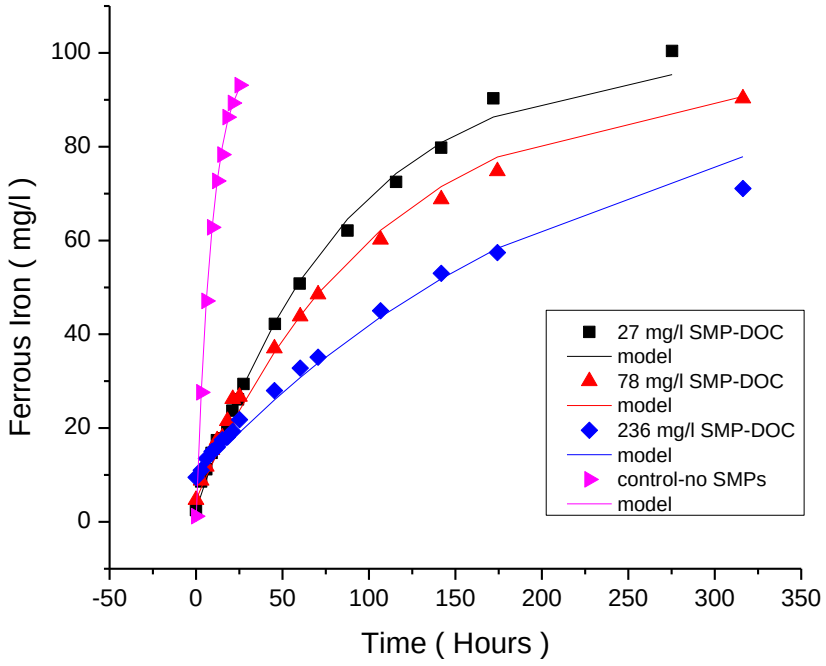

Figure 3-11. Fitted data of the pyrite oxidation experiments with lysis derived SMPs. Symbols represent experimental data and the lines are obtained using equations of the first-order rate models obtained from the nonlinear regressions.

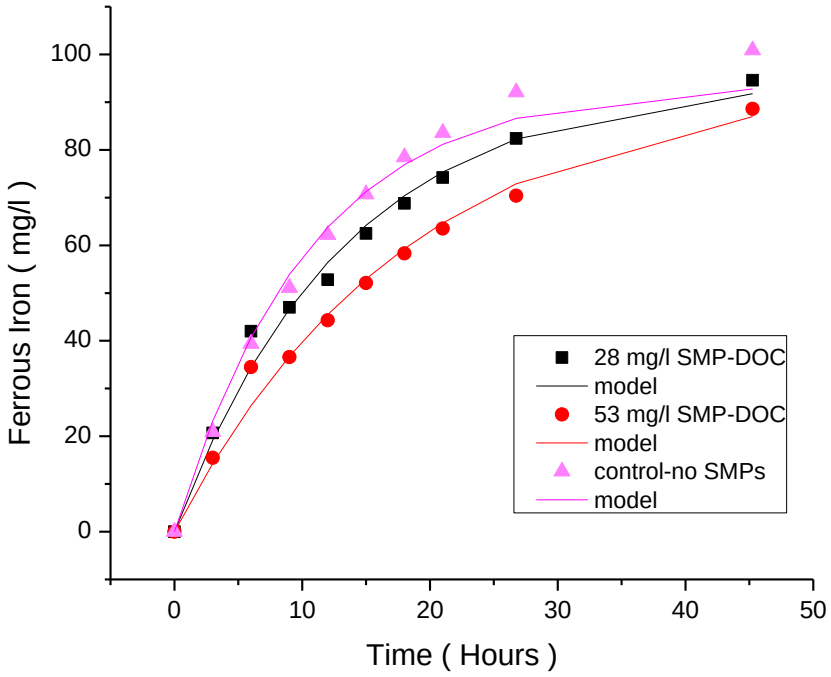

Figure 3-12. Fitted data of the pyrite oxidation experiments with growth derived SMPs. Symbols represent experimental data and the lines are obtained using equations of the first-order rate model obtained from the nonlinear regressions.

The rate of pyrite oxidation decreased steadily for the three lysis product SMP concentrations. The average first-order reaction constant for the control flasks was 0.108 ± 0.003 hr^{-1}. When lysate SMP was added at a concentration of 27 mg/l DOC, the rate constant was 0.012 ± 0.01 hr^{-1}, a reduction of 89%. The rate constant followed a decreasing trend at higher SMP-DOC concentrations of 78 and 236 mg/l DOC, with associated first-order rate constants of 0.009 ± 0.002 hr^{-1} and 0.004 ± 0.001 hr^{-1}, respectively. The added first-order reaction constant reduction per mg/l of SMP-DOC for the 78 and 236 mg/l DOC treatments were only 1% of that of the 27 mg/l DOC treatment. This is suggestive of the near saturation of the 90 mg/l (1.6 mM) ferric iron added by a 27 mg/l DOC or lower concentration of SMP. Muller and Raymond (1984) have shown that iron transport by Ferrioxamine B, D1, D2 and E

siderophores was a saturable process. None of the lysis treatments achieved a plateau in ferrous iron increase within the 300-hour experiment. In comparison, the Fe2+ accumulation for Fe-DFAM complexes reached a plateau concentration in less than 150 hours, similar to the control (Figure 3-13). One explanation for the difference is that SMP-ferric iron complexes are weaker than siderophore complexes allowing either lower activity of the complexed ferric iron or dissociation of the complex and release of free ferric ions. (Rose and Waite (2005) reported that the superoxide reduction of ferric iron complexed by salicylate, 5-sulfosalicylate, Deferoxamine B, or EDTA produced more complexed than free ferrous iron, indicating reduction of iron in the complexed form rather than complex dissociation followed by ferric iron reduction. Here it needs to be clear that the comparison with known siderophores is made only as a way of evaluating possible mechanisms of interaction between SMPs and iron. It should not be taken as a suggestion that the SMPs used in this work are actually siderophores produced by acidophilic heterotrophs.

The lysate SMP produced a significantly larger decrease in the pyrite oxidation rate than an equivalent DOC concentration from growth products, with respective decreases from the control rate constant of 89% and 27%. One possible reason for the growth product's weaker inhibition of pyrite oxidation as compared to similar carbon equivalent lysis solutions could be the smaller fraction of < 1 KDa molecules. The specific classes of molecules found in the amw fraction (< 1 KDa) for the lysis derived SMP are unknown. Lysis of cells is known to release proteins, polysaccharides, nucleic acids, and lipids (Sutherland and Wilkinson, 1971). The autoclaving technique used on the culture liquid to obtain lysis SMP is expected to release lower amw molecules through hydrolysis (Campbell *et al.*, 1978). Amino acids in particular are

expected to be released during hydrolysis of cytoplasmic proteins. It has been shown that certain amino acids such as aspartic acid have the ability to chelate ferric iron down to a pH of 2.5 (Smythe and Schmidt, 1930). Since the fluorescence EEM spectra modeling has shown that greater than 70% of the lysate SMP solution contain protein like components, interaction of iron and amino acids may have a significant role on the inhibition of pyrite oxidation. The autoclaving process used to induce lysis, although being a time efficient laboratory technique, may result in much more lower amw hydrolysis products compared to an environmental lysis process. Lysis of cells in the environment involves endogenous decay processes during starvation periods, cryptic growth, and autolysin enzymes (Mason *et al.*, 1986).

The first order rate constant, K, for the bulk ultrafiltration experiment was found to be significantly lower than the <1 KDa one (0.009 ± 0.001 vs. 0.012 ± 0.001 hr^{-1}) suggesting contribution of fractions >10 KDa to the slowing down effect of pyrite oxidation. No significant difference was present between the <1 KDa and <10 KDa lysate solution rates. As demonstrated earlier, saturation of the added iron by a low SMP-DOC concentration makes it difficult to compare the results from the calculation of the reduction of the pyrite oxidation rate constant for a mg/l SMP-DOC for the fractions with amw less than and greater than 10 KDa. Put in a different way, it is difficult to differentiate between the DOC concentration effect and the chemical distinction for the amw >10 KDa fraction.

The first order reaction modeling for the deferoxamine mesylate pyrite oxidation experiments done with the initial ferric iron (ICP-OES iron test values) did not converge. Instead, the initial 1-10 phenanthroline measured ferric iron was used for the modeling and the rate constant K determined. Further modeling with both the initial soluble ferric iron and the

rate constant as unknowns yielded a best fit initial ferric iron within 10 % of the 1-10 phenanthroline measured ferric iron for all three DFAM treatments suggesting this is the right choice of initial ferric iron for the first order reaction model. The rate constants obtained were 0.037 ± 0.003, 0.039 ± 0.006, 0.047 ± 0.007, and 0.108 ± 0.009 hr^{-1} for the 270, 540, 812 mg/l DFAM, and control treatments respectively. The rate constants for all three DFAM treatments were not significantly different from each other at the 95% confidence interval. Since it has been shown that a portion of the ferric iron is likely to be completely complexed with DFAM and kept from reacting, a rate constant closer to that of the control's was expected for the remaining presumably free ferric iron. However, the initial rate for the DFAM treatments was about 62% less than the rate of the control with no DFAM. This may be due to possible extra complexation happening to the DFAM-Fe complex. At pH 1.8, most of the primary complexes formed with DFAM will be found as monohydroxamate and bishydroxamate species and thus will have free hydroxyl and carbonyl groups. Thus secondary complexes of ferric iron may form with these groups, albeit weaker than the main DFAM-Fe complexes and so allowing pyrite oxidation with a slower rate. The effect can also be due secondary complexes of DFAM-Fe to the pyrite surface. Kalinowski et al. (2000) has shown that deferoxamine mesylate forms surface complexes with iron on the surface of hornblende.

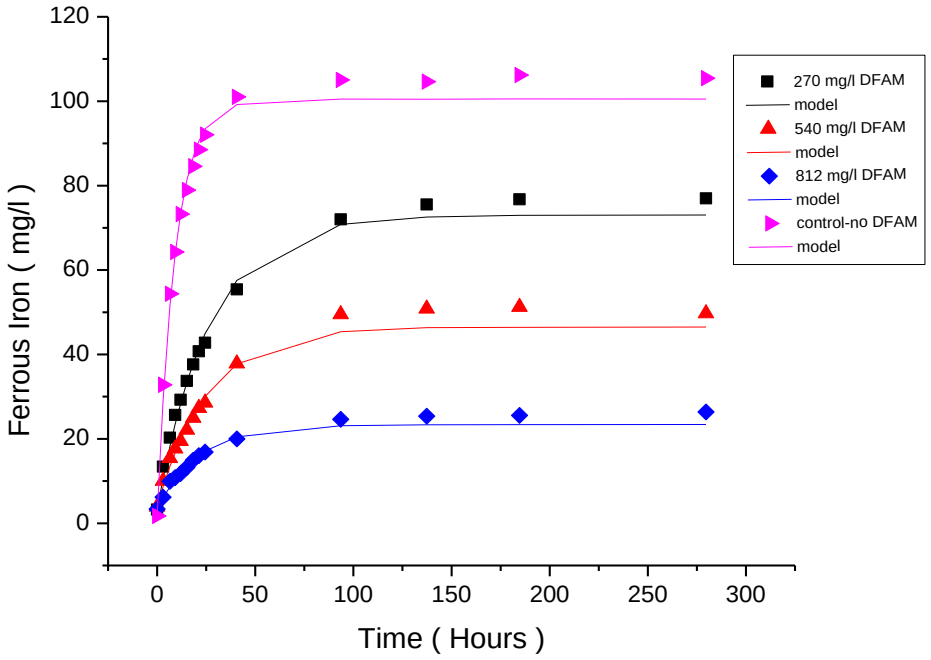

Figure 3-13. Ferrous iron production during pyrite oxidation experiments containing deferoxamine mesylate. Experiments were done in 200 ml, pH 1.8 solutions and contained 2.0 g of pyrite and initial ferric iron concentration of about 85 mg/l ferric iron. Symbols represent experimental data and the lines are obtained using equations of first-order rate models obtained by nonlinear regression.

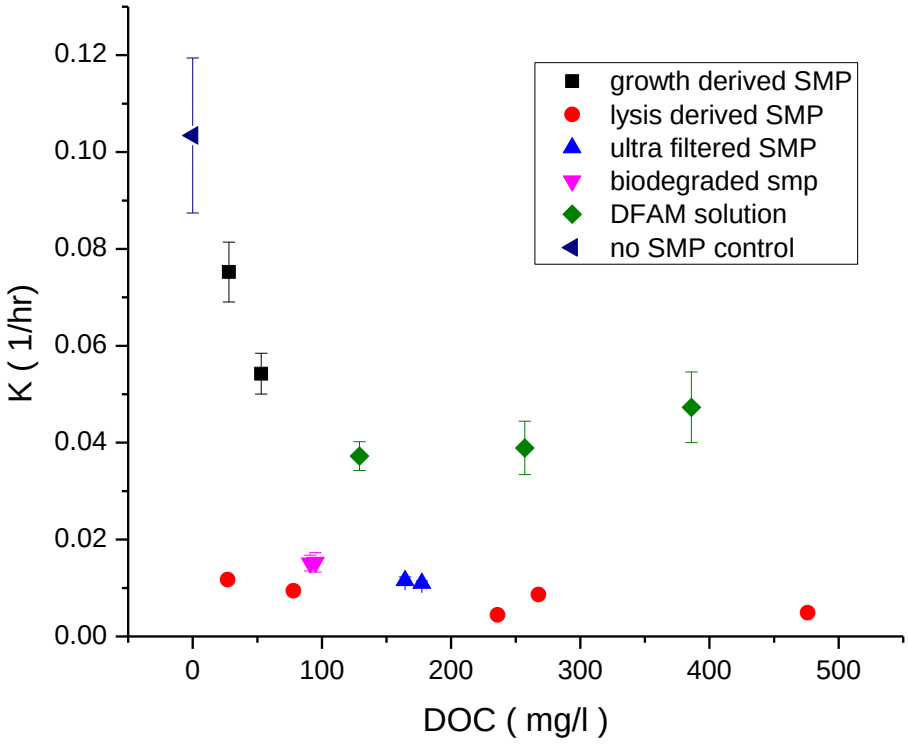

Figure 3-14. First order pyrite oxidation rate constants as a function of SMP-DOC concentrations. Data from UF experiments are for apparent molecular weight fractions <1 KDa, and <10 KDa. The biodegradation experiments data are from the two biodegraded filtrates with the one containing ferric iron prior to biodegradation. The unfiltered bulk UF treatment and the sterile biodegradation treatment are added to the three lysis experiments and make up the above 5 lysis derived SMP data points. The DFAM treatments contained 129, 257, and 386 mg/l DFAM-DOC. Error bars represent 95% confidence intervals for the rate constants.

The biodegradation pyrite oxidation experiments indicated an equal rate of pyrite oxidation for the two biodegraded solutions, with and without ferric iron (a K of 0.015 ± 0.002 hr^{-1}). The pyrite oxidation rate for the sterile biodegradation experiment filtrate had a K of 0.005 ± 0.001 $hr^{-1}$and is significantly less than that of the two biodegraded filtrates. This demonstrates that the biodegraded fraction does have an impact on the slowing down of pyrite oxidation.

As the pyrite oxidation rates determined for the various SMP treatments were shown to depend mainly on the SMP-DOC content, an SMP-DOC inhibition model was developed.

$$k = k_{max} * \frac{k_{smp}}{k_{smp} + c}$$

Where k_{max} (hr^{-1}) is the average pyrite oxidation rate constant of the no SMP control treatments, k_{smp} is the inhibition constant in mg/l SMP-DOC, c is the SMP-DOC concentration of the various considered treatments and k is the fitted pyrite oxidation rate constant (hr^{-1}). The respective SMP-DOC values were used to calculate k_{smp} by minimizing the squared residual between the k (inhibition model prediction) and the pyrite oxidation experiment derived rate constants. The inhibition model runs were done for all SMP treatments and the lysis derived SMP treatments. The model result for all SMP treatments is seen in Figure 3-15. A best fit solution was obtained at k_{smp} of 21.7 ± 14.3 mg/l SMP-DOC and an associated R^2 of 0.749. The model run for only the lysis derived SMP treatments resulted in an R^2 of 0.953 and a k_{smp} of 7.5 ± 4.7 mg/l SMP-DOC for the best fit solution (Figure 3-16). The model for only the lysis derived SMP treatments had a higher correlation coefficient and narrower range for the 95% confidence intervals of the determined k_{smp} compared to the model for all SMP treatments. This is not surprising as the lysis derived SMP were shown to have much more inhibition impact than the growth derived SMP. The low k_{smp} of 7.5 mg/l SMP-DOC for the lysis derived SMP inhibition model indicates the sensitivity of the pyrite oxidation rate to the presence of a relatively low SMP-DOC concentration. The model also shows the decreasing effect of the lysis derived SMP-DOC on the rate of pyrite oxidation within the range of concentrations of SMP-DOC used.

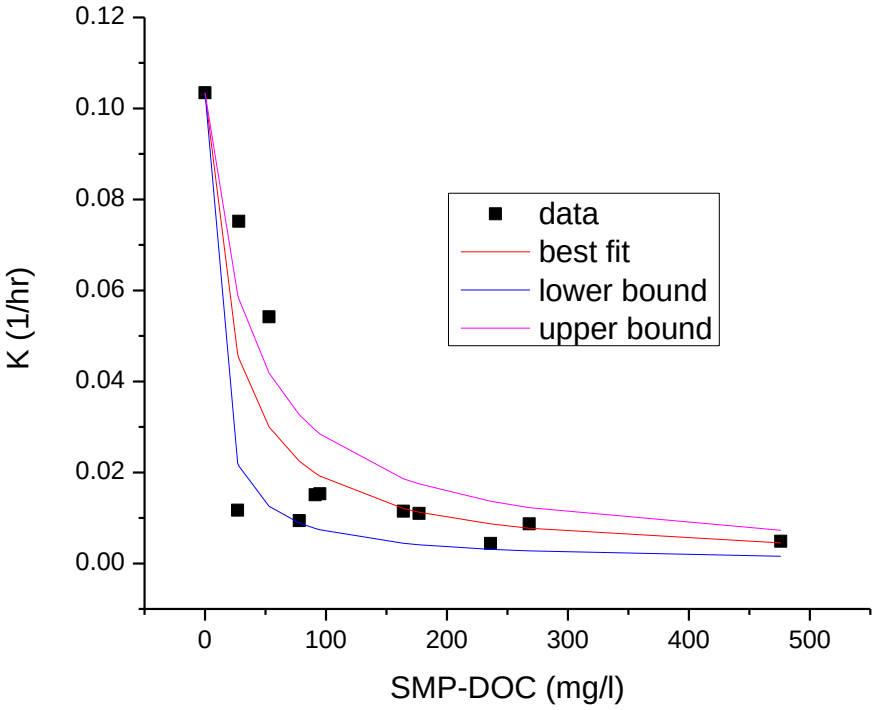

Figure 3-15. SMP pyrite oxidation Inhibition model run results for all the SMP treatments. The best fit line represents the inhibition model predicted rate constants at the best fit inhibition constant, k_{smp} of 21.7 mg/l SMP-DOC. The 95% confidence levels on k_{smp} were used to generate a lower and upper bound predictions for K. The inhibition model was run for all SMP treatments (n=12).

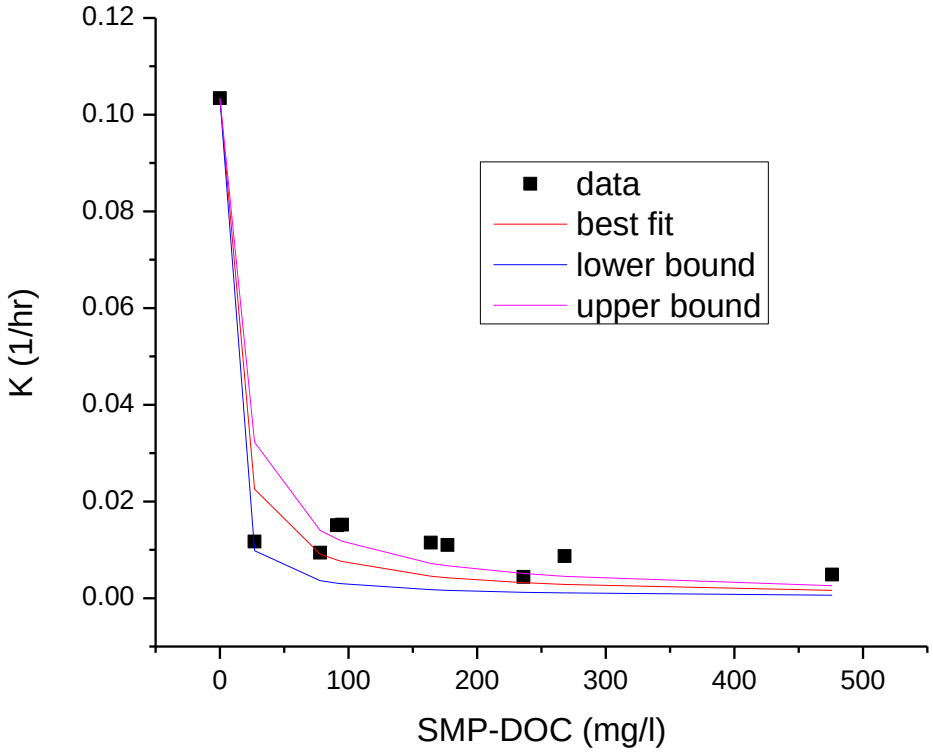

Figure 3-16. SMP pyrite oxidation Inhibition model run results for lysis derived SMP treatments. The best fit line represents the inhibition model predicted rate constants at the best fit inhibition constant, k_{smp} of 7.5 mg/l SMP-DOC. The 95% confidence levels on k_{smp} were used to generate a lower and upper bound predictions for K. The inhibition model was run for all lysis derived SMP treatments including the ultra-filtered and biodegraded SMP (n=10).

3.3.5 Implications

Most research on AMD remediation by addition of organic carbon to mine wastes has focused on oxygen depletion and inhibition of bacterial iron oxidation. However, it is likely that the chemical oxidation of pyrite by ferric iron is the slower step in the acid mine drainage formation cycle when oxygen is available for bacterial growth. In that case, complexation of ferric iron by internal cycling of microbial organic compounds as demonstrated in this study may be an important secondary process in mine site remediation.

The study of the remediation of mine waste sites by carbon addition is a complex task requiring many resources. An alternative approach is the use of mathematical models to simulate and investigate the biochemical and geochemical changes expected to happen during remediation. This work provides quantitative information on the concentration of SMP generated from acidophilic heterotrophic cultures of known initial organic carbon substrate. A predictive model has also been developed for lysis derived SMP-DOC of up to 500 mg/l to predict pyrite oxidation rate constant when pyrite is not limiting. Preliminary results have also been obtained about the extent of biodegradation of SMP. These results can be integrated with AMD remediation models and help advance the investigation of mine waste remediation.

3.4 Conclusions

Soluble microbial products (SMP) resulting from growth or lysis of cultures enriched from mine waste rock reduce the rate of chemical oxidation of pyrite by ferric iron, possibly by formation of organo-ferric iron complexes. The rate decrease was proportional to the SMP-DOC concentration for both growth and lysis derived SMPs as quantified by fitting a first-order rate model to ferrous iron production data. For the same SMP-DOC concentrations, lysis derived SMPs had much more impact on reduction of the rate of pyrite oxidation than growth derived SMPs. Low molecular weight compounds, < 1 KDa were dominantly present in the lysis derived SMPs. Experiments with the siderophore deferoxamine mesylate (DFAM) showed that complexation of ferric iron led to the inhibition of pyrite oxidation suggesting complexation may be the mechanism of interaction between SMPs and ferric iron.

3.5 References

Bilgin, A. A., Silverstein, J. and Jenkins, J. D. (2004). Iron respiration by Acidiphilium cryptum at pH 5. *Fems Microbiology Ecology* **49**(1): 137-143.

Boero, V. J., Bowers, A. R. and Eckenfelder, W. W. (1996). Molecular weight distribution of soluble microbial products in biological systems. *Water Science and Technology* **34**(5-6): 241-248.

Bond, P. L., Druschel, G. K. and Banfield, J. F. (2000). Comparison of acid mine drainage microbial communities in physically and geochemically distinct ecosystems. *Applied and Environmental Microbiology* **66**(11): 4962-+.

Breault, R. F., Colman, J. A., Aiken, G. R. and McKnight, D. (1996). Copper speciation and binding by organic matter in copper-contaminated streamwater. *Environmental Science & Technology* **30**(12): 3477-3486.

Brothers, L. A., Engel, M. H. and Elmore, R. D. (1996). The late diagenetic conversion of pyrite to magnetite by organically complexed ferric iron. *Chemical Geology* **130**(1-2): 1-14.

Bunescu, A., Besse-Hoggan, P., Sancelme, M., Mailhot, G. and Delort, A. M. (2008). Fate of the nitrilotriacetic Acid-Fe(III) complex during photodegradation and biodegradation by Rhodococcus rhodochrous. *Applied and Environmental Microbiology* **74**(20): 6320-6326.

Campbell, L. K., Knox, K. W. and Wicken, A. J. (1978). Extractability of cell-wall polysaccharide from lactobacilli and streptococci by autoclaving and by dilute acid. *Infection and Immunity* **22**(3): 842-851.

Chen, M., Wang, W. X. and Guo, L. D. (2004). Phase partitioning and solubility of iron in natural seawater controlled by dissolved organic matter. *Global Biogeochemical Cycles* **18**(4).

Cory, R. M. and McKnight, D. M. (2005). Fluorescence spectroscopy reveals ubiquitous presence of oxidized and reduced quinones in dissolved organic matter. *Environmental Science & Technology* **39**(21): 8142-8149.

Dong, M. M., Mezyk, S. P. and Rosario-Ortiz, F. L. (2010). Reactivity of Effluent Organic Matter (Ef0M) with Hydroxyl Radical as a Function of Molecular Weight. *Environmental Science & Technology* **44**(15): 5714-5720.

Dudal, Y., Sevenier, G., Dupont, L. and Guillon, E. (2005). Fate of the metal-binding soluble organic matter throughout a soil profile. *Soil Science* **170**(9): 707-715.

Edwards, K. J., Bond, P. L. and Banfield, J. F. (2000). Characteristics of attachment and growth of Thiobacillus caldus on sulphide minerals: a chemotactic response to sulphur minerals? *Environmental Microbiology* **2**(3): 324-332.

Francis, A. J. and Dodge, C. J. (1993). Influence of complex structure on the biodegradation of iron-citrate complexes. *Applied and Environmental Microbiology* **59**(1): 109-113.

Ganesh, R., Robinson, K. G., Reed, G. D. and Sayler, G. S. (1997). Reduction of hexavalent uranium from organic complexes by sulfate- and iron-reducing bacteria. *Applied and Environmental Microbiology* **63**(11): 4385-4391.

Gao, H. Z. and Zepp, R. G. (1998). Factors influencing photoreactions of dissolved organic matter in a coastal river of the southeastern United States. *Environmental Science & Technology* **32**(19): 2940-2946.

Gross, S. and Robbins, E. I. (2000). Acidophilic and acid-tolerant fungi and yeasts. *Hydrobiologia* **433**(1-3): 91-109.

Hayen, H. and Volmer, D. A. (2006). Different iron-chelating properties of pyochelin diastereoisomers revealed by LC/MS. *Analytical and Bioanalytical Chemistry* **385**(3): 606-611.

Holakoo, L., Nakhla, G., Yanful, E. K. and Bassi, A. S. (2006). Chelating properties and molecular weight distribution of soluble microbial products from an aerobic membrane bioreactor. *Water Research* **40**(8): 1531-1538.

Huang, G. T., Jin, G., Wu, J. H. and Liu, Y. D. (2008). Effects of glucose and phenol on soluble microbial products (SMP) in sequencing batch reactor systems. *International Biodeterioration & Biodegradation* **62**(2): 104-108.

Johnson, D. B. (1995). Acidophilic microbial communities - candidates for bioremediation of acidic mine effluents. *International Biodeterioration & Biodegradation* **35**: 41-58.

Johnson, D. B., Yajie, L. and Okibe, N. (2008). "Bioshrouding" - a novel approach for securing reactive mineral tailings. *Biotechnology Letters* **30**(3): 445-449.

Kalinowski, B. E., Liermann, L. J., Brantley, S. L., Barnes, A. and Pantano, C. G. (2000). X-ray photoelectron evidence for bacteria-enhanced dissolution of hornblende. *Geochimica Et Cosmochimica Acta* **64**(8): 1331-1343.

Kim, D. and Strathmann, T. J. (2007). Role of organically complexed iron(II) species in the reductive transformation of RDX in anoxic environments. *Environmental Science & Technology* **41**(4): 1257-1264.

Kuo, W. C. and Parkin, G. F. (1996). Characterization of soluble microbial products from anaerobic treatment by molecular weight distribution and nickel-chelating properties. *Water Research* **30**(4): 915-922.

Liu, G. L., Fernandez, A. and Cai, Y. (2011). Complexation of Arsenite with Humic Acid in the Presence of Ferric Iron. *Environmental Science & Technology* **45**(8): 3210-3216.

Lottermoser , B. (2003). Mine wastes: characterization, treatment and environmental impacts. Berlin, Heidelberg, and New York. *Springer*.

Luther, G. W., Kostka, J. E., Church, T. M., Sulzberger, B. and Stumm, W. (1992). Seasonal iron cycling in the salt-marsh sedimentary environment - the importance of ligand complexes with fe(ii) and fe(iii) in the dissolution of fe(iii) minerals and pyrite, respectively. *Marine Chemistry* **40**(1-2): 81-103.

Luther, G. W., Shellenbarger, P. A. and Brendel, P. J. (1996). Dissolved organic Fe(III) and Fe(II) complexes in salt marsh porewaters. *Geochimica Et Cosmochimica Acta* **60**(6): 951-960.

Magnuson, T. S., Hodges-Myerson, A. L. and Lovley, D. R. (2000). Characterization of a membrane-bound NADH-dependent Fe3+ reductase from the dissimilatory Fe3+-reducing bacterium Geobacter sulfurreducens. *Fems Microbiology Letters* **185**(2): 205-211.

Marchand, E. A. and Silverstein, J. (2002). Influence of heterotrophic microbial growth on biological oxidation of pyrite. *Environmental Science & Technology* **36**(24): 5483-5490.

Marchand, E. A. and Silverstein, J. (2003). The role of enhanced heterotrophic bacterial growth on iron oxidation by Acidithiobacillus ferrooxidans. *Geomicrobiology Journal* **20**(3): 231-244.

Mason, C. A., Hamer, G. and Bryers, J. D. (1986). The death and lysis of microorganisms in environmental processes. *Fems Microbiology Reviews* **39**(4): 373-401.

McKnight, D. M., Bencala, K. E., Zellweger, G. W., Aiken, G. R., Feder, G. L. and Thorn, K. A. (1992). Sorption of dissolved organic-carbon by hydrous aluminum and iron-oxides occurring at the confluence of deer creek with the snake river, summit county, colorado. *Environmental Science & Technology* **26**(7): 1388-1396.

McKnight, D. M., Feder, G. L., Thurman, E. M., Wershaw, R. L. and Westall, J. C. (1983). Complexation of copper by aquatic humic substances from different environments. *Science of the Total Environment* **28**(JUN): 65-76.

McKnight, D. M. and Morel, F. M. M. (1980). Copper complexation by siderophores from filamentous blue-green-algae. *Limnology and Oceanography* **25**(1): 62-71.

Moses, C. O., Nordstrom, D. K., Herman, J. S. and Mills, A. L. (1987). Aqueous pyrite oxidation by dissolved-oxygen and by ferric iron. *Geochimica Et Cosmochimica Acta* **51**(6): 1561-1571.

Muller, G. and Raymond, K. N. (1984). Specificity and mechanism of ferrioxamine-mediated iron transport in streptomyces-pilosus. *Journal of Bacteriology* **160**(1): 304-312.

Neilands, J. B. (1995). Siderophores - structure and function of microbial iron transport compounds. *Journal of Biological Chemistry* **270**(45): 26723-26726.

Osorio, H., Martinez, V., Nieto, P. A., Holmes, D. S. and Quatrini, R. (2008). Microbial iron management mechanisms in extremely acidic environments: comparative genomics evidence for diversity and versatility. *Bmc Microbiology* **8**. 203

Rose, A. L. and Waite, T. D. (2003). Kinetics of iron complexation by dissolved natural organic matter in coastal waters. *Marine Chemistry* **84**(1-2): 85-103.

Rose, A. L. and Waite, T. D. (2005). Reduction of organically complexed ferric iron by superoxide in a simulated natural water. *Environmental Science & Technology* **39**(8): 2645-2650.

Smythe, C. V. and Schmidt, C. L. A. (1930). Studies on the mode of combination of iron with certain proteins, amino acids, and related compounds. *Journal of Biological Chemistry* **88**(1): 241-269.

Sutherland, I. W. and Wilkinson, J. F. (1971). Chapter IV Chemical Extraction Methods of Microbial Cells. *Methods in Microbiology*. J. R. N. a. D. W. Ribbons, *Academic Press*. **Volume 5, Part B:** 345-383.

Tyson, G. W., Chapman, J., Hugenholtz, P., Allen, E. E., Ram, R. J., Richardson, P. M., Solovyev, V. V., Rubin, E. M., Rokhsar, D. S. and Banfield, J. F. (2004). Community structure and metabolism through reconstruction of microbial genomes from the environment. *Nature* **428**(6978): 37-43.

Tyson, G. W., Lo, I., Baker, B. J., Allen, E. E., Hugenholtz, P. and Banfield, J. F. (2005). Genome-directed isolation of the key nitrogen fixer Leptospirillum ferrodiazotrophum sp nov from an acidophilic microbial community. *Applied and Environmental Microbiology* **71**(10): 6319-6324.

CHAPTER 4. THE ROLE OF PORE REACTIONS ON ACID MINE DRAINAGE GENERATION IN WASTE ROCK

Abstract

The generation of acid mine drainage (AMD) from waste rock piles is a process involving numerous biological, geochemical and hydrologic processes. This research investigated AMD production from waste rock piles with a focus on the contribution of rock pore reactions. Four columns packed with waste rock were run in series to simulate AMD generation in waste rock piles. Iron, trace metals, and sulfate concentrations as well as, pH, and the number of acidophilic iron oxidizing and heterotrophic organisms were determined for both bulk liquid and rock pore liquid. The porosity and water saturation of rock samples were measured. Results showed the rock pore liquid containing 6 to 17 times higher concentrations of iron compared to the bulk liquid. Metals and sulfate followed the same trend. Heterotrophic acidophilic microorganisms in pore liquid were on average 2 orders of magnitude more than the bulk liquid, whereas there were about the same number of iron oxidizing organisms in both liquid regions. A conservative pulse tracer test confirmed the presence of a dual porosity system with an elongated tail and a tracer recovery of 58% and 68% after 1 and 20 days respectively. An average ferric iron production of $5.7^{*}\ 10^{-9}$ mol/Kg-S of waste rock mass was obtained. The research shows the importance of reactions in rock pores and the diffusive transport of the products for the generation of AMD in waste rock piles and underscores the need for remediation efforts to focus on these active regions.

4.1 Introduction

4.1.1 AMD introduction

Waste rock piles are used as a form of mine waste disposal. These piles contain sulfide minerals which when oxidized by oxygen and ferric iron can release harmful heavy metals. The transport of these contaminants to surface and ground waters are of serious concern to aquatic plants and animals (Warner 1971; Gray, 1998; Peplow and Edmonds, 2005; Pond *et al.*, 2008). Water treatment facilities receiving metal contaminated raw water are also forced to spend extra resources on treatment. In the USA alone there are an estimated 550,000 or more abandoned mines (Lyon *et al.*, 1993). The task of cleaning up these mines and properly storing the waste rock, tailings and other waste has become a public burden.

4.1.2 Waste rock piles

Waste rock piles can be made up of mm to boulder sized rocks, with varying mineralogical content. Waste rock piles can be as tall as tens of meters and can cover several square kilometers (Blowes *et al.*, 2003). At low pH (< 3.5), ferric iron is the primary oxidant of sulfide resulting in ferrous iron and sulfate (equation 4-1). The ferrous iron is predominantly converted to ferric iron by the action of iron oxidizing organisms which use oxygen as the terminal electron acceptor (equation 4-2). The overall rate of sulfide oxidation and acidity production as well as heavy metal release is dependent on the activity of these autotrophic organisms (Singer and Stumm, 1970).

$$FeS_2 + 14Fe^{3+} + 8H_2O \rightarrow 15Fe^{2+} + 2SO_4^{2-} + 16H^+ \quad \text{.....(4-1)}$$

$$4Fe^{2+} + O_2 + 4H^+ \rightarrow 4Fe^{3+} + 2H_2O \text{.....(4-2)}$$

Oxygen and water availability are important parameters in the proliferation of these aerobic organisms. The transport of oxygen and water is dependent on factors such as the mineralogy, size of pile, the bulk porosity, and the fine material content (Edwards *et al.*, 2000; Stockwell *et al.*, 2006). Individual rocks have different porosities and these give rise to varying rates of oxygen and water transport to rock pores through diffusion and advection. As soluble ferrous iron is mainly generated at the interface of a sulfide surface, iron oxidizing organisms prefer to live closer to these solid surfaces (Edwards *et al.*, 2000). Experiments have shown the attachment of iron oxidizing organisms through a biofilm to pyrite grains with an accumulation of ferric iron to very high concentrations inside the biofilm (Gehrke *et al.*, 1998; Gehrke *et al.*, 2001; Sand and Gehrke, 2006). This dependence of the organsims on the chemical reaction step of sulfide oxidation can also create a dependence of their activity on the residence time of a liquid in contact with a sulfide surface. A longer residence time can lead to ferric iron accumulation.

Addition of an external source of organic carbon to mine waste has been proposed as a remediation approach with the growth of heterotrophic acidophiles resulting in the competition for oxygen, and reactive sulfide surfaces with autotrophic organsims as well as the reduction of ferric iron activity by hetrotrophic microbial products (Marchand and Silverstein, 2002; Bilgin *et al.*, 2004; Johnson *et al.*, 2008). A better understanding of the waste rock sulfide reaction sites in terms of the biological, chemical and transport processess happening can aid in the design of an effective organic carbon addition strategy. Previous waste rock pile and column experiments have focused on geochemical and microbial interpretation of bulk liquid samples (Stromberg and Banwart, 1999; Blowes *et al.*, 2003). These however represent an

aggregate of what is happening in microenvironments of the pile material and thus do not contribute as much in understanding the processess in these reactive microenvironments.

This work investigated the production of acid mine drainage in waste rock packed columns. The main focus of the research was comparing the chemical and microbial activity measured from waste rock pore liquid and bulk liquid samples. The physical properties of selected individual rocks were carefully measured. The liquid transport in the columns was studied by using a conservative tracer.

4.2 Materials and Methods

4.2.1 Research set up

Waste rock from an abandoned mine near Leadville, CO was used to pack five conical bottom tanks. About 150 kilograms of waste rock was packed in each column. The particle sizes ranged between 2.5 and 8.5 cm in diameter. The tanks were 46.4 cm diameter and the height of the packed rocks was 69.2 cm. A perforated plate separated the conical part of the tank from the rocks and provided unconstrained draining. Valves were fitted to the bottom of the tanks for sampling and flow control. Liquid was fed to the top of the columns through ¼ inch id tubing at the center of the cover and on to a splash plate. Enhanced flow distributors were installed to C4, C3 and C5 on days 120, 130 and 225 respectively. The flow distributors were made with an acrylic material and featured 20 drip needles distributed on 40.6 cm diameter and 0.63 cm thick sealed cylinder. Four of the tanks were connected in series with effluent from one tank being pumped to the top of the next tank and so on. Schematic of the tanks is provided in Figure 4-1. Two side sampling ports were used to obtain rock samples. A central humidity probe was used to measure humidity and temperature inside the tanks. All humidity and temperature measurements were done at a fixed depth of 30.5 cm from the top of the packed rocks. The tanks are referred to as columns for the subsequent sections.

4.2.2 Flow experiments

The columns were packed with rocks and filled up completely with water to measure the bulk porosity and to get rid of any existing precipitates on the rock surfaces. Following this, the liquid was completely drained and the flow experiments were started. Liquid was circulated

at 500 ml/min through C1 and kept in an 80 liter reservoir at a set 5 day reservoir liquid residence time. The recirculation flow of C1 was undertaken for 75 days prior to starting the four column series flow experiment (data for the first 75 days not shown). Thereafter, the reservoir liquid of C1 was used as a seed by pumping a portion of the liquid at 11 ml/min to C2 and in series through C3, C4 and C5. Column 1 was run in a recirculation mode throughout the experiment and was hydraulically distinct from the other four columns. Liquid effluent samples from the bottom of each column were collected and filtered through a 0.22 um nylon filter and analyzed for pH, sulfate, total dissolved iron, dissolved ferrous iron and selected metals. Measurement of dissolved oxygen and enumeration of acidophilic iron oxidizing and acidophilic heterotrophic microorganisms by means of the most probable number was undertaken from unfiltered column effluent samples. Solid rock samples were used to enumerate the pore liquid microorganisms.

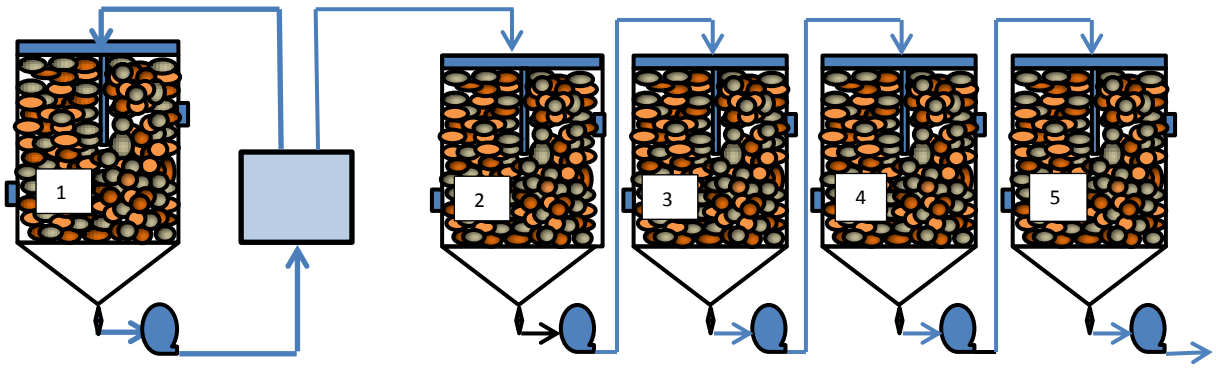

Figure 4-1. Schematics of the column experiment set up. The end of the cylindrical part of the columns had a perforated plate allowing the free drainage of liquid to the conical part. Column 1 has a recirculating reservoir which was daily wasted and fed with water to maintain a 5 day residence time. Liquid from the reservoir was applied at 11 ml/min to column 2 and in series to all the other columns.

4.2.3 Porosity and saturation measurement

The porosity and saturation measurements used 30 rock samples from each of the columns. The rocks were taken from five different depths (0, 23.4, 28.9, 33.3, and 54 cm). The depths were measured from the top of the packed rocks. The rocks were taken out of the columns and were put on a plastic for 15 minutes to get rid of surface liquid. The initial weights were then taken and the rocks oven dried at 80 degree centigrade for 24 hours. Following this, their dry weights were recorded. They were then put in a water bath for at least 6 hours and then put in a water filled vacuum chamber under 80 KPa vacuum for 5 more hours. Thereafter air-saturated weights were taken after drying of surface liquid for 15 minutes. The apparent immersed weight was then measured by suspending the rocks in water. Porosity, P, was calculated using the formula,

$$\mathrm{P} = \frac{(\text{ air saturated weight} - \text{dry weight})}{(\text{air saturated weight} - \text{apparent immersed weight})}$$

Water Saturation, S, was calculated as follows:

$$\mathrm{S} = \frac{(\text{initial weight} - \text{dry weight})}{\mathrm{P} * (\text{air saturated weight} - \text{apparent immersed weight})}$$

4.2.4 Rock pore liquid measurement

A total of 6 rocks were sampled at a depth of 15 cm from each column. The weights were between 146 and 164 g. Following the initial weight check, two rocks were put in a single container (thus 3 containers for each column). The containers had 400 ml of a pH 1.8, 20 mg/l benzoic acid solution to prevent microbial activity. The mixture was mixed at 100 rpm and

sampled for (Fe2), (Fe tot) and pH. Selected samples were analyzed for sulfate and metals. At the end of the experiment, the volume and porosity of the rocks were measured.

4.2.5 Enumeration of microorganisms

Enumeration of iron oxidizing and carbon consuming organisms was done using the most probable number method (MPN). Appropriate media was pipeted to 12 culture tubes, the samples added and serially diluted either at 1:5 or 1:10 ratios. Each dilution was then transferred to eight wells (thus 12*8). The MPN plates were then incubated for 3-5 weeks and the most dilutions at which growth occurred was identified and converted into number using a statistical table (Rowe *et al.*, 1977).

The media of both groups of organisms contained minerals (0.81 g/l NH_4Cl, 0.1 g/l KCl , 0.5 g/l K_2HPO_4 , 0.5 g/l $MgSO_4.7H_2O$, 0.19 g/l $CaCl_2.2H_2O$ and 0.02 g/l $FeSO_4.7H_2O$). The iron oxidizing organisms media contained 8.9 g/l ferrous iron ($FeSO_4.7H_2O$) substrate and the above minerals acidified to pH 2.5 using 3N HCl. The acidophilic heterotrophic organisms media had 0.106 g/l trypticase soy broth, 1.0 g/l glucose, 0.1 g/l yeast extract, and a 50 mg/l resazurin, all adjusted to pH 2.5 using 3N HCl. At low pH resazurin changes from pink to colorless during oxidation of glucose. The mineral media was sterilized by autoclaving at 121 degree centigrade and 15 psi for 20 minutes while the rest of the media were filter sterilized through sterile 0.22 um cellulose acetate filters.

Bulk liquid samples were taken directly from column effluents. Rock samples were put in a solution of 0.3 % sodium pyrophosphate, 0.22 % sodium polyphosphate and 0.1 % tween-80 (Aldrich Chemical Co) for 4-6 hours (Jenkins, 2006). There after the mixture was allowed to

settle to remove precipitates and the supernatant used as the inoculation sample. The porosity, and water saturation of the rock samples used for the MPN test were also measured. The pore liquid volume was then used to calculate the dilution factor from which the microbial numbers in the rock pore liquid were determined.

4.2.6 Tracer test

A 2 M bromide (NaBr) solution was injected for 5 minutes to the top of C2. This corresponds to 8.79 g (0.11 mol) of Br^-. The column effluent from C5 was monitored with a bromide probe (Cole Parmer Corp) connected to a YSI mV meter. Calibration standards were prepared by dissolving NaBr into previously collected C5 effluent to account for the high ionic strength of the column effluent. The probe was periodically recalibrated to account for a possible drift.

4.2.7 Analytical methods

Ferrous and total soluble iron was measured using the 1-10 phenanthroline method. Hydroxylamine HCl was used to reduce (Fe3) to (Fe2) followed by the color producing complexation reaction with 1-10 phenanthroline. (Fe3) was calculated as the difference of the (Fe tot) and (Fe2). Sulfate was measured on a Dionex IC (DX-500) using an anion column (AS14) and a CD20 conductivity detector. An elluent containing 8 mM Na_2CO_3 and a 1 mM $NaHCO_3$ was used. pH was measured using an Accumet combination electrode and meter. Metal analysis was done using ICP-OES or ICP-MS (LEGS Lab, Department of Geological Sciences, University of

Colorado). Dissolved oxygen was measured using a YSI 5901 BOD probe and a YSI 52 meter. Air temperature and humidity were measured using a Dickson-TM320 model sensor and logger.

4.3 Results and Discussion

4.3.1 Column effluent results

The ferrous and total iron measurement results indicated the dominance of ferric iron in all column effluents. Ferrous iron was generally under 10 mg/l while ferric iron concentration reached as high as 2800 mg/l in the C5 effluent from an initial concentration of 700 mg/l. The ferric iron values increased along the cascade from C2 to C5 (Figure 4-2). The pH measurements decreased with increasing ferric iron; C5 having the lowest pH at about 1.6 (Figure 4-3). The seed liquid from the reservoir of C1, stayed at about 500 mg/l ferric iron and a pH of 2.2. The sulfate measurements for C5 showed the general trend exhibited by the ferric iron value of C5. It steadily increased from 8 to 20.5 g/l over the duration of the experiment (Figure 4-4).

Three of the four cascade columns had close to saturation humidity values with most readings being greater than 95% (Figure 4-5). C5 had much lower saturation and it was mostly close to the ambient saturation. This low saturation was not explained. The installment of an enhanced flow distributor for C5 on day 225 did not cause the humidity to increase. Other physical and flow configurations of C5 were the same as the other three columns.

The metal analysis on C5 effluents of days 21, 92 and 191 for As, Pb, Cd, Mn, Mg, Cu, Al, and Zn returned low mg/l levels (Figure 4-6). The most concentrated metal was Zn with an average of 8 mg/l. The lowest was Cd with an average of 0.3 mg/l. The sample for day 191 was run for the four cascade columns. Except for Mg, the rest of the metals increased in level from C2 to C5 (Figure 4-7). Mg concentration increased from C1 to C2 but decreased thereafter for each column in the series. The metals trend along the flow path is consistent with increased leaching of metals at lower pHs. The irregularity of magnesium to these trends was not

explained. PHREEQC speciation results did not show any over saturated magnesium containing minerals.

Iron production for each column were calculated by subtracting the molar iron concentration of a given column output from the input concentration and multiplying it by the flow rate and normalizing it to the waste rock mass for each column (Figure 4-8). The average production for C2 and C5 were $4.6*10^{-9}$ and $4.1*10^{-9}$ mol/ (kg-s) respectively. C3 and C4 have a higher average iron production of $8.3*10^{-9}$ and $1.2*10^{-8}$ mol/(kg-s) respectively. The iron production from columns 4 and 3 showed an increase after the installment of enhanced flow distributors on days 120 and 130 respectively. An increased iron production was also seen for C5 following the installment of an enhanced flow distributor for C5 on day 225. The increased iron production seen with the installment of the enhanced flow distributors could be because increased liquid distribution brings about liquid coverage to more of the rock surfaces. This in turn can result in increased diffusional exchange with pore liquid and increased rock surface sulfide oxidation reactions. The estimated total mass of iron released from the columns is 5900 g. Of these C2 had the lowest with a contribution of 900 g whereas C3 and C5 each had about 1550 g and C4 had the highest with close to 2000 g.

The calculation of the mass of pyrite oxidized using the total released iron results in about 13.7 kg, which is about 2 % of the total rock mass. This number is most likely a conservative number as part of the iron is likely to precipitate out as suggested by the sulfate data. The particular waste rocks used for the experiments have previously been shown to have about 22% sulfide content in mineralogical testing (Jenkins, 2006).

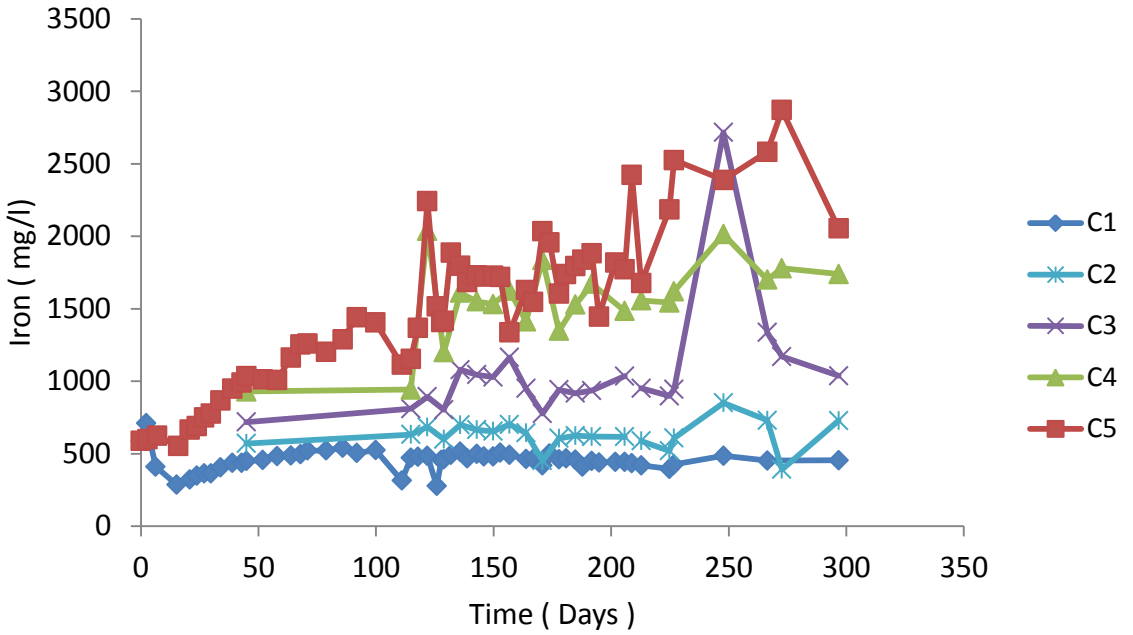

Figure 4-2. Ferric iron concentration for effluents of columns 1-5. The ferrous iron concentrations for all columns were mostly less than 20 mg/l. The ferric iron was calculated as a difference of the total soluble iron and soluble ferrous iron measurements.

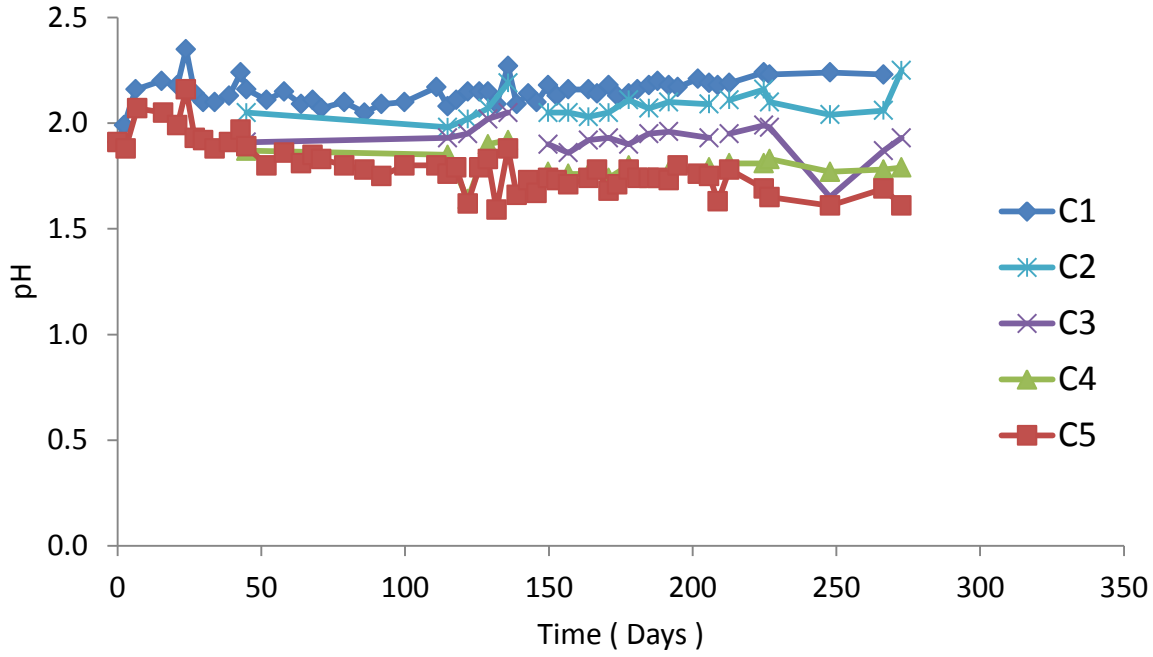

Figure 4-3. Measured pH for effluents of columns 1-5. pH measurements were done on 0.22 µm filtered samples and were undertaken within an hour of sample collection.

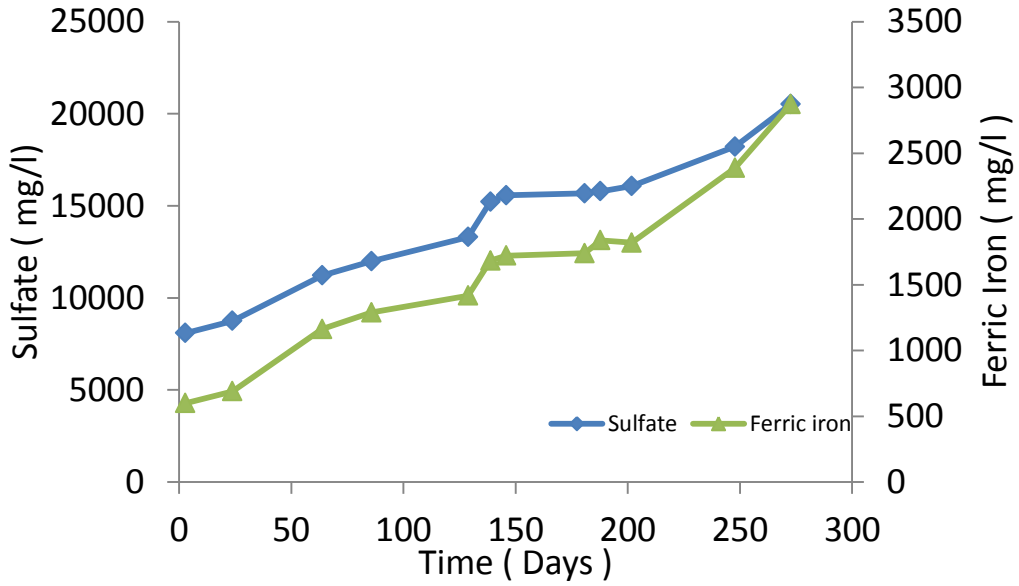

Figure 4-4. Sulfate and ferric iron concentrations for selected samples of column 5 effluent. Please note the separate y axes.

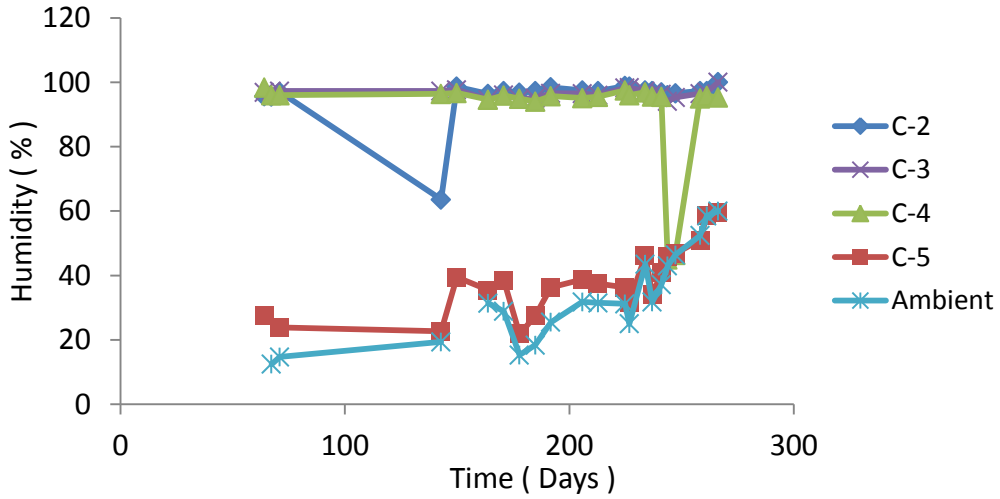

Figure 4-5. Humidity measurement results at a depth of 30.5 cm for columns 2-5 along with ambient humidity measurements.

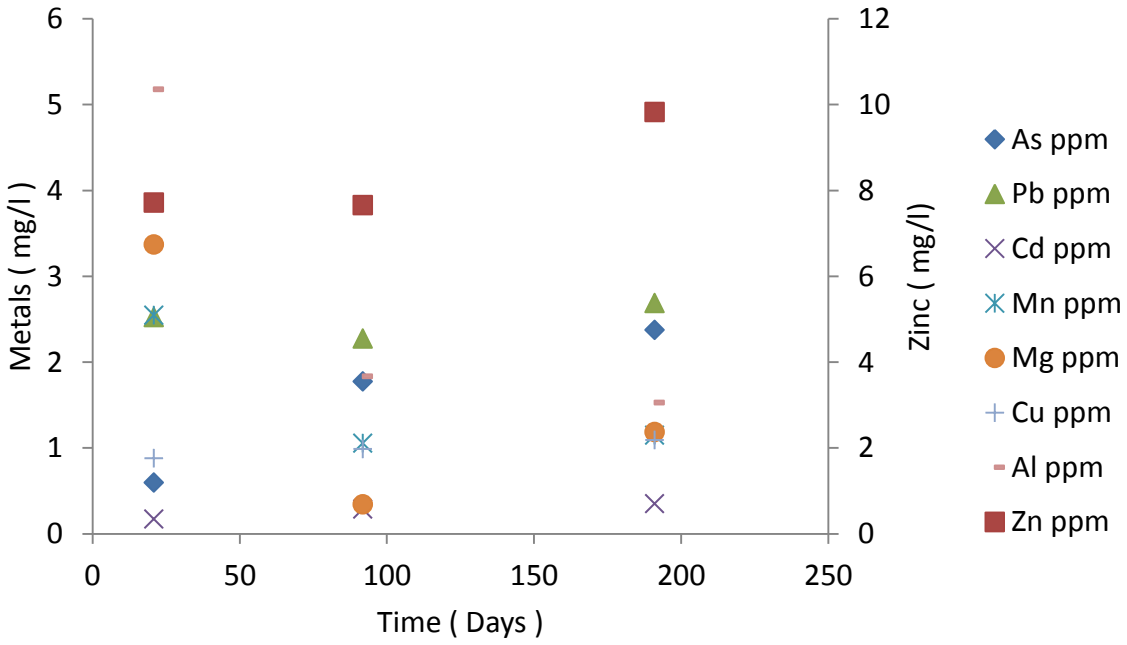

Figure 4-6. Metal analysis of selected elements for column 5 effluent on days 21, 92 and 191. A separate right axis has been made for zinc concentrations for a better display of the data.

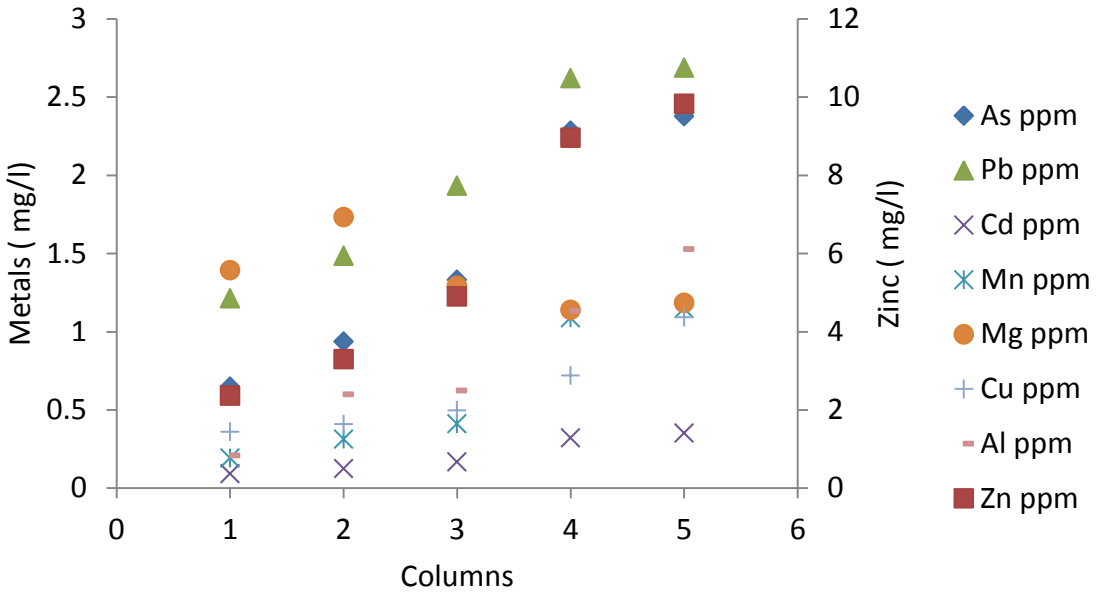

Figure 4-7. Metal analysis results of selected elements for effluent of columns 1-5 on day 191. A separate right axis has been made for zinc concentrations for a better display of the data.

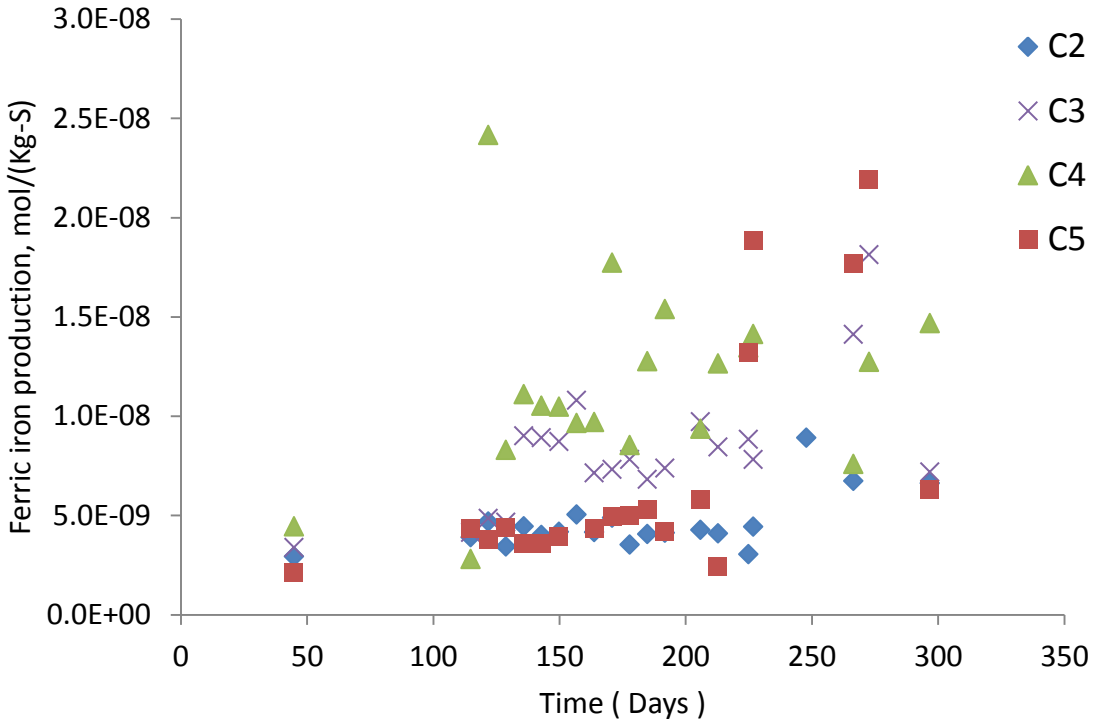

Figure 4-8.The ferric iron production is the net moles of ferric iron released from each of columns 2-5 per kg of waste rock per second.

4.3.2 Microorganism enumeration (MPN) results

The columns 2-5 effluent average MPN values for iron oxidizers and heterotrophs were 93,000 ± 7016 and 259 ± 206 per ml respectively. The average pore liquid MPN values on the other hand were 70,000 ± 20,000 and 135,000 ± 69,000 per ml. The MPN results for all four column effluent samples indicated about 2 orders of magnitude more MPN values for iron oxidizing organisms compared to acidophilic heterotrophic organisms (figure not included). There were about half an order of magnitude more iron oxidizers in the pore liquid compared to the respective column effluents for columns 3 and 4 (Figure 4-9). In columns 2 and 5 however, the iron oxidizing column effluent MPNs were more than the pore liquid values albeit very small difference (Figure 4-9). The heterotrophic pore liquid MPNs for all columns were at

least 2 orders of magnitude more than their respective column effluent MPN values (Figure 4-10).

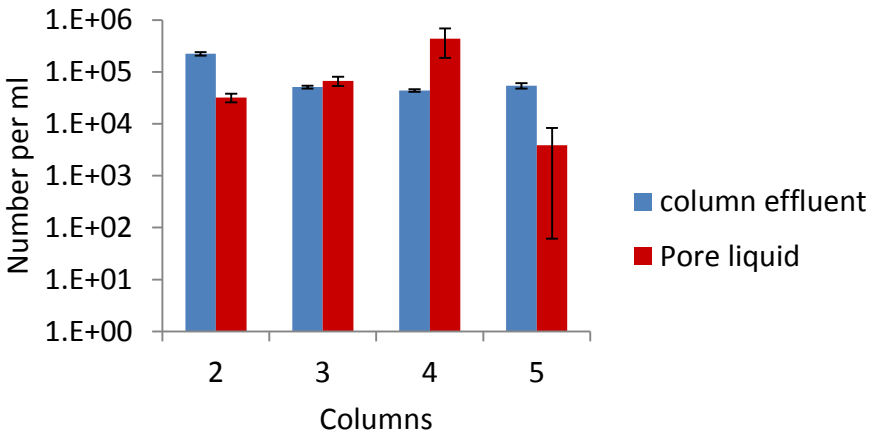

Figure 4-9. MPNs of iron oxidizing organisms for column effluent and pore liquid samples of columns 2-5. Error bars represent the standard errors predicted for each test.

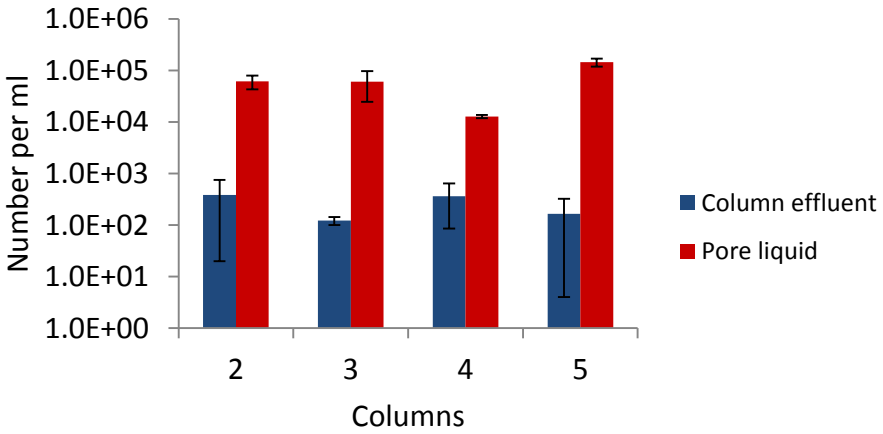

Figure 4-10. MPNs of acidophilic heterotrophs done for column effluent and pore liquid of columns 2-5. Error bars represent the standard errors predicted for each test.

4.3.3 Saturation and porosity measurement results

The waste rock measurements indicated that the average rock porosity for all columns was between 4 and 6 % (Figure 4-11). The minimum measured porosity was 1.6% while the maximum was 20.8 %. Column 5 had the most variability in the porosity of the rocks tested. The water saturation results showed that C3, C4, and C5 rock samples had an average of 91, 84, and 87 % saturation respectively (Figure 4-12). C2 had the lowest at an average of 74%. A plot of the average rock saturation results of all column samples for a given depth indicated that the surface rock samples have the lowest water saturation levels (Figure 4-13). A linear fit to the water saturation vs. depth data had an R^2 of 0.74.

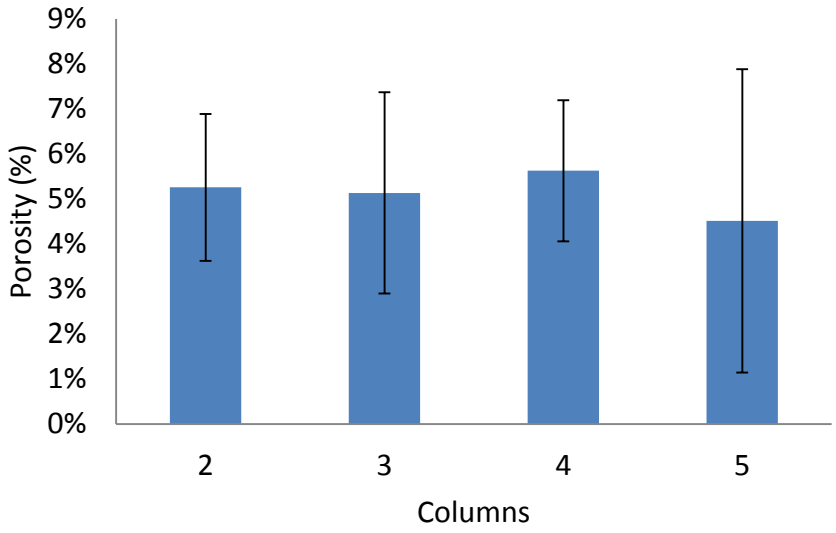

Figure 4-11. Average rock porosity for samples of columns 2-5 (n=30). Error bars represent standard deviation for the results.

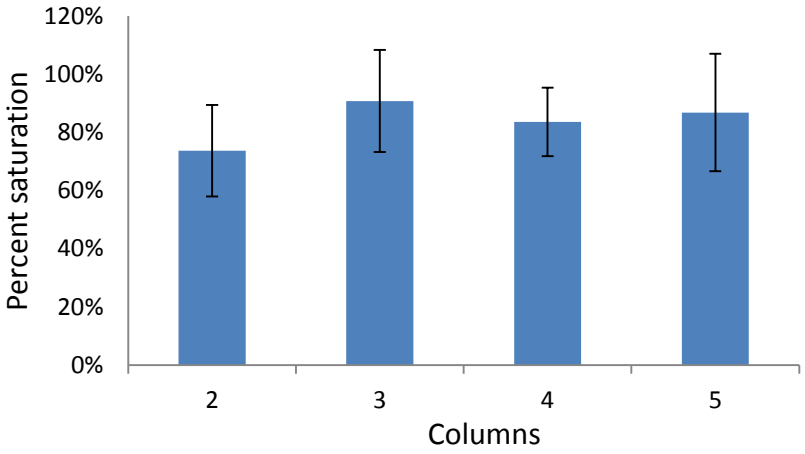

Figure 4-12. Average water saturation for samples of columns 2-5 (n=30). Error bars represent standard deviation for the results.

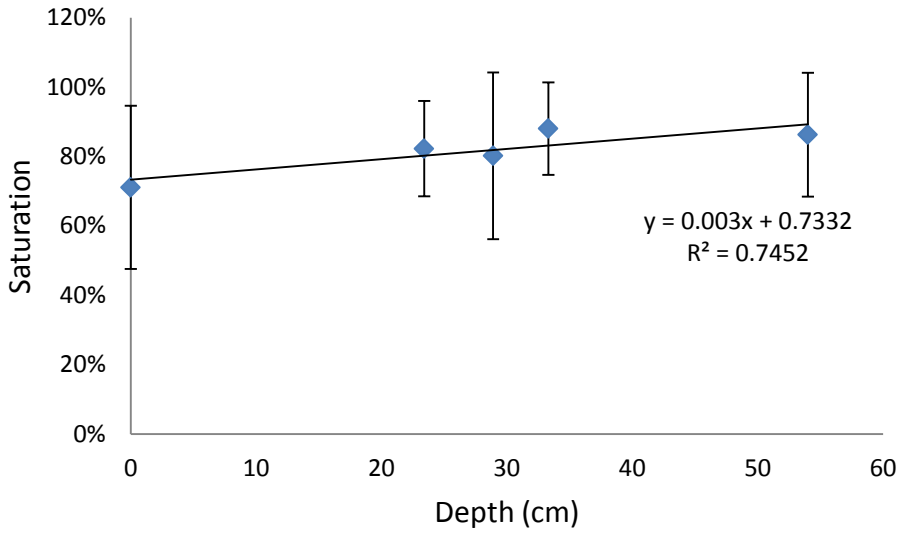

Figure 4-13. A plot of the average water saturation of rock samples in all columns at each of the 5 depths. Error bars represent standard deviation for the results.

4.3.4 Pore liquid chemistry measurement results

The iron concentrations in the rock diffusion experiments increased rapidly initially and slowed down with time. The last sample (6th day) concentrations were used to calculate the pore liquid iron content. The rock pore volume measurement results (obtained from porosity and whole rock volume) for each of the rocks was used along with the average water saturation levels for the columns to calculate the pore liquid volume. There after dilution values were calculated using the volume of liquid in the diffusion buckets and data for the pore liquid iron content was generated. The same dilution factors were used for sulfate and metal pore liquid concentration calculations. The obtained pore liquid iron concentrations were higher than the respective column effluent values for all columns (Figure 4-14). The ratios of pore liquid to column effluent iron concentrations for columns 2, 3, 4, and 5 were 17, 10, 6, and 6

respectively. The sulfate results also indicated a higher pore sulfate concentration than the column liquid. The ratios for sulfate were 19, 6, 5, and 4 for C2, C3, C4 and C5 respectively. The four column average pore liquid sulfate concentration was about 100 g/l, while the iron average was 13.1 g/l.

Metal analysis of 9 elements was done for the pore liquid samples. The highest pore liquid metal concentrations were for Zn and Pb with an average of 114 and 140 mg/l respectively. These corresponded to 25 and 70 times more concentrations than the respective column effluent results. Most of the other analyzed metals (Al, As, Mn, and Mg) were at least 5 times more concentrated in the pores than the respective column effluent measurements. The exceptions were Cd and Cu with about the same concentration for both pore liquid and column effluent samples.

The demonstrated high iron concentrations in pore liquid can result in a very fast rate of pyrite oxidation as this oxidation is dependent on the ferric iron concentration (Moses *et al.*, 1987; Williamson and Rimstidt, 1994; Fowler *et al.*, 2001). This in fact is suggested by the much higher concentration of sulfate and metals in the pore liquids as compared to the column effluents. The fact that 2 orders of magnitude higher Heterotrophic microbial counts were obtained for the pore liquid compared to the respective column effluent is an indirect evidence of a much more established activity of autotrophic community in the rock pore liquid. This is because acidophilic heterotrophs are known to depend on the microbial products of autotrophs in these organic carbon scarce environments (Jenkins, 2006; Johnson and Hallberg, 2009). Direct evidence of a more established iron oxidizing community in the pore liquid as compared to the column effluent was not seen with the autotrophic MPN results. This result was not fully

explained but it can be because the iron oxidizing organisms are used to sulfide attached growth and thus could not acclimate to growing in sessile incubations during the MPN test.

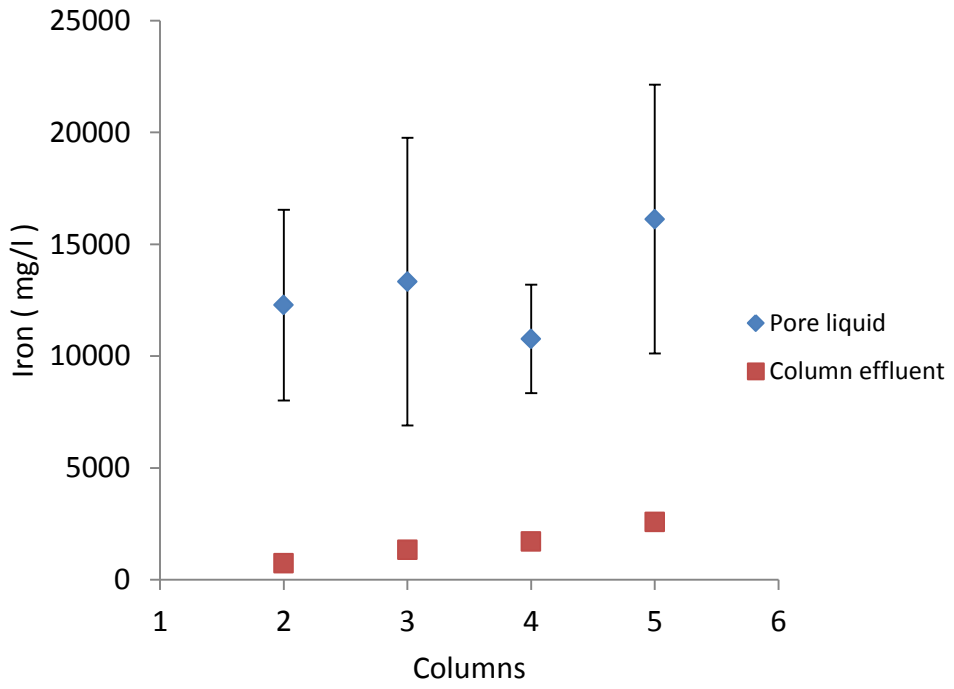

Figure 4-14. Pore liquid and column effluent total soluble iron concentrations for columns 2-5. Error bars represent standard deviation of results (n=3).

4.3.5 Tracer test results

The peak of the bromide appeared 2.6 hours after the tracer injection. This peak concentration was 0.0189 M (Figure 4-15). This is about 1% of the injected 2 M concentration. The bromide mass recovery at this time was about 10 %. A day into the injection, about 58% mass recovery was made. 20 days into the test, the effluent of C5 had $3.6*10^{-6}$ M bromide which was about an order of magnitude higher than the detection limit. At this time, the mass recovery was 68%.

A drainage test was done at an earlier date by shutting down the input liquid at C2 and collecting the effluent of C5. This resulted in the collection of a total of 700 ml of liquid in 11.5 hours. Half of this liquid was collected in the first 2 hours. Assuming a compete dispersion of the 55 ml of tracer injected in the 700 ml of bulk liquid available at any time in the four columns , the resulting concentration would be 0.15 M. This is however 1 order of magnitude higher than the peak tracer concentration. This is evidence of the extensive diffusion into the rock pores. The long tail and the low tracer recovery is likely due to a slow back diffusion from the rock pore liquid to the bulk liquid (Reimus *et al.*, 2003; Cvetkovic, 2010; Waber *et al.*, 2011). This can be because of a low bromide concentration gradient between the pore liquid and bulk liquid.

At an average rock pore volume of 5.1% and 86% water saturation, a pore liquid total volume of 10.5 liters for the four columns is calculated. The 700 ml of bulk liquid available at any time in the four columns is only 0.3 % of the 224.6 liter void space in the four columns. Although not all pore liquid will be available for chemical and bacterial reactions, the pore liquid volume is significantly more than the bulk liquid and thus diffusion to the bulk liquid may well be a limiting factor in the transport of chemical species in and out of the pore liquid. This in fact may be the other reason for the elongated tail and low tracer recovery. The long tail and low tracer recovery can also be an indication of a long pore liquid residence time as diffusion and not slow advection is the likely process dominating solute transport (Cvetkovic, 2010).

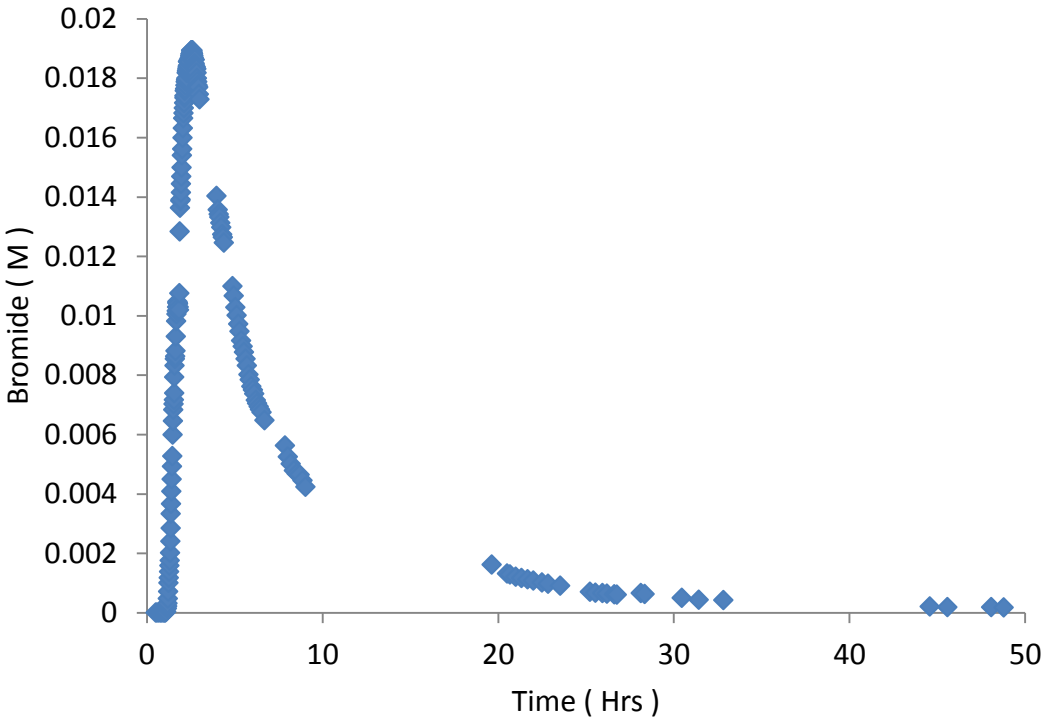

Figure 4-15. Bromide molar concentration for C5 effluent. The peak bromide concentration was 0.0189 M and appeared 2.6 hours after the tracer injection. A day into the tracer injection 58% of the tracer mass was recovered.

4.3.6 Geochemical modeling

The oxidation of pyrite by ferric iron results in a sulfate to ferric iron theoretical mass ratio of 0.29 (equation 4-1). The calculation of the ratio for most of the measured bulk liquid samples was actually between 0.10 and 0.14. This could be because of the precipitation of ferric iron. At a pH of 3 and below , ferric iron is known to form jarosite in the presence of sulfate and other elements such as K, Na , and Ag (Dutrizac and Jambor, 2000; Kawano and Tomita, 2001; Majzlan and Myneni, 2005). PHREEQC (Parkhurst and Appelo, 1999) was used to model the speciation of column 5 effluent and pore liquid samples. The results showed K-jarosite ($KFe_3(SO_4)_2(OH)_6$) , hematite (Fe_2O_3) , and goethite (FeOOH) to be super saturated with respect

to both the column effluent and pore liquid samples. Anglesite ($PbSO_4$), anhydrite ($CaSO_4$), and gypsum ($CaSO_4$:$2H_2O$) were in addition shown to be super saturated with respect to the pore liquid sample (Table 4-1). A calculation was made by assuming the discrepancy between the theoretical and measured ferric iron to sulfate ratio for the column effluent to have resulted from formation of a jarosite mineral. New ferric iron and sulfate concentrations were then calculated by using the ratio of ferric iron to sulfate in jarosite and the average of the new ratio of sulfate to ferric iron was found to be 0.24 as compared to the previous average of 0.11. This new ratio is much closer to the theoretical ratio of 0.29. Hematite and goethite precipitation can possibly explain the rest of the discrepancy.

Although noisy, an Increasing total iron production with time was seen from C5 concentration-time profile (Figure 4-2) and iron production calculations using only the effluent of C5 and the input to C2 (not shown). One explanation for this could be the solubilization of the above described iron precipitates. The demonstrated low bulk liquid saturation of the columns could also cause diffusion limitations and cause increase of pore liquid iron concentration with time. The flow paths inside the columns are expected to change with time resulting in diffusion from pores having increased iron concentration as well as solubilization of formerly unreached precipitates.

Table 4-1. Selected PHREEQC speciation results for the average pore liquid chemistry results of C5. The input for the speciation contained mg/l of, Fe^{3+} – 15,100, Fe^{2+}-100, SO_4^{2-}78,700, Al-31, Cu-2.2, Zn-74, Mn-8.4, Mg-10, Cd-0.5, Pb-177, K-12,643, Na-0 and Ca-9,887. The pH was 1.6 and the pE was set at 12.

Species	SI (saturation index)	Log (IAP)	Formula
Anglesite	1.94	-5.87	$PbSO_4$
Anhydrite	1.30	-3.05	$CaSO_4$
$Fe(OH)_3$	-3.49	1.40	
Gypsum	1.51	-3.07	$CaSO_4:2H_2O$
Goethite	2.30	1.41	FeOOH
Hematite	6.61	2.83	Fe_2O_3
$Pb(OH)_2$	-9.44	-1.18	
Jarosite-K	4.67	-4.31	$KFe_3(SO_4)_2(OH)_6$
Melanterite	-3.02	-5.27	$FeSO_4:7H_2O$

4.3.7 Implications

The presented work has shown the presence of a fairly water saturated and active AMD producing rock pores despite low bulk water saturation. Waste rock piles generally have low bulk water saturation during a dry season (Vaughn *et al.*, 1999; Nichol *et al.*, 2005). AMD reactions in saturated rock pores can thus be the dominant process happening during the dry season. During the spring snow melt, flushing of the pores and the matrix water can then export AMD into the environment (Vaughn *et al.*, 1999; Sracek *et al.*, 2004). Thus efforts of AMD prevention in waste rock piles such as organic carbon or bactericide addition has to focus

on delivering these into rock pore liquids. Different strategies may be used to accomplish this. The hydrology at a given waste rock pile can be studied and a time when the rocks are the least saturated can be chosen to deliver the needed liquid. In waste rock piles with significant fines, saturation of the fine material with the remediation liquid of choice may result in an extended diffusive exchange with rock pore liquids.

Biological or chemical treatments that seal rock pores can significantly contribute to the reduction of AMD. Organic carbon addition may result in heterotrophic growth and production of biofilm and other particulate forms of carbon that can help seal the pores. Chemical applications such as phosphate and silicate have previously been shown to minimize pyrite oxidation by forming ferric-phosphate and ferric-silicate coats on pyrite grains (Nyavor and Egiebor, 1995; Evangelou, 2001). More research is needed on waste rock piles to find similar or even non-reactive and low pH resistant materials that may provide long term sealing of rock pores.

4.4 Conclusions

The waste rock pore liquids contained (6-17) and (4-19) times more iron and sulfate respectively than bulk liquid column effluents. Heterotrophic microbial enumeration and other trace metal results followed the same trend as above indicating that enhanced pyrite oxidation occurs in the rock pores. The waste rock columns featured a very low bulk liquid saturation at less than 1% and had much more rock pore liquid than bulk liquid (10.5 l of pore liquid compared to 0.7 l of bulk liquid). A relatively high liquid saturation (74 to 91 %) was maintained by the waste rocks despite this low bulk saturation. The tracer result showed an extended tailing with low recovery suggesting a diffusion controlled system with possible limitations caused by low bulk saturation and low diffusion gradient. Over saturation of minerals such as k-jarosite, hematite and goethite showed the mineralogical limitation on ferric iron and explained some of the discrepancy between the theoretical and measured ferric iron to sulfate mass ratio. AMD prevention efforts aimed at waste rock piles should address the important pore liquid reactions as well as the related residence time and diffusion limitation factors. Organic carbon based AMD prevention efforts have to involve the design of techniques to deliver organic carbon substrate to rock pore liquids.

4.5 References

Bilgin, A. A., Silverstein, J. and Jenkins, J. D. (2004). Iron respiration by Acidiphilium cryptum at pH 5. *Fems Microbiology Ecology* **49**(1): 137-143.

Blowes , D. W., Ptacek , C. J., Jambor , J. L. and Weisener , C. G. (2003). The geochemistry of acid mine drainage. *Treatise on geochemistry*. B. S. Lollar. Toronto, Canada., *Elsevier*. **9:** 149-204.

Cvetkovic, V. (2010). Diffusion-controlled tracer retention in crystalline rock on the field scale. *Geophysical Research Letters* **37**, L13401.

Dutrizac, J. E. and Jambor, J. L. (2000). Jarosites and their application in hydrometallurgy. *Sulfate Minerals - Crystallography, Geochemistry and Environmental Significance* **40**: 405-452.

Edwards, K. J., Bond, P. L., Druschel, G. K., McGuire, M. M., Hamers, R. J. and Banfield, J. F. (2000). Geochemical and biological aspects of sulfide mineral dissolution: lessons from Iron Mountain, California. *Chemical Geology* **169**(3-4): 383-397.

Evangelou, V. P. (2001). Pyrite microencapsulation technologies: Principles and potential field application. *Ecological Engineering* **17**(2-3): 165-178.

Fowler, T. A., Holmes, P. R. and Crundwell, F. K. (2001). On the kinetics and mechanism of the dissolution of pyrite in the presence of Thiobacillus ferrooxidans. *Hydrometallurgy* **59**(2-3): 257-270.

Gehrke, T., Hallmann, R., Kinzler, K. and Sand, W. (2001). The EPS of Acidithiobacillus ferrooxidans - a model for structure-function relationships of attached bacteria and their physiology. *Water Sci Technol* **43**(6): 159-67.

Gehrke, T., Telegdi, J., Thierry, D. and Sand, W. (1998). Importance of extracellular polymeric substances from Thiobacillus ferrooxidans for bioleaching. *Applied and Environmental Microbiology* **64**(7): 2743-2747.

Gray, N. F. (1998). Acid mine drainage composition and the implications for its impact on lotic systems. *Water Research* **32**(7): 2122-2134.

Jenkins, J. D. (2006). Role of flow and organic carbon on acid mine drainage remediation in waste rock. Ph.D. thesis. *University of Colorado***.**

Johnson, D. B. and Hallberg, K. B. (2009). Carbon, Iron and Sulfur Metabolism in Acidophilic Micro-Organisms. *Advances in Microbial Physiology, Vol 54*. R. K. Poole. **54:** 201-255.

Johnson, D. B., Yajie, L. and Okibe, N. (2008). "Bioshrouding" - a novel approach for securing reactive mineral tailings. *Biotechnology Letters* **30**(3): 445-449.

Kawano, M. and Tomita, K. (2001). Geochemical modeling of bacterially induced mineralization of schwertmannite and jarosite in sulfuric acid spring water. *American Mineralogist* **86**(10): 1156-1165.

Lyon, J. S., Hilliard, T. J. and Bethell, T. N. (1993). Burden of gilt Washington, DC, *Mineral Policy Center*.

Majzlan, J. and Myneni, S. C. B. (2005). Speciation of iron and sulfate in acid waters: Aqueous clusters to mineral precipitates. *Environmental Science & Technology* **39**(1): 188-194.

Marchand, E. A. and Silverstein, J. (2002). Influence of heterotrophic microbial growth on biological oxidation of pyrite. *Environmental Science & Technology* **36**(24): 5483-5490.

Moses, C. O., Nordstrom, D. K., Herman, J. S. and Mills, A. L. (1987). AQUEOUS PYRITE OXIDATION BY DISSOLVED-OXYGEN AND BY FERRIC IRON. *Geochimica Et Cosmochimica Acta* **51**(6): 1561-1571.

Nichol, C., Smith, L. and Beckie, R. (2005). Field-scale experiments of unsaturated flow and solute transport in a heterogeneous porous medium. *Water Resources Research* **41**(5).

Nyavor, K. and Egiebor, N. O. (1995). Control of pyrite oxidation by phosphate coating. *Science of the Total Environment* **162**(2-3): 225-237.

Parkhurst, D. L. and Appelo, C. A. J. (1999). *User's guide to PHREEQC: A computer program for speciation, batch-reaction, one dimensional* tra*nsport, and inverse geomchemical calculation*. Denver, CO, *U.S. Geological Survey*

Peplow, D. and Edmonds, R. (2005). The effects of mine waste contamination at multiple levels of biological organization. *Ecological Engineering* **24**(1-2): 101-119.

Pond, G. J., Passmore, M. E., Borsuk, F. A., Reynolds, L. and Rose, C. J. (2008). Downstream effects of mountaintop coal mining: comparing biological conditions using family- and genus-level macroinvertebrate bioassessment tools. *Journal of the North American Benthological Society* **27**(3): 717-737.

Reimus, P., Pohll, G., Mihevc, T., Chapman, J., Haga, M., Lyles, B., Kosinski, S., Niswonger, R. and Sanders, P. (2003). Testing and parameterizing a conceptual model for solute transport in a fractured granite using multiple tracers in a forcedgradient test. *Water Resources Research* **39**(12).

Rowe, R., Todd, R. and Waide, J. (1977). Microtechnique for most-probable-number analysis. *Applied and Environmental Microbiology* **33**(3): 675-680.

Sand, W. and Gehrke, T. (2006). Extracellular polymeric substances mediate bioleaching/biocorrosion via interfacial processes involving iron(III) ions and acidophilic bacteria. *Research in Microbiology* **157**(1): 49-56.

Singer, P. C. and Stumm, W. (1970). Acidic mine drainage . Rate-determining step. *Science* **167**(3921): 1121-&.

Sracek, O., Choquette, M., Gelinas, P., Lefebvre, R. and Nicholson, R. V. (2004). Geochemical characterization of acid mine drainage from a waste rock pile, Mine Doyon, Quebec, Canada. *Journal of Contaminant Hydrology* **69**(1-2): 45-71.

Stockwell, J., Smith, L., Jambor, J. L. and Beckie, R. (2006). The relationship between fluid flow and mineral weathering in heterogeneous unsaturated porous media: A physical and geochemical characterization of a waste-rock pile. *Applied Geochemistry* **21**(8): 1347-1361.

Stromberg, B. and Banwart, S. (1999). Weathering kinetics of waste rock from the Aitik copper mine, Sweden: scale dependent rate factors and pH controls in large column experiments. *Journal of Contaminant Hydrology* **39**(1-2): 59-89.

Vaughn, R. B., Stanton, M. R. and Horton, R. J. (1999). A year in the life of a mine dump: A diachronic case study. *Tailings and Mine Waste'99*, Balkema.

Waber, H. N., Gimmi, T. and Smellie, J. A. T. (2011). Effects of drilling and stress release on transport properties and porewater chemistry of crystalline rocks. *Journal of Hydrology* **405**(3-4): 316-332.

Warner , R. (1971). Distribution of Biota in a Stream Polluted by Acid Mine-Drainage *ohio journal of science* **71**: 202-215.

Williamson, M. A. and Rimstidt, J. D. (1994). The kinetics and electrochemical rate-determining step of aqueous pyrite oxidation. *Geochimica Et Cosmochimica Acta* **58**(24): 5443-5454.

CHAPTER 5. SUMMARY AND CONCLUSIONS

5.1 Summary of research

The motivation behind the research are mine waste rock piles and in particular abandoned ones that are contributing drainage of low pH and heavy metal affecting the environment in various ways. The key process responsible for this is the oxidation of sulfide minerals by ferric iron and oxygen. The regeneration of the sulfide oxidation by product ferrous iron by iron oxidizing organisms sustains the sulfide oxidation and increases the rate by many orders of magnitude. Water and oxygen has to be present near a sulfide surface for these reactions to happen. Waste rock piles contain rocks of various sizes, mineralogical content, and porosities. The estimation of how much acid mine drainage is produced mainly depends on understanding transport of water and oxygen in a pile.

One proposed solution is remediation of the piles by addition of organic carbon substrate to stimulate native heterotrophic organisms. Based on previous investigations and theoretical knowledge, heterotrophic growth is proposed to bring about biochemical, geochemical and physical changes that affect the acid mine drainage generation reactions. The extent of remediation of acid mine drainage can be estimated if a knowledge of these changes and the rate at which they happen is known. The main remediation mechanisms proposed are the competition for oxygen between iron oxidizing and heterotrophic organisms, the interaction of heterotrophic microbial products with ferric iron and resulting in the reduction of pyrite oxidation, and the reduction in sulfide reactive surface by heterotrophic extracellular polymeric substances. All these processes first start by the metabolization of organic carbon

substrates. What happens once all the substrate is metabolized will depend on cycling of the various organic carbon containing forms. The above mentioned remediation processes will need to happen on sulfide surfaces that are actively producing acid mine drainage.

This research had three focus areas. The first was the investigation of the growth of acidophilic heterotrophs on glucose and the effect of environmental factors such as pH and DO on growth. The end purpose here was quantification of the growth kinetics to be able to predict consumption of oxygen. The second focus was the investigation of the interaction of the microbial products of acidophilic heterotrophs and ferric iron and the resulting effect on sulfide oxidation. The third focus was on getting more understanding about microenvironments undergoing active acid mine drainage generation within waste rock piles. This third focus of the research was motivated by the need to identify actively reacting sulfide surfaces within waste rock piles and understand the various parameters that affect them to aid in the design of organic carbon addition.

5.1.1 Chapter 2 – Growth kinetics

Waste rock enrichments were grown on glucose substrate, supplemental yeast extract and mineral media. Growth experiments were also done without supplemental yeast extract. The effect of pH on growth was studied by doing experiments at various initial pH of 1.1 to 6.0. The glucose substrate utilization and biomass growth kinetics was studied by doing glucose limited experiments at pH 3.0. Oxygen depletion experiments were done to assess the affinity of the organisms to dissolved oxygen. Phospholipid fatty acid analysis was done on a sample of

the culture for domain level characterization and enumeration. Monod kinetic parameters were predicted from the growth experiments.

5.1.2 Chapter 3-SMP ferric iron interaction

Growth derived and lysis derived SMPs were obtained from mine waste rock enrichments grown on glucose and mineral media. Various concentrations of these SMPs were mixed with ferric iron and pyrite and the reaction products monitored. Characterization of the SMPs was done using SEC and fluorescence EEM techniques. Additional molecular size characterization of the lysis derived SMPs was done with ultra-filtration and the filtration fractions mixed with ferric iron and used for pyrite oxidation experiments. Biodegradation and the after biodegradation interaction with ferric iron and pyrite was tested for the lysis derived SMPs.

5.1.3 Chapter 4-Waste rock AMD generation

Water was recirculated through a waste rock packed column. Part of this recirculating liquid was applied to four other waste rock columns connected in series. Various water chemistry measurements, iron oxidizing and glucose consuming metabolic microbial enumerations were performed on the column effluents. The above chemical and microbial enumerations were done for rock pore liquids by putting rock samples in well mixed solutions for diffusion of rock pore contents. A conservative tracer with a pulse input was applied to the columns to investigate the movement of liquid through the waste rocks.

5.2 Conclusions

5.2.1 Chapter 2

- The enrichment was shown to utilize a simple carbohydrate substrate efficiently.
- Determination of monod kinetic growth parameters was made and this would enable incorporation into an AMD remediation model to predict competition for oxygen with iron oxidizers.
- The oxygen half saturation constant showed that the enrichments are able to utilize glucose at low concentrations of dissolved oxygen. The value obtained was close to or lower than previously published dissolved oxygen concentrations shown to limit the growth of iron oxidizing organisms.
- The enrichment's maximum specific growth rate was much higher than that reported for *A. cryptum* providing further evidence that *A. cryptum* is not a good AMD model organism.
- The growth of the enrichment down to pH 1.5 suggests growth is possible in rock pores or other microenvironments where the pH typically gets below 2.0.
- Eukaryotes constituted a significant part of the enrichment. This is consistent with their recent detection in extremely low pH environments and warrants further research.

5.2.2 Chapter 3

- Both growth and lysis derived SMPs were able to slow down pyrite oxidation by ferric iron. Lysis derived SMPs had more pronounced effect than growth derived SMPs for the same SMP-DOC concentration.

- Lysis derived SMPs were shown to result in a significant reduction of the pyrite oxidation rate even at a 1:3.6, SMP-DOC to mg/l ferric iron ratio.
- The formation of weak SMP complexes with ferric iron was indicated as shown in the comparison with the strong iron chelator , deferoxamine mesylate.
- Ferric iron containing lysis derived SMPs were shown to be highly biodegradable. The results however were not conclusive on whether the SMP-ferric complexes biodegraded or not.
- A quantitative relationship was developed for predicting a pyrite oxidation rate constant given a lysis derived SMP-DOC. This relationship can be used as part of an AMD remediation model in cases where pyrite is not limiting.

5.2.3 Chapter 4

- Individual waste rocks had fairly high water saturation despite very low bulk water saturation. Big waste rock piles can have this phenomenon in the interior of a pile where high air humidity may be maintained. This has significance for chemical and microbial activity in the rock pores.
- Rock pore liquids featured much higher concentrations of iron, sulfate, metals, and heterotrophic microorganisms compared to the column effluents. This is indicative of the presence of active pore regions where high pyrite oxidation rates are maintained. It is important from the view point of organic carbon remediation to deliver selected substrates to these active regions.

- Extensive diffusion to the rock pores was shown with low tracer recovery caused by a presumed long pore residence time and slow back diffusion. This indicates that the transport of contaminants from pores to bulk liquid is the limiting process in terms of the export of AMD.
- Although rock pores contain significant volume of reaction space, the transport limitations can create an opportunity for remediation processes in pores to limit or stop AMD reactions.

5.3 Recommendations for future research endeavors

- It will be important to study the growth of acidophilic heterotrophs on wide range of substrates including locally available organic carbon sources such as wood chips and manure.
- The dissolved oxygen and mineralogical controls that influence the acidophilic heterotroph's use of electron acceptors other than oxygen has to be identified and the kinetics of these metabolisms determined.
- The transport and storage of carbon in rock pores and bulk liquids of a waste rock pile has to be investigated experimentally and/or using mathematical models.
- The pH, ferric iron, and sulfate concentrations in microenvironments of a waste rock pile can be more extreme than drainage concentrations. Thus growth of acidophilic heterotrophs in these microenvironments has to be investigated.
- The lysis rate of heterotrophic cells under laboratory and field conditions has to be determined.
- Work on direct evidence of complex formation during the interaction of SMPs with iron and on the biological stability of the complex will provide useful rates for evaluating the remediation scheme.
- Waste rock piles with significant content of fines (sand and gravel size) may have different microenvironments than the waste rock set up used in this work. It is thus important to do experiments and modeling to understand the effect of fines on transport of water and oxygen including saturation of rock pores and the fine material matrix.

BIBILIOGRAPHY

Amos, R. T., Mayer, K. U., Blowes, D. W. and Ptacek, C. J. (2004). Reactive transport modeling of column experiments for the remediation of acid mine drainage. *Environmental Science & Technology* **38**(11): 3131-3138.

Andre, B. and Stroncek, J. (2008). Kinetics study of Acidiphilium Cryptum in glucose media. University of Colorado. Personal communication.

Andre, B. J., Rajaram, H. and Silverstein, J. (2009). Generation of acid mine drainage: Reactive transport models incorporating geochemical and microbial kinetics. Ph.D. thesis. University of Colorado.

Azam, S., Wilson, G. W., Herasymuik, G., Nichol, C. and Barbour, L. S. (2007). Hydrogeological behaviour of an unsaturated waste rock pile: a case study at the Golden Sunlight Mine, Montana, USA. *Bulletin of Engineering Geology and the Environment* **66**(3): 259-268.

Baker, B. J. and Banfield, J. F. (2003). Microbial communities in acid mine drainage. *Fems Microbiology Ecology* **44**(2): 139-152.

Baker, B. J., Tyson, G. W., Goosherst, L. and Banfield, J. F. (2009). Insights into the Diversity of Eukaryotes in Acid Mine Drainage Biofilm Communities. *Applied and Environmental Microbiology* **75**(7): 2192-2199.

Banfield, J. F., Verberkmoes, N. C., Hettich, R. L. and Thelen, M. P. (2005). Proteogenomic approaches for the molecular characterization of natural microbial communities. *Omics-a Journal of Integrative Biology* **9**(4): 301-333.

Berthelot, D., Leduc, L. G. and Ferroni, G. D. (1993). Temperature studies of iron-oxidizing autotrophs and acidophilic heterotrophs isolated from uranium mines. *Canadian Journal of Microbiology* **39**(4): 384-388.

Bhatnagar, M. and Singh, G. (1991). Growth-inhibition and leakage of cellular material from thiobacillus-ferrooxidans by organic-compounds. *Journal of Environmental Biology* **12**(4): 385-399.

Bilgin, A. A. (2004). Enhancement of bacterial iron respiration as a means to inhibit acid mine drainage. Ph.D. thesis. *University of Colorado.*

Bilgin, A. A., Harrington, J. M. and Silverstein, J. (2007). Enhancement of bacterial iron and sulfate respiration for in situ bioremediation of acid mine drainage sites: a case study. *Minerals & Metallurgical Processing* **24**(3): 139-144.

Bilgin, A. A., Silverstein, J. and Hernandez, M. (2005). Effects of soluble ferri - Hydroxide complexes on microbial neutralization of acid mine drainage. *Environmental Science & Technology* **39**(20): 7826-7832.

Bilgin, A. A., Silverstein, J. and Jenkins, J. D. (2004). Iron respiration by Acidiphilium cryptum at pH 5. *Fems Microbiology Ecology* **49**(1): 137-143.

BLM. (2011). "http://www.blm.gov/wo/st/en/prog/more/Abandoned_Mine_Lands/abandoned_mine_site.html" Feb 2011. Retrieved 2/12, 2012. Bureau of Land Management.

Blowes , D. W., Ptacek , C. J., Jambor , J. L. and Weisener , C. G. (2003). The geochemistry of acid mine drainage. *Treatise on geochemistry*. B. S. Lollar. Toronto, Canada., *Elsevier*. **9:** 149-204.

Boero, V. J., Bowers, A. R. and Eckenfelder, W. W. (1996). Molecular weight distribution of soluble microbial products in biological systems. *Water Science and Technology* **34**(5-6): 241-248.

Bond, P. L., Druschel, G. K. and Banfield, J. F. (2000). Comparison of acid mine drainage microbial communities in physically and geochemically distinct ecosystems. *Applied and Environmental Microbiology* **66**(11): 4962-+.

Bond, P. L., Smriga, S. P. and Banfield, J. F. (2000). Phylogeny of microorganisms populating a thick, subaerial, predominantly lithotrophic biofilm at an extreme acid mine drainage site. *Applied and Environmental Microbiology* **66**(9): 3842-3849.

Borichewski, R.M. (1967). Keto acids as growth-limiting factors in autotrophic growth of thiobacillus thiooxidans. *Journal of Bacteriology* **93**(2): 597-&.

Breault, R. F., Colman, J. A., Aiken, G. R. and McKnight, D. (1996). Copper speciation and binding by organic matter in copper-contaminated streamwater. *Environmental Science & Technology* **30**(12): 3477-3486.

Bridge, T. A. M. and Johnson, D. B. (2000). Reductive dissolution of ferric iron minerals by Acidiphilium SJH. *Geomicrobiology Journal* **17**(3): 193-206.

Brothers, L. A., Engel, M. H. and Elmore, R. D. (1996). The late diagenetic conversion of pyrite to magnetite by organically complexed ferric iron. *Chemical Geology* **130**(1-2): 1-14.

Bunescu, A., Besse-Hoggan, P., Sancelme, M., Mailhot, G. and Delort, A. M. (2008). Fate of the nitrilotriacetic Acid-Fe(III) complex during photodegradation and biodegradation by Rhodococcus rhodochrous. *Applied and Environmental Microbiology* **74**(20): 6320-6326.

Campbell, L. K., Knox, K. W. and Wicken, A. J. (1978). Extractability of cell-wall polysaccharide from lactobacilli and streptococci by autoclaving and by dilute acid. *Infection and Immunity* **22**(3): 842-851.

Carey, S. K., Barbour, S. L. and Hendry, M. M. (2005). Evaporation from a waste-rock surface, Key Lake, Saskatchewan. *Canadian Geotechnical Journal* **42**(4): 1189-1199.

Chen, M., Wang, W. X. and Guo, L. D. (2004). Phase partitioning and solubility of iron in natural seawater controlled by dissolved organic matter. *Global Biogeochemical Cycles* **18**(4).

Coram, N. J. and Rawlings, D. E. (2002). Molecular relationship between two groups of the genus Leptospirillum and the finding that Leptosphillum ferriphilum sp nov dominates South African commercial biooxidation tanks that operate at 40 degrees C. *Applied and Environmental Microbiology* **68**(2): 838-845.

Cory, R. M. and McKnight, D. M. (2005). Fluorescence spectroscopy reveals ubiquitous presence of oxidized and reduced quinones in dissolved organic matter. *Environmental Science & Technology* **39**(21): 8142-8149.

Cvetkovic, V. (2010). Diffusion-controlled tracer retention in crystalline rock on the field scale. *Geophysical Research Letters* **37**, L13401.

Dalzell, D. J. B. and Macfarlane, N. A. A. (1999). The toxicity of iron to brown trout and effects on the gills: a comparison of two grades of iron sulphate. *Journal of Fish Biology* **55**(2): 301-315.

Das, B. K., Roy, A., Koschorreck, M., Mandal, S. M., Wendt-Potthoff, K. and Bhattacharya, J. (2009). Occurrence and role of algae and fungi in acid mine drainage environment with special reference to metals and sulfate immobilization. *Water Research* **43**(4): 883-894.

Dong, M. M., Mezyk, S. P. and Rosario-Ortiz, F. L. (2010). Reactivity of Effluent Organic Matter (Ef0M) with Hydroxyl Radical as a Function of Molecular Weight. *Environmental Science & Technology* **44**(15): 5714-5720.

Dopson, M., Lovgren, L. and Bostrom, D. (2009). Silicate mineral dissolution in the presence of acidophilic microorganisms: Implications for heap bioleaching. *Hydrometallurgy* **96**(4): 288-293.

Dudal, Y., Sevenier, G., Dupont, L. and Guillon, E. (2005). Fate of the metal-binding soluble organic matter throughout a soil profile. *Soil Science* **170**(9): 707-715.

Dutrizac, J. E. and Jambor, J. L. (2000). Jarosites and their application in hydrometallurgy. *Sulfate Minerals - Crystallography, Geochemistry and Environmental Significance* **40**: 405-452.

Edwards, K. J., Bond, P. L. and Banfield, J. F. (2000). Characteristics of attachment and growth of Thiobacillus caldus on sulphide minerals: a chemotactic response to sulphur minerals? *Environmental Microbiology* **2**(3): 324-332.

Edwards, K. J., Bond, P. L., Druschel, G. K., McGuire, M. M., Hamers, R. J. and Banfield, J. F. (2000). Geochemical and biological aspects of sulfide mineral dissolution: lessons from Iron Mountain, California. *Chemical Geology* **169**(3-4): 383-397.

Edwards, K. J., Gihring, T. M. and Banfield, J. F. (1999). Seasonal variations in microbial populations and environmental conditions in an extreme acid mine drainage environment. *Applied and Environmental Microbiology* **65**(8): 3627-3632.

Eggleston, C. M., Voros, J., Shi, L., Lower, B. H., Droubay, T. C. and Colberg, P. J. S. (2008). Binding and direct electrochemistry of OmcA, an outer-membrane cytochrome from an iron reducing bacterium, with oxide electrodes: A candidate biofuel cell system. *Inorganica Chimica Acta* **361**(3): 769-777.

Evangelou, V. P. (2001). Pyrite microencapsulation technologies: Principles and potential field application. *Ecological Engineering* **17**(2-3): 165-178.

Ferris, F. G., Schultze, S., Witten, T. C., Fyfe, W. S. and Beveridge, T. J. (1989). Metal interactions with microbial biofilms in acidic and neutral ph environments. *Applied and Environmental Microbiology* **55**(5): 1249-1257.

Fortin, D., Davis, B. and Beveridge, T. J. (1996). Role of Thiobacillus and sulfate-reducing bacteria in iron biocycling in oxic and acidic mine tailings. *Fems Microbiology Ecology* **21**(1): 11-24.

Fowler, T. A., Holmes, P. R. and Crundwell, F. K. (2001). On the kinetics and mechanism of the dissolution of pyrite in the presence of Thiobacillus ferrooxidans. *Hydrometallurgy* **59**(2-3): 257-270.

Francis, A. J. and Dodge, C. J. (1993). Influence of complex structure on the biodegradation of iron-citrate complexes. *Applied and Environmental Microbiology* **59**(1): 109-113.

Ganesh, R., Robinson, K. G., Reed, G. D. and Sayler, G. S. (1997). Reduction of hexavalent uranium from organic complexes by sulfate- and iron-reducing bacteria. *Applied and Environmental Microbiology* **63**(11): 4385-4391.

Gao, H. Z. and Zepp, R. G. (1998). Factors influencing photoreactions of dissolved organic matter in a coastal river of the southeastern United States. *Environmental Science & Technology* **32**(19): 2940-2946.

Gehrke, T., Hallmann, R., Kinzler, K. and Sand, W. (2001). The EPS of Acidithiobacillus ferrooxidans - a model for structure-function relationships of attached bacteria and their physiology. *Water Sci Technol* **43**(6): 159-67.

Gehrke, T., Telegdi, J., Thierry, D. and Sand, W. (1998). Importance of extracellular polymeric substances from Thiobacillus ferrooxidans for bioleaching. *Applied and Environmental Microbiology* **64**(7): 2743-2747.

Gemmell, R. T. and Knowles, C. J. (2000). Utilisation of aliphatic compounds by acidophilic heterotrophic bacteria. The potential for bioremediation of acidic wastewaters contaminated with toxic organic compounds and heavy metals. *Fems Microbiology Letters* **192**(2): 185-190.

Gilchrist, S., Gates, A., Szabo, Z. and Lamothe, P. J. (2009). Impact of AMD on water quality in critical watershed in the Hudson River drainage basin: Phillips Mine, Hudson Highlands, New York. *Environmental Geology* **57**(2): 397-409.

Gray, N. F. (1998). Acid mine drainage composition and the implications for its impact on lotic systems. *Water Research* **32**(7): 2122-2134.

Gross, S. and Robbins, E. I. (2000). Acidophilic and acid-tolerant fungi and yeasts. *Hydrobiologia* **433**(1-3): 91-109.

Harrison, A. P. (1981). Acidiphilium-cryptum gen-nov, sp-nov, heterotrophic bacterium from acidic mineral environments. *International Journal of Systematic Bacteriology* **31**(3): 327-332.

Hayen, H. and Volmer, D. A. (2006). Different iron-chelating properties of pyochelin diastereoisomers revealed by LC/MS. *Analytical and Bioanalytical Chemistry* **385**(3): 606-611.

Herlihy, A. T., Kaufmann, P. R., Mitch, M. E. and Brown, D. D. (1990). Regional estimates of acid-mine drainage impact on streams in the mid-atlantic and southeastern united-states. *Water Air and Soil Pollution* **50**(1-2): 91-107.

Holakoo, L., Nakhla, G., Yanful, E. K. and Bassi, A. S. (2006). Chelating properties and molecular weight distribution of soluble microbial products from an aerobic membrane bioreactor. *Water Research* **40**(8): 1531-1538.

Huang, G. T., Jin, G., Wu, J. H. and Liu, Y. D. (2008). Effects of glucose and phenol on soluble microbial products (SMP) in sequencing batch reactor systems. *International Biodeterioration & Biodegradation* **62**(2): 104-108.

Huang, X. and Evangelou, V. P. (1994). Suppression of pyrite oxidation rate by phosphate addition. *Environmental Geochemistry of Sulfide Oxidation* **550**: 562-573.

Jansen, M. and Groman, D. (1993). The Effect of High Concentrations of Iron on Impounded American Lobsters: A Case Study. *Journal of Aquatic Animal Health* **5**(2).

Jenkins, J. D. (2006). Role of flow and organic carbon on acid mine drainage remediation in waste rock. Ph.D. thesis. *University of Colorado***.**

Johnson, D. B. (1995). Acidophilic microbial communities - candidates for bioremediation of acidic mine effluents. *International Biodeterioration & Biodegradation* **35**: 41-58.

Johnson, D. B. and Bridge, T. A. M. (2002). Reduction of ferric iron by acidophilic heterotrophic bacteria: evidence for constitutive and inducible enzyme systems in Acidiphilium spp. *Journal of Applied Microbiology* **92**(2): 315-321.

Johnson, D. B. and Hallberg, K. B. (2003). The microbiology of acidic mine waters. *Research in Microbiology* **154**(7): 466-473.

Johnson, D. B. and Hallberg, K. B. (2005). Acid mine drainage remediation options: a review. *Science of the Total Environment* **338**(1-2): 3-14.

Johnson, D. B. and Hallberg, K. B. (2009). Carbon, Iron and Sulfur Metabolism in Acidophilic Micro-Organisms. *Advances in Microbial Physiology, Vol 54*. R. K. Poole. **54:** 201-255.

Johnson, D. B. and McGinness, S. (1991). Ferric iron reduction by acidophilic heterotrophic bacteria. *Applied and Environmental Microbiology* **57**(1): 207-211.

Johnson, D. B., Yajie, L. and Okibe, N. (2008). "Bioshrouding" - a novel approach for securing reactive mineral tailings. *Biotechnology Letters* **30**(3): 445-449.

Kalinowski, B. E., Liermann, L. J., Brantley, S. L., Barnes, A. and Pantano, C. G. (2000). X-ray photoelectron evidence for bacteria-enhanced dissolution of hornblende. *Geochimica Et Cosmochimica Acta* **64**(8): 1331-1343.

Kawano, M. and Tomita, K. (2001). Geochemical modeling of bacterially induced mineralization of schwertmannite and jarosite in sulfuric acid spring water. *American Mineralogist* **86**(10): 1156-1165.

Kim, D. and Strathmann, T. J. (2007). Role of organically complexed iron(II) species in the reductive transformation of RDX in anoxic environments. *Environmental Science & Technology* **41**(4): 1257-1264.

Kuo, W. C. and Parkin, G. F. (1996). Characterization of soluble microbial products from anaerobic treatment by molecular weight distribution and nickel-chelating properties. *Water Research* **30**(4): 915-922.

Kusel, K., Roth, U. and Drake, H. L. (2002). Microbial reduction of Fe(III) in the presence of oxygen under low pH conditions. *Environmental Microbiology* **4**(7): 414-421.

Kyhn, C. and Elberling, B. (2001). Frozen cover actions limiting AMD from mine waste deposited on land in Arctic Canada. *Cold Regions Science and Technology* **32**(2-3): 133-142.

Lindsay, M. B. J., Ptacek, C. J., Blowes, D. W. and Gould, W. D. (2008). Zero-valent iron and organic carbon mixtures for remediation of acid mine drainage: Batch experiments. *Applied Geochemistry* **23**(8): 2214-2225.

Liu, G. L., Fernandez, A. and Cai, Y. (2011). Complexation of Arsenite with Humic Acid in the Presence of Ferric Iron. *Environmental Science & Technology* **45**(8): 3210-3216.

Liu, M. S., Branion, R. M. R. and Duncan, D. W. (1988). The effects of ferrous iron, dissolved-oxygen, and inert solids concentrations on the growth of thiobacillus-ferrooxidans. *Canadian Journal of Chemical Engineering* **66**(3): 445-451.

Lottermoser , B. (2003). Mine wastes: characterization, treatment and environmental impacts. Berlin, Heidelberg, and New York. *Springer*.

Lu, J., Chen, T. H., Wu, J., Wilson, P. C., Hao, X. Y. and Qian, J. H. (2011). Acid tolerance of an acid mine drainage bioremediation system based on biological sulfate reduction. *Bioresource Technology* **102**(22): 10401-10406.

Luther, G. W., Kostka, J. E., Church, T. M., Sulzberger, B. and Stumm, W. (1992). Seasonal iron cycling in the salt-marsh sedimentary environment - the importance of ligand complexes with fe(ii) and fe(iii) in the dissolution of fe(iii) minerals and pyrite, respectively. *Marine Chemistry* **40**(1-2): 81-103.

Luther, G. W., Shellenbarger, P. A. and Brendel, P. J. (1996). Dissolved organic Fe(III) and Fe(II) complexes in salt marsh porewaters. *Geochimica Et Cosmochimica Acta* **60**(6): 951-960.

Lyon, J. S., Hilliard, T. J. and Bethell, T. N. (1993). Burden of gilt Washington, DC, *Mineral Policy Center*.

Magnuson, T. S., Hodges-Myerson, A. L. and Lovley, D. R. (2000). Characterization of a membrane-bound NADH-dependent Fe3+ reductase from the dissimilatory Fe3+-reducing bacterium Geobacter sulfurreducens. *Fems Microbiology Letters* **185**(2): 205-211.

Majzlan, J. and Myneni, S. C. B. (2005). Speciation of iron and sulfate in acid waters: Aqueous clusters to mineral precipitates. *Environmental Science & Technology* **39**(1): 188-194.

Marchand, E. A. (2000). The role of induced heterotrophic microbial growth in mitigating the effects of acid mine drainage. Ph.D. thesis. *University of Colorado.*

Marchand, E. A. and Silverstein, J. (2002). Influence of heterotrophic microbial growth on biological oxidation of pyrite. *Environmental Science & Technology* **36**(24): 5483-5490.

Marchand, E. A. and Silverstein, J. (2003). The role of enhanced heterotrophic bacterial growth on iron oxidation by Acidithiobacillus ferrooxidans. *Geomicrobiology Journal* **20**(3): 231-244.

Mason, C. A., Hamer, G. and Bryers, J. D. (1986). The death and lysis of microorganisms in environmental processes. *Fems Microbiology Reviews* **39**(4): 373-401.

McKibben, M. A. and Barnes, H. L. (1986). Oxidation of pyrite in low-temperature acidic solutions - rate laws and surface textures. *Geochimica Et Cosmochimica Acta* **50**(7): 1509-1520.

McKnight, D. M., Bencala, K. E., Zellweger, G. W., Aiken, G. R., Feder, G. L. and Thorn, K. A. (1992). Sorption of dissolved organic-carbon by hydrous aluminum and iron-oxides occurring at the confluence of deer creek with the snake river, summit county, colorado. *Environmental Science & Technology* **26**(7): 1388-1396.

McKnight, D. M., Feder, G. L., Thurman, E. M., Wershaw, R. L. and Westall, J. C. (1983). Complexation of copper by aquatic humic substances from different environments. *Science of the Total Environment* **28**(JUN): 65-76.

McKnight, D. M. and Morel, F. M. M. (1980). COPPER COMPLEXATION BY SIDEROPHORES FROM FILAMENTOUS BLUE-GREEN-ALGAE. *Limnology and Oceanography* **25**(1): 62-71.

Meruane, G. and Vargas, T. (2003). Bacterial oxidation of ferrous iron by Acidithiobacillus ferrooxidans in the pH range 2.5-7.0. *Hydrometallurgy* **71**(1-2): 149-158.

Moses, C. O., Nordstrom, D. K., Herman, J. S. and Mills, A. L. (1987). Aqueous pyrite oxidation by dissolved-oxygen and by ferric iron. *Geochimica Et Cosmochimica Acta* **51**(6): 1561-1571.

Muller, G. and Raymond, K. N. (1984). Specificity and mechanism of ferrioxamine-mediated iron transport in streptomyces-pilosus. *Journal of Bacteriology* **160**(1): 304-312.

Neilands, J. B. (1995). Siderophores - structure and function of microbial iron transport compounds. *Journal of Biological Chemistry* **270**(45): 26723-26726.

Nichol, C., Smith, L. and Beckie, R. (2005). Field-scale experiments of unsaturated flow and solute transport in a heterogeneous porous medium. *Water Resources Research* **41**(5).

Nordstrom, D. K. and Alpers, C. N. (1999). Negative pH, efflorescent mineralogy, and consequences for environmental restoration at the Iron Mountain Superfund site, California. *Proceedings of the National Academy of Sciences of the United States of America* **96**(7): 3455-3462.

Nyavor, K. and Egiebor, N. O. (1995). Control of pyrite oxidation by phosphate coating. *Science of the Total Environment* **162**(2-3): 225-237.

Osorio, H., Martinez, V., Nieto, P. A., Holmes, D. S. and Quatrini, R. (2008). Microbial iron management mechanisms in extremely acidic environments: comparative genomics evidence for diversity and versatility. *Bmc Microbiology* **8**. 203

Parkhurst, D. L. and Appelo, C. A. J. (1999). *User's guide to PHREEQC: A computer program for speciation, batch-reaction, onedimensional* tr*ansport, and inverse geomchemical calculation*. Denver, CO, *U.S. Geological Survey*

Patidar, S. K. and Tare, V. (2008). Soluble microbial products formation and their effect on trace metal availability during anaerobic degradation of sulfate laden organics. *Water Science and Technology* **58**(4): 749-755.

Peplow, D. and Edmonds, R. (2005). The effects of mine waste contamination at multiple levels of biological organization. *Ecological Engineering* **24**(1-2): 101-119.

Pond, G. J., Passmore, M. E., Borsuk, F. A., Reynolds, L. and Rose, C. J. (2008). Downstream effects of mountaintop coal mining: comparing biological conditions using family- and genus-level macroinvertebrate bioassessment tools. *Journal of the North American Benthological Society* **27**(3): 717-737.

Pronk, J. T., Meesters, P. J. W., Vandijken, J. P., Bos, P. and Kuenen, J. G. (1990). Heterotrophic growth of thiobacillus-acidophilus in batch and chemostat cultures. *Archives of Microbiology* **153**(4): 392-398.

Rampinelli, L. R., Azevedo, R. D., Teixeira, M. C., Guerra-Sa, R. and Leao, V. A. (2008). A sulfate-reducing bacterium with unusual growing capacity in moderately acidic conditions. *Biodegradation* **19**(5): 613-619.

Reimus, P., Pohll, G., Mihevc, T., Chapman, J., Haga, M., Lyles, B., Kosinski, S., Niswonger, R. and Sanders, P. (2003). Testing and parameterizing a conceptual model for solute transport in a fractured granite using multiple tracers in a forcedgradient test. *Water Resources Research* **39**(12).

Rose, A. L. and Waite, T. D. (2003). Kinetics of iron complexation by dissolved natural organic matter in coastal waters. *Marine Chemistry* **84**(1-2): 85-103.

Rose, A. L. and Waite, T. D. (2005). Reduction of organically complexed ferric iron by superoxide in a simulated natural water. *Environmental Science & Technology* **39**(8): 2645-2650.

Rowe, R., Todd, R. and Waide, J. (1977). Microtechnique for most-probable-number analysis. *Applied and Environmental Microbiology* **33**(3): 675-680.

Sand, W. and Gehrke, T. (2006). Extracellular polymeric substances mediate bioleaching/biocorrosion via interfacial processes involving iron(III) ions and acidophilic bacteria. *Research in Microbiology* **157**(1): 49-56.

Schaeffer, W. I. and Umbreit, W. W. (1963). Phosphotidylinositol as a wetting agent in sulfur oxidation by thiobacillus thiooxidans. *Journal of Bacteriology* **85**(2): 492-&.

Singer, P. C. and Stumm, W. (1970). Acidic mine drainage . Rate-determining step. *Science* **167**(3921): 1121-&.

Smythe, C. V. and Schmidt, C. L. A. (1930). Studies on the mode of combination of iron with certain proteins, amino acids, and related compounds. *Journal of Biological Chemistry* **88**(1): 241-269.

Sracek, O., Choquette, M., Gelinas, P., Lefebvre, R. and Nicholson, R. V. (2004). Geochemical characterization of acid mine drainage from a waste rock pile, Mine Doyon, Quebec, Canada. *Journal of Contaminant Hydrology* **69**(1-2): 45-71.

Stockwell, J., Smith, L., Jambor, J. L. and Beckie, R. (2006). The relationship between fluid flow and mineral weathering in heterogeneous unsaturated porous media: A physical and geochemical characterization of a waste-rock pile. *Applied Geochemistry* **21**(8): 1347-1361.

Stromberg, B. and Banwart, S. (1994). Kinetic modeling of geochemical processes at the aitik mining waste rock site in northern sweden. *Applied Geochemistry* **9**(5): 583-595.

Stromberg, B. and Banwart, S. (1999). Weathering kinetics of waste rock from the Aitik copper mine, Sweden: scale dependent rate factors and pH controls in large column experiments. *Journal of Contaminant Hydrology* **39**(1-2): 59-89.

Stromberg, B. and Banwart, S. A. (1999). Experimental study of acidity-consuming processes in mining waste rock: some influences of mineralogy and particle size. *Applied Geochemistry* **14**(1): 1-16.

Sturman, P. J. (2004). Control of acid rock drainage from mine tailings through the addition of dissolved organic carbon. Ph.D. thesis. Montana State University.

Sutherland, I. W. and Wilkinson, J. F. (1971). Chapter IV Chemical Extraction Methods of Microbial Cells. *Methods in Microbiology*. J. R. N. a. D. W. Ribbons, *Academic Press*. **Volume 5, Part B:** 345-383.

Thurman, E. M. (1985). Organic geochemistry of natural waters. Dordrecht; Hingham; Boston, MA, USA, *Kluwer Academic*.

Tokunaga, T. K., Olson, K. R. and Wan, J. M. (2005). Infiltration flux distributions in unsaturated rock deposits and their potential implications for fractured rock formations. *Geophysical Research Letters* **32**(5).

Tran, A. B., Miller, S., Williams, D. J., Fines, P. and Wilson, G. W. (2003). Geochemical and mineralogical characterisation of twocontrasting waste rock dumps – the INAP waste rock dumpcharacterization project. 6th International Conference onAcid Rock Drainage, *Austral. Inst. Mining Metall. Publ. Ser***:** 939–948.

Tyson, G. W., Chapman, J., Hugenholtz, P., Allen, E. E., Ram, R. J., Richardson, P. M., Solovyev, V. V., Rubin, E. M., Rokhsar, D. S. and Banfield, J. F. (2004). Community structure and metabolism through reconstruction of microbial genomes from the environment. *Nature* **428**(6978): 37-43.

Tyson, G. W., Lo, I., Baker, B. J., Allen, E. E., Hugenholtz, P. and Banfield, J. F. (2005). Genome-directed isolation of the key nitrogen fixer Leptospirillum ferrodiazotrophum sp nov from an acidophilic microbial community. *Applied and Environmental Microbiology* **71**(10): 6319-6324.

Vaughn, R. B., Stanton, M. R. and Horton, R. J. (1999). A year in the life of a mine dump: A diachronic case study. *Tailings and Mine Waste'99*, Balkema.

Waber, H. N., Gimmi, T. and Smellie, J. A. T. (2011). Effects of drilling and stress release on transport properties and porewater chemistry of crystalline rocks. *Journal of Hydrology* **405**(3-4): 316-332.

Warner , R. (1971). Distribution of Biota in a Stream Polluted by Acid Mine-Drainage *ohio journal of science* **71**: 202-215.

Waybrant, K. R., Ptacek, C. J. and Blowes, D. W. (2002). Treatment of mine drainage using permeable reactive barriers: Column experiments. *Environmental Science & Technology* **36**(6): 1349-1356.

Williamson, M. A. and Rimstidt, J. D. (1994). The kinetics and electrochemical rate-determining step of aqueous pyrite oxidation. *Geochimica Et Cosmochimica Acta* **58**(24): 5443-5454.

Yanful, E. K. and Orlandea, M. P. (2000). Controlling acid drainage in a pyritic mine waste rock. Part II: Geochemistry of drainage. *Water Air and Soil Pollution* **124**(3-4): 259-284.